PATTERN RECOGNITION AND FEATURE EXTRACTION USING LIDAR-DERIVED ELEVATION MODELS IN GIS: A COMPARISON BETWEEN VISUALIZATION TECHNIQUES AND AUTOMATED METHODS FOR IDENTIFYING PREHISTORIC DITCH-FORTIFIED SITES IN NORTH DAKOTA

A Thesis
Submitted to the Graduate Faculty
of the
North Dakota State University
of Agriculture and Applied Science

By

Matthew Jeffery Radermacher

In Partial Fulfillment of the Requirements
for the Degree of
MASTER OF SCIENCE

Major Department:
Sociology and Anthropology

October 2016

Fargo, North Dakota

North Dakota State University
Graduate School

Title

Pattern recognition and feature extraction using lidar-derived elevation models in GIS: a comparison between visualization techniques and automated methods for identifying prehistoric ditch-fortified village sites in North Dakota

By

Matthew J. Radermacher

The Supervisory Committee certifies that this ***disquisition*** complies with North Dakota State University's regulations and meets the accepted standards for the degree of

MASTER OF SCIENCE

SUPERVISORY COMMITTEE:

Jeffrey T. Clark
Chair

Thomas Riley

Stephanie Day

Michael Michlovic

Approved:

10/11/2016
Date

Jeffrey Bumgarner
Department Chair

ABSTRACT

As technologies advance in the fields of geology and computer science, new methods in remote sensing, including data acquisition and analyses, make it possible to accurately model diverse landscapes. Archaeological applications of these systems are becoming increasingly popular, especially in regards to site prospection and the geospatial analysis of cultural features. Different methodologies were used to identify fortified ditch features of anthropogenic origin using aerial lidar from known prehistoric sites in North Dakota. The results were compared in an attempt to develop a system aimed at detecting similar, unrecorded morphological features on the landscape. The successful development of this program will allow archaeological investigators to review topography and locate specific features on the surface that otherwise could be difficult to identify as a result of poor visibility in the field.

ACKNOWLEDGMENTS

This research would not have been possible without the hard work and dedication of the talented individuals from the Computer Science, Geoscience, and Sociology/Anthropology departments at North Dakota State University. The members of this multi-disciplinary team brought distinct expertise and skills to make this project a success. These individuals include Project Director and GIS specialist Stephanie Day, Professor Emeritus of Geology Donald Schwert, Professor of Anthropology Jeffrey Clark, Assistant Professor of Anthropology (University of Hawaii) Seth Quintus, Professor of Computer Science Anne Denton, and graduate students Shuhang Li and Nolita Motu. Special thanks to ND NASA EPSCoR for providing the seed money and the original grant writers for making this project a reality.

Lastly, none of this would have been possible without funding and support from North Dakota State University. This institution provided the technology that made this project a possibility and without that, it would have been nothing more than an idea. Thanks to Thesis committee members Jeffrey Clark (Chair), Thomas Riley, Stephanie Day, and Michael Michlovic for providing advice and guidance throughout this entire process. Special thanks to Kate Ulmer for assisting with administrative support. Finally, I would like to thank Ava, Eli, my wife Trista, and the rest of my family and friends, for tolerating me during the last couple of years and giving me the motivation and will to complete this… it would not have been possible without any of you.

TABLE OF CONTENTS

LIST OF TABLES

LIST OF FIGURES

LIST OF ABBREVIATIONS

CRM…….Cultural Resource Management

CW……continuous waveform

DEM…….Digital Elevation Model

EPSCoR.....Experimental Program to Stimulate Competitive Research

FW……full waveform

GIS……...Geographical Information Systems

lidar……...light detection and ranging

LRM…….Local Relief Model

NASA.....National Aeronautics and Space Administration

ND.....North Dakota

NDSU.....North Dakota State University

NEPV..... Northeastern Plains Village

WEKA.....Waikato Environment for Knowledge Analysis

LIST OF APPENDIX TABLES

CHAPTER 1. INTRODUCTION

Locating archaeological sites during surface inventories can oftentimes be difficult due to terrain and other environmental factors. In areas with limited ground exposure, overlying vegetation cover can make the identification of cultural materials seem quite impossible. Artifact scatters frequently get missed and although certain morphological features can show topographic change on the surface, they, too, are sometimes overlooked. Ground surveys can additionally be very expensive or time consuming, and with limited operating budgets, field crews often have to work with limited personnel under strict deadlines. Unfortunately, this may cause a decrease in work quality and result in an incomplete record of the cultural properties identified within an area.

As computational technologies – hardware and software – have advanced, new methods and capabilities for geospatial analysis have emerged to enhance archaeological investigations. Most notably, remote sensing provides an opportunity for researchers to perform visual inspections on spatial data for the purpose of archaeological prospection. Among the remote sensing techniques, aerial lidar (light detection and ranging) is increasingly providing data for large areas, making it possible to accurately model and analyze diverse landscapes. Perhaps the most advantageous aspect of lidar data is in giving the researcher the ability to filter out overlying vegetation to display bare-surface models (Devereux et al. 2005; Crow et al. 2007; Doneus et al. 2008; Lasaponara 2010). Although this technique does not reveal subsurface anomalies, morphological features such as the numerous types of anthropogenic earthworks found around the world can be mapped and defined in great detail.

More recent investigations into the feasibility of using these datasets for the purpose of automatic feature extraction have been promising. By programming computer algorithms with machine learning techniques, these systems can mine through large amounts of data in search of specific patterns for features of interest. The demonstrable success in detecting features in urban landscapes as well as prehistoric occupations highlight the effectiveness of that approach and illustrate how it can provide the archaeological toolkit with an additional application for site prospection (Rottensteiner and Briese 2002; Sohn et al. 2007; Hermosilla et al. 2011; Trier et al. 2009; Trier et al. 2012; Trier and Zortea 2012).

This project aims to build upon this work by comparing detection methods for a specific feature type, fortification ditches, that is found at sites in North Dakota (ND) as well as abroad. These features represent linear trenches that have been excavated into the ground surface, and typically surround campsites or villages. By programming the automated extraction software with previously known samples, it is hoped that similar but unrecorded features on the surface may be discovered. The successful development of this technology has immense implications for archaeology and cultural heritage management, which could increase the number of known sites and in turn our understanding of the past.

Funding for this research was provided by a seed grant from ND NASA (National Aeronautics and Space Administration) EPSCoR (Experimental Program to Stimulate Competitive Research) titled *Using Machine Learning in Earth Sciences Research to Discern Anthropogenic vs. Natural Landform Features within Remote Sensing Data Sets.* (NASA EPSCoR RID NNX13AB20A, sub-award 10137-18182). As a dual-component project it aims to examine the possibility of using data acquired from aerial lidar and high-resolution satellite imagery to detect anthropogenic features and automate the extraction process. A set of

earthworks from two very distinct landscapes were to be considered for analysis: house terraces, ditches, and mounds on a steep, densely covered tropical island in the U. S. Territory of American Samoa, in Western Polynesian, and the earth lodge depressions, fortification ditches, and mounds found at riverside occupations in the open, low-relief plains of North Dakota. These locations were chosen because of their contrasting topography and vegetation, and the similarity in size and morphology between the feature types. This provides useful datasets to test the technology in different areas to determine its applicability in complementary yet distinct settings. This thesis will be the product of a portion of this larger research agenda by focusing on North Dakota features, more specifically, the fortification ditches found at sites along the Sheyenne and Maple rivers in the Southeastern part of the state.

Environmental Setting

This research examines the viability of using remotely sensed data to model the distribution of specific archaeological properties on the landscape. Features in question include fortified, ditched sites located on the Sheyenne and Maple rivers of the southern Red River basin in North Dakota (Figure 1). These sites were occupied by Plains Village groups. As the local landscape has been heavily influenced by continental glaciers, the region is defined by topography of relatively low relief, intersected only by the banks of local drainages. Once an expansive grassland, much of the region has since been repurposed for agricultural uses, and economically productive crops dominate the vegetation in the area. The remaining floral assemblage includes various prairie grasses and forbs, as well as small patches of deciduous woods near water sources. Unfortunately, many sites have been lost due to intensive landscape modification through plowing, and many others can go unnoticed because of the thick

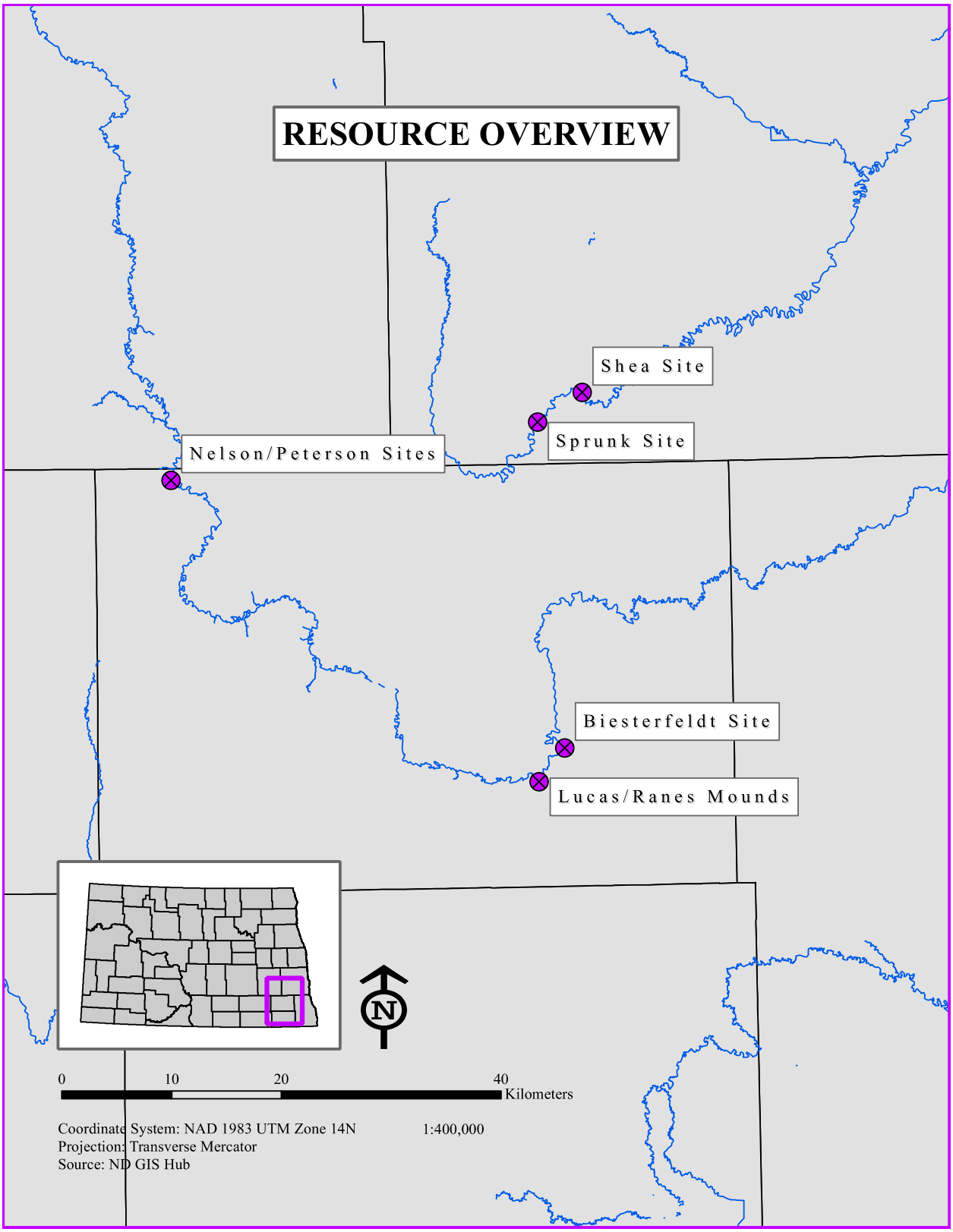

Figure 1. Cultural resources along the Sheyenne and Maple Rivers used in this study.

overgrowth that can impede the visual indications of topographic features during certain points of the year. With the recent increase in locally available, high-resolution remotely sensed datasets acquired for flood mitigation, it is hypothesized that specific disparities between the signals from features and the surrounding landscape can be recognized and used in the extraction process. Previously recorded sites along rivers in this region provide several examples of fortification ditches that will be used for analysis and the programming of the automated detection system.

Sites and Features

Known sites used for the development of this research include the Shea and Sprunk sites located on the Maple River, as well as Biesterfeldt, Nelson, Peterson, and Lucas sites found along the banks of the Sheyenne River (see chapter 2). The Shea, Sprunk, Biesterfeldt, Nelson, and Peterson sites provide excellent samples of fortification ditches for analysis. These features can be described as linear or curvilinear excavated trenches that encircle or partially encircle an occupation area, or village, for the interpreted purpose of defense, and can be found at numerous Northern Plains sites. An additional ditched feature at Lucas Mounds provides another example but is notably different and may represent an earthwork that was used for ceremonial purposes, as it is associated with a nearby mound cluster (Holley and Kalinowski 2008). However, the morphology seems similar enough to the other examples and should be compatible with the program.

Research Questions

This project aims to assess various visualization techniques of the lidar data, and develop/compare automated and semi-automated extraction programs based on the topographic pattern analysis of fortification ditches. Using a remotely sensed lidar-derived digital elevation model (DEM), it is hoped that the precise measurements of the features can provide enough detail to create accurate predictive models. The primary research questions are as follows:

- What visualization technique best represents the physical extent of these features for manual interpretations of the data?
- Which characteristic of these features, or combination of characteristics, will provide the highest degree of accuracy in detecting known sites through automated and semi-automated methods of feature extraction?
- Since the automated system will primarily detect anomalies based on morphological shape, is it possible to distinguish between the targeted feature type, and those of similar shape but of other cultural or natural origins, based on interpretations of these non-intrusive datasets alone?

To address these questions, several visualization layers (e.g., hillshades, slope severity, directional aspect, curvature profile, constrained color shading, and Local Relief Model) were created for interpretation in order to determine which qualities will be used for the programming. An algorithm was then developed in conjunction with North Dakota State University (NDSU) Computer Science personnel using machine learning and data mining techniques. The program was trained using data from a collection of known sites to identify the landscape patterns associated with the features. The training was followed by testing for accuracy on similar, previously recorded occupations to determine which characteristics and datasets were most

suitable for the application. This step provides researchers with an estimated degree of precision that this system can hope to achieve. If an algorithm is successfully developed, an attempt will be made to address issues of positive tests resulting from similarly shaped landforms such as modern agricultural or road ditches, vehicle ruts, abandoned river meanders, etc. Finally, the efficiency of the automated program was compared to a manual operation that attempts to detect the same features using similar characteristics based off a simple reclassification scheme within ArcGIS.

Thesis Organization

Following this introductory chapter, Chapter 2 reviews advancements in computer technology that has greatly impacted the field of archaeology. It briefly covers the progression of computers in the recent past, including the advent of GIS, spatial analysis, remote sensing, visualization techniques, and data extraction methods used in contemporary research.

Chapter 3 introduces the objectives of this project and describes how the research questions will be answered. The program design and methods employed are outlined including data acquisition, analysis of visualization techniques, and algorithm development including the training/testing on known features. A semi-automated method will additionally be introduced and comparatively tested on the same datasets. Statistics will be measured based on the true-positive, true-negative, false-positive, and false-negative results to assess the precision and accuracy of the separate approaches.

A detailed landscape description can be found in Chapter 4, which includes the cultural affiliations, or phases, that the occupations belong to. Additionally, it will define the form and

function of fortification ditches as well as the sites used for this study and the previous investigations carried out there.

Chapter 5 compares the results of the project and the degree of success in detecting anthropogenic features within the defined parameters. Feature visualizations of the different techniques will be displayed and subjectively compared. Each training and test dataset will be quantified and described in detail to determine the potential of the two methods. Additionally, a commentary will be provided for errors incurred during the research and troubleshooting steps to remedy the issues.

Chapter 6 concludes this study by addressing the viability and limitations of the methods employed in regard to the targeted research area, as well as areas both regionally and globally. This final chapter discusses potential areas to which the technology can be applied for future projects, and prospects for where it can be taken with further development.

As a preliminary investigation into the development of these systems for archaeological prospection, this study, and others like it, will provide a base for future work and advancements in the technology. It is hypothesized that the programs will function productively, but to an unknown extent, as there is a possibility of attaining false-positive results of non-features and false-negative results from others that were missed. Either way, the results should provide measurements of accuracy and precision that provide guidance for additional work to proceed in regard to the automatic and semi-automatic extraction of morphological features in a variety of settings.

CHAPTER 2. BACKGROUND

Computer Applications and Archaeology

The impact of computer technologies on societies around the globe in recent decades has been unprecedented and altered the way people interact with their environments. With so many systems dependent on computers to function properly, their continual use is essential and has ultimately culminated in the creation of entire institutions devoted to ensuring their constant operation. From nuclear programs and emergency services to banking and everything in between, the world as we know it is ultimately dependent on the existence of the processing power that these tools provide. They have made certain tasks easier to accomplish but in turn have created additional problems themselves. Researchers have spent countless hours devoted to troubleshooting these problems, and their research has advanced computers to the sophisticated machines they are today. From the first specialized units that took up entire rooms, to the miniaturized versions that many humans carry with them today, these systems have significantly impacted contemporary cultures across the world.

Technological advancements over the previous decades have had tremendous impacts in the field of archaeology. Computer software provides a platform for researchers to enter data with the ability to efficiently code information, allowing them to search for patterns and correlations for both intra- and inter-site relationships between identified cultural remains (Whallon 1972). The large amount of storage capacity creates endless amounts of datasets that can easily be transferred and accessed by individuals from numerous agencies. Illustration software offers ways to create accurate digital images of features or artifacts and function as enhanced forms of graphical communication between vested parties (Boast et al. 2011).

Advanced modeling systems provide ways to create detailed representations of cultural properties that can be used for comprehensive analysis at research institutions or public displays at interpretive centers (Stanco et al. 2011). This is by no means an exhaustive list of all the potential uses that computers provide for cultural investigators, but reflects on some of the significant implications they can provide to archaeological study.

GIS and Spatial Technologies

The application of Geographic Information Systems (GIS) and other spatial technologies in archaeology have recently become quite popular for site recording, visualization, modeling, data management, and the statistical analyses of artifacts and features (e.g., Kvamme 1999; McCoy and Ladefoged 2009). GIS represents the interface between landscape, hardware, software, and data, to organize information into a comprehensive package for analysis and interpretation by a human component. Using highly precise global positioning instruments to acquire targeted information in space, data can be referenced to a geographic coordinate system for visualization on various software platforms. Records from a variety of sources can be integrated into extensive datasets to better understand site complexities as well as the context in which they are located in scales of time and place. Having quick access to the information allows investigators to spend more time answering research questions and developing new ways to explore cultural materials and human impacts on the environment.

From exploring artifact and feature distribution through a single site, to spatially defining and analyzing regional settlement patterns, the impact of this technology has been immense in archaeology over the past 20 years. Especially in regard to Cultural Resource Management (CRM) and its prevalence in the United States, this technology facilitates the expedited transfer

of data between clients and concerned parties for development projects (Ebert 2004). During these undertakings, project corridors and associated areas of potential effects can oftentimes change due to environmental factors or cultural properties that could be affected. Being able to send updated files electronically between involved parties speeds up the process and allows the projects to be carried out in an efficient and productive manner. Many state historical preservation offices, including North Dakota, now even require data files to be submitted with site reports for cultural resource assessments. With so much emphasis being placed on GIS with site recording, it has been imperative for current researchers and field workers to learn and adapt to the technology. Sophisticated, handheld computers are now being brought into the field so archaeological properties can be digitally recorded at the source, allowing easy access to the information from any point recorded (Tripcevich 2004; Tripcevich et al. 2010).

This software has allowed investigators to view cultural resources in new ways and facilitates the (re)discovery of important information of both recorded sites and new finds. As excavation is undoubtedly a destructive process, the data we record is all that is preserved, while the original context of the material is permanently destroyed. These technologies allow that information to be stored in easy–to-access formats, and incredibly detailed maps and models of archaeological sites can be created for further study and analysis. In regard to existing collections, the paper files that were first created to document sites can be digitized and that information displayed in a GIS, allowing subsequent analysis and the potential discovery of information not previously known.

The ability of these techniques to assist in the archaeological prospection of sites has been a central component in the importance of GIS to the discipline. Having access to highly detailed and accurate digital maps prior to fieldwork allows researchers to visually inspect a

region to identify cultural properties themselves, or areas having high potential for sites. Being able to differentiate the contrasts between known cultural properties with the surrounding landscape permits investigators to begin preliminary interpretations before ever being in the field (Neubauer 2004). Classification of archaeological features can be defined on maps using different visualization techniques, creating the detailed site models used for spatial analysis. These data can then be used to identify areas with high integrity for targeted excavation and material recovery, thereby increasing the efficiency and productivity of the work.

Utilities that provide the opportunity for subsurface prospection at archaeological sites have provided tremendous results in being able to detect buried cultural properties such as artifact clusters and other living surfaces, as well as hearths, post holes, pits, ditches, and architecture (Kvamme 2003). These geophysical surveys can produce detailed maps of cultural resources several meters deep without having to place a shovel in the ground. Non-destructive methods including magnetometry, electrical resistivity, electromagnetic conductivity, and ground penetrating radar have been indispensable for researchers, as they attempt to gather as much information in the field as possible while preventing unnecessary damage. Although each of these systems is valuable as a standalone product, the integration of multiple techniques and datasets is beneficial to attaining a holistic understanding and perspective of subsurface materials.

Upgrades of the tools used to remotely sense and acquire these types of data are under constant development and improvement, which allows researchers to better understand landscape modification and settlement distribution. Recent uses of aerial lidar for archaeological reconnaissance provide large datasets on regional scales that can be used to document the cultural resources located within defined areas (Doneus et al. 2006; Challis et al. 2008). These

data are becoming increasingly available for larger areas and facilitates additional avenues of archaeological analysis.

Remote Sensing and lidar

Although aerial surveys have been successfully employed for most of the 20th century in field research (Bewley 2003), their limitations are abundant. Smaller scale photographs of specific sites can be used to define their boundaries, but large photosets over regional landscapes create distortions in many objects. Lighting conditions need to be perfect to obtain detailed images and cloud cover can greatly impede the process, however, the shading of certain objects can actually make them more visible, depending on the situation. These shortcomings severely limit the visibility of numerous details in the aerial images that archaeologists study. Despite these shortcomings, aerial images are still in use and will likely continue to be employed in varying capacities, even as new developments in remote sensing techniques provide researchers with accurate landscape models prior to ground survey and are becoming increasingly popular for both academic research and cultural heritage management (Cowley 2009; Corns and Shaw 2013; Crutchley 2013).

Advancements in laser-based technologies have developed quite rapidly and can be used to create extremely detailed maps of the earth's surface, and in turn can improve archaeological landscape understanding (Risbol 2013). Both terrestrial and aerial laser scanning systems are currently used in archaeology to document the landscape for varying purposes (Opitz 2013). As the lidar data acquired for this study are a central component of the research, a brief overview of how the aerial reconnaissance technology works and data are obtained is necessary. Briefly summarized, an aircraft travels over a designated area taking highly precise readings of the

ground surface. From these data, detailed models are created using specialized software to produce extremely accurate topographic maps, which are then used by individuals and researchers from numerous disciplines for a variety of applications. A more detailed explanation follows.

As an active sensing system, the scanning assembly emits a laser beam that is reflected off the first surface it hits back to the unit (Wehr and Lohr 1999). The time is measured between the sent and received light signals, and that measurement is used calculate the distance from the scanner to the surface. Two ranging principles are commonly applied to measurements: pulsed, which transmit individual light beams, and continuous wave (CW), or full-waveform (FW), lasers that emit a constant beam of light. CW lasers measure the phase difference between the transmitted and received signal and can be used with multiple frequencies to achieve higher resolution. The properties of the surface must also be considered when using these units, as the reflective qualities of various surfaces can differ. For example, certain wavelength frequencies will work better in areas of dense vegetation compared to surfaces with exposed sediment or those covered with snow or water. Considering the acquisition of the data itself, the scan pattern of the surface is influenced by the laser pulse, flight path conditions, and topography. Calibrated data is derived from measured points compared to the flight speed, height, and position (i.e., roll, pitch, and yaw), and referenced to a geographic coordinate system. The scanned points are placed in a .pos data file with their location in space characterized by x, y, and z values; x and y being the two-dimensional grid location while z designates the elevation.

From these data, further processing can then be accomplished to produce a digital elevation model (DEM). All points are first sorted and displayed in relation to a referenced coordinate system. The size of the grid is dependent on project specifications but multiple points

will be available for each unit. Different filtering algorithms can be used to remove non-ground points, such as buildings and vegetation, to obtain a bare-surface model (described in detail below). From this, the data are interpolated into a raster grid based on an average of measurements for individual units, where certain areas with incomplete data can be estimated from the nearest points. The resulting DEM that is produced can be described as a grid of equally sized units with specific elevation values. Subsequent post-processing steps can be performed to develop additional layers for visualization and analysis. For instance, these data can be viewed in differing scales of color to best represent and display the targeted information on mapping software.

The resulting high-quality landscape models and maps that this technology has made available over the previous decades have now been successfully utilized by historical and archaeological researchers of the past (Opitz and Cowley 2013). Their attempts at applying the data to not just simply map site boundaries and the artifacts within them, but to answer more broadly based research questions regarding settlement distribution, exchange networks, material provenance, and others, have been enlightening to say the least. Having immediate access to large amounts of data and the processing capabilities that this technology provides has increased the efficiency in workflow, as computers have limited the amount of labor the human component needs to perform. This allows more time and effort to be devoted to interpretation, although it is still a tedious undertaking to visually inspect the potential wealth of data acquired for analysis. New methods are under constant development that facilitate enhanced visualizations as well as data integration and cross-referencing to examine varying modes of investigation. Perhaps the most beneficial aspect that lidar can already provide archaeologists is its ability to remove from

overlying vegetation from the dataset, allowing researchers to view a bare surface model of the landscape.

This ability to reveal archaeological features hidden under woodland canopies in aerial photographs has greatly benefitted archaeologists in their task of identifying and recording cultural resources (Devereux et al. 2005). The application of this technique has thereby significantly increased the number of recognized pre-historic and historic properties within forested regions. Processing algorithms and vegetation removal filters have been used effectively to contrast between ground and foliage and identify potential archaeological features with minimal topographic context (Lasaponara 2010). Generally, these methods discriminate between terrain and off-terrain points by removing outlying data caused by errors in the acquisition process or interruption by other objects. Data obtained from full waveform scanners encompass the entire range of surface information from each pulse as multiple signals are received, and can be used to remove overlying vegetation or architecture (Doneus et al. 2008). However, it is important to recognize that distinctive types of flora will produce significantly different pulse patterns in their return signals. Differences in vegetation type, such as canopy and understory, influence the effectiveness of lidar in these areas, and can both be used to differentiate between ground and non-ground points (Crow et al. 2007). The recognition of these limitations and combination of techniques can be used to develop our perspectives and increase our understanding of the processes involved in refining the data, resulting in clearer images and the potential discovery of unknown sites too difficult to see in the field.

This has had tremendous implications for the spatial analysis of cultural properties, as we have never before been able to examine the bare ground surface from aerial photography alone, and investigators have had to rely on maps created in the field. Entire landscapes over large

regions can now be accurately visualized and interpreted by field researchers as areas with high potential to yield cultural remains (Hess 2013). The use of landscape indicators for the purpose of site prediction has been useful for the prospection of archaeological resources (Fry et al. 2004). Based on proximity to arable land, water, or other resources conducive to human activity, certain landscapes have higher potential for previous occupations than others. The possibility of identifying unknown sites is now even greater as technologies, processing speed, and storage capacity, build through constant improvements, which decreases the time spent on-screen and field research can more narrowly focus on targeted areas for study (Ainsworth et al. 2013).

Visualization Techniques

In order for site location predictions to be successful, physical attributes of the morphological features need to be considered in the analysis. Measurements from the DEM can be used to create additional layers from various tools within GIS software. These secondary datasets created from the lidar-derived elevation models provide quantifiable values based on certain characteristics, and include such properties as the degree of slope and curvature of a surface. These layers can then be viewed in GIS under varying conditions for interpretive analyses. Transparencies can be added to view multiple layers at once, and certain limits can be placed on the data to constrict the amount of information being displayed. Additional values can be altered to increase clarity, and sometimes by simply altering the color scheme, specific features on the surface can be more clearly defined and recognized from visual inspections.

Challis et al. (2011) inspected a suite of visualization techniques in a variety of regions in the United Kingdom to assess their viability. It included an examination of constrained color shading, slope, hillshade, principal component analysis, local-relief models, and solar insolation

models for various earthworks and structures. A high level of detail must be attained from the lidar data to produce thorough and accurate interpretations, and these techniques offer additional perspectives for archaeological properties under numerous conditions. Constrained color shading limits the displayed elevation values to a specific range that features of interest would be located. This creates a higher degree of contrast between the immediately surrounding landscape, essentially removing other landforms at different elevations. By eliminating hills and low relief areas, such as floodplains, a greater level of detail can be attained for areas of occupation by displaying the color scale over a smaller range of data. Clarity is enhanced and makes for improved visualization of geomorphological features on map documents. Slope analysis calculates surface angles and the severity of relief measured in degrees (0-90) or as percentage (0-100). Observable geomorphological structures become quite obvious during visual inspections but subtle features may be less so. Hillshading, which produces a hypothetical shadow from the sun, has long been used on topographic maps to more easily define features from their contours and has become ingrained into digital cartography, as well. It enhances the visual representation of areas with higher relief values but is limited by illumination from only a single point that can create shadows that hide other details. To remedy this, principal component analysis compiles a multi-azimuthal model of hillshades with 16 illuminations from a 360 degree spectrum (Devereux et al. 2008). The resulting image has fewer distortions and the sharp contrasts between features in low-relief areas become clearly noticeable. Local-relief models attempt to eliminate the natural topographic variation of an area to focus only on the archaeological properties (Hesse 2010). This is accomplished by subtracting the generalized terrain values that primarily define the landscape from the DEM, while leaving those within the range of targeted features that can then be clearly identified. The object of that exercise is to

display those features from the data while eliminating large-scale landforms to emphasize the archaeological properties without being distracted by the natural relief. Solar insolation models attempt to estimate the amount of radiation from the sun received at the surface. To achieve this, a viewshed of the observable sky must be made for each surface unit and coupled with sunmaps to complete the calculation. These data become quite useful for the analysis of land-use models in relation to human activity that would have occurred in shaded areas, under intense sunlight, or none at all.

Other researchers have examined a multitude of visualization techniques, including some that were previously mentioned, and others used for additional levels of analysis. A comparison between slope, aspect, principal component analysis, local-relief models, and sky-view factor highlights the differences in visualization techniques (Bennet et. al 2008). Similar conclusions are attained from the aforementioned methods but the addition of directional aspect to the equation creates another avenue for analysis. Although large features may be quite visible from other techniques, subtle features may not be. The slope may not be as great and will subsequently affect hillshading, which will result in less clarity. However, the surface direction that a unit faces could be quite useful for identifying features as additional patterns can emerge even on smaller features. Sky-view factor takes the viewshed of individual units to calculate the amount of diffuse light received by the surface (Kokalj et al. 2011). Similar to solar insolation models, it attempts to more clearly define archaeological features and increase their visibility compared to hillshading methods (Kokalj et al. 2013). Additional analyses employing viewshed methods have become popular for the interpretation of landscape uses (Challis et al. 2011). With additional parameters, some techniques have even taken human visual acuity into consideration. A fuzzy viewshed approach attempts to analyze the landscape based on an individuals view from

a certain point (Ogurn 2006). Areas closer to the observation point are plainly visible with clarity decreasing with distance.

It must be emphasized that no one technique will reveal the entire range of pertinent information, and some combination of techniques may be needed to yield better results. Additionally, the human component must be noted, as well as the recognition that prior knowledge and experience affect archaeological interpretations (Doneus and Kuhteiber 2013; Halliday 2013; Palmer 2013). Each landscape must be considered as a unique circumstance and as such, visualization methods must be measured on an individual basis. These techniques are very useful for analysis and interpretation, including the identification of features and regional patterns of distribution, as well as their range of variation in morphological form. However, these are primarily based on visual inspections of the data and must be quantified into functional values for computer-based applications.

Automatic Feature Extraction

Recent investigations have examined the accuracy of using certain physical indicators to predict where specific morphological features are located on the surface. By using the aforementioned values related to physical form, analysts search for patterns of attributes present in known samples to create templates that can be used for reference collections. By recognizing and understanding these forms, they can then search for other instances by inspecting the visual data represented on maps, or the lines of code themselves. However, this can be extremely difficult due to the tedious and time-consuming process of analyzing and interpreting vast amounts of data. In an attempt to automate this data extraction process, archaeologists have teamed up with computer scientists to create such systems by developing algorithms using

machine learning and data mining techniques (Cowley 2012). By training a computer program to detect patterns in the data, the resulting output should differentiate between areas that represent archaeological properties from those that do not and classify the individual units as such.

Although these methods have been evolving for over a decade, most previous research on automated feature extraction has been involved with building detection in urban landscapes. By directly analyzing the lidar point clouds and the individual measurements of each, the building and non-building points can be separated and used to create a digital terrain model (Rottensteiner and Briese 2002). By examining the height differences in the point values between the actual surface, buildings, and other off-terrain points that are not structures, highly accurate cityscape models can be created with the targeted classification information. Hoping to increase the accuracy and efficiency of building detection, much research has focused on the integration and collaboration of a data fusion between lidar data and high-resolution satellite imagery (Sohn et al. 2007; Hermosilla et al. 2011). These systems aim to both detect and describe buildings by threshold-based classifications of the lidar point clouds, and object-based classification of imagery by using chromatic clues to differentiate between vegetation indices and its presence or absence. These techniques have had success rates up to 90% and highlight their effectiveness in classifying the differences in surface properties on a landscape (Rottensteiner and Briese 2002; Sohn et al. 2007; Hermosilla et al. 2011).

Using similar methodological approaches, a group of Norwegian researchers have attempted to locate circular shaped pit structures using both aerial lidar and high-resolution satellite imagery (Trier et al. 2009; Trier et al. 2012). Their effort to detect archaeological depressions used previously known samples as templates for training the system. Differentiating

from the previously mentioned studies that examined the lidar point cloud, this research attempted to use a raster image of the elevation data to classify and detect features by their size and shape. The independent use of satellite imagery offered information on vegetation differences in low relief areas, but still classified types by size. The results were placed on probability scales in their likelihood of being correct detections and subsequently field-checked for verification. In either case, a fair amount of false-positive detections occurred, but were easily disregarded after visual inspection. After the success of their initial studies, the program has been expanded to search for additional cultural properties and detect such features as grave mounds, stone fences, and old roads (Trier and Zortea 2012).

Significant results have been produced from these studies, and although the systems are often termed "automatic," a more appropriate term may be "semi-automated" forms of feature extraction. Computers may automatically calculate and process the information, but the methods of training and modifying the programing parameters are heavily operator involved. Additionally, the output and results may be automatically obtained but are quite useless without the visual inspection by a human component and the knowledge-based interpretations offered by trained archaeologists. With an increase in the use of these technologies over wider geographic areas and varying categories of features, refinements in the programming can be made to tailor them towards specific units of analysis and highlight their applicability for examining different regions of the world.

CHAPTER 3. RESEARCH OBJECTIVES AND METHODS

Research Objectives

Traditional archaeological methods include the extensive recording of artifacts, features, occupations, and landscape changes resulting from past human activity. This most often involves detailed descriptions of both surface and subsurface collections, which typically results in the destruction of the original context in which the objects or features were found. Although this information is preserved in the archaeological record, investigators must be wary to carefully record their findings, as to preserve the integrity of further research. More recently, many researchers have been advocating the use of non-intrusive methods for field investigations (e.g., magnetometry, ground-penetrating radar, etc.), as useful data can be obtained without destroying the sites and the context of the information. Remotely sensed data, and more specifically that from lidar, falls under this category and provides a useful avenue for archaeologists to examine large areas of land and potential cultural properties without ever leaving a desk

The primary goal of the research under discussion here is to address the possibility of using certain morphological characteristics to define fortification ditches by their lidar-derived surface measurements. Therefore, the principal question of concern is: *What geomorphological attribute, or attributes, will provide the most accurate results when using lidar-derived surface measurements to define ditched features?* The unique context of these features should offer enough specific detail to distinguish them from the surrounding topography. Although visualizations such as the various hillshading and viewshed methods are useful for certain modes of analysis, they are not practical for this research due to their interpretive qualities. In addition, the research team on this project determined that other characteristics are more discerning. For

this study, we determined that only the physical qualities from direct measurements of the features should be used. Specifically, degree of slope, directional aspect, and curvature profiles of the features were chosen as the most likely variables to yield positive results. During visual inspections of the lidar data these parameters provided adequate differences to define the features, and they could be easily transferred to the automated program.

A secondary question of concern to this project deals with the possibility of attaining positive results from similarly shaped features of other cultural or natural origins, as the system will primarily detect anomalies based on morphological shape. Other manmade features of concern to this project include modern agricultural ditches and those found adjacent to roads, as well as ruts from repeated vehicular activity in non-paved areas. Naturally derived features such as the numerous oxbow lakes and abandoned meanders of the adjacent rivers near to which these sites are located, could potentially be mistaken for fortification ditches. Though it is possible that the anthropogenic features will be small enough and contained within well-defined contexts to avoid this issue, the system could still misinterpret some natural features as cultural. To mitigate these issues, visual inspection of the data can be conducted and, where possible, verified in the field through ground-truthing. After development, the algorithm can also be tested on known features of other cultural or natural origins to assess the degree of similarity between them and the output results to be expected.

Methods

Data Acquisition, Preprocessing, and Visualization Tools

Lidar data for the Red River Basin were collected through aerial survey in 2012 using a Leica ALS50_II MPiA sensor with sub-meter point spacing. Fugro Horizons Inc., a company

specializing in geospatial mapping solutions, processed the raw point data to create a classified LAS file and interpolated a 1-meter DEM. The data are available in multiple units and only those that covered the geographic region of concern were selected and combined for study. The resulting datasets provide a list of square-meter cells, georeferenced to spatial locations, which define individual elevation values and can be visualized as a map layer. Different color schemes can be used to best display the image, and parameters can be altered to specify the information being portrayed. Secondary layers can then be created from this information that represent additional details and can be viewed separately or in conjunction with other datasets.

From the spatial data acquired for this project, known features were classified within ArcGIS by delineating the boundaries of fortification ditches from the surrounding areas on the DEM, and a separate raster layer was subsequently created that assigned specific values to feature and non-feature cells. This was accomplished by manually visualizing the elevation data and tracing the approximate location of the outside boundary. It must be noted that according to the site reports that the average width of these ditches is around three meters. When determining the boundaries a buffer of several meters was applied to each site to ensure that the entire feature was included and identified as such. Secondary datasets including slope, aspect, and curvature of these features were additionally created using tools available in the GIS software package. These functions process the existing data with moving window neighborhood operations, which assigns values to individual cells based on a larger cluster adjoining it. This means that the characteristics of the surrounding cells must be considered when determining the value for a central unit. For example, slope is a measurement of the degree in angle a surface displays. This cannot be determined by examining a single elevation measurement alone, but by considering the

surrounding cells and their elevation the program calculates the maximum and minimum differences between all units in the window and assigns a corresponding value to the central cell.

For this study, the characteristics chosen for quantitative analysis are defined as follows and illustrated in Figure 2. In addition to these, a DEM with hillshade, multi-azimuthal hillshade, constrained color model, and local relief model were made for the visual comparison component of this study.

- **Slope:** Measured in degrees between 0-90, this characteristic defines the angle of a surface in relation to a horizontal plane. For ditches, the sides should be both steeper than its top/bottom and from the generally flat surrounding landscape, resulting in a higher degree of slope for those portions.
- **Aspect:** This characteristic measures the direction a surface is facing. The sides of ditches will face inward at directly opposite intervals and should have corresponding values approximately 180 degrees apart.
- **Curvature:** Surface curvature represents whether a cell is convex or concave in profile. Compared to mounds or hills, which would be 'positive', fortification ditches should indicate a 'negative' value as they represent a depression from the excavation and removal of soil.

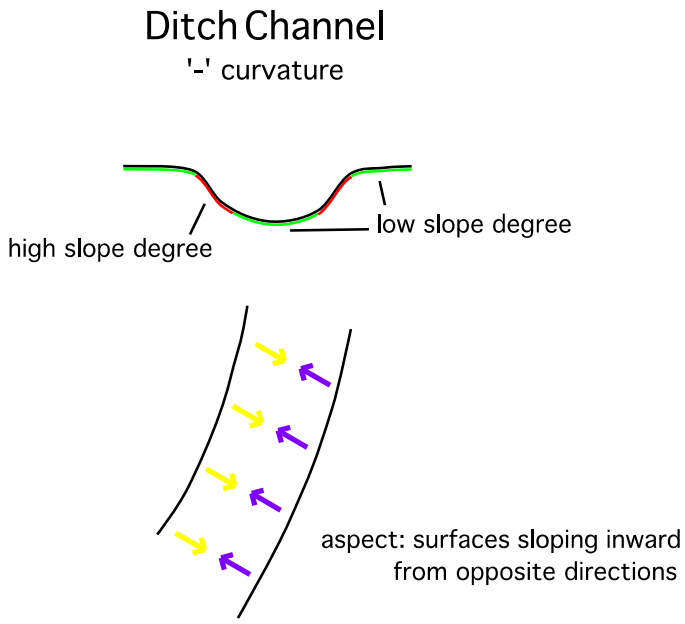

Figure 2. Ditched feature characteristics.

Semi-automated Feature Detection

A simple process within ArcGIS using reclassification tools was used in an attempt to define the fortification ditches. A manual examination of certain values found in cells characterized as features was compared to those on the surrounding landscape. For example, a greater range of slope severity on the sides of the ditches differs from the relatively flat topography of the adjacent cells. A reclassification of the raster dataset, which displays those cells that meet the criteria differently than those surrounding, should provide a decent visual representation that efficiently distinguishes those areas. Since the aspect displays the direction a surface faces, and all ranges will be represented in cells throughout the landscape, this characteristic is unlikely to provide useful results. For that reason, the degree of slope as well as curvature was used for this element of testing.

Three separate tests were completed to assess multiple results for different ranges of slope severity and curvature. By manually examining random cells within the ditches for each dataset, three distinct values were chosen for each test. Regarding slope severity, the ranges used were 3-15°, 5-15°, and 7-15°. For curvature, the three tests were >0, >3, and >5. Each case results in only two distinct values or classes. For slope this meant one for the targeted range of slope and one for anything that does not fall within that category, and for curvature one for anything less than the targeted value and one representing anything greater. If successfully integrated, the resulting map should define the ditch quite well, as the color of those cells representing the ditch will contrast with those surrounding that are not part of the feature.

If successful outputs result from the three separate slope and three separate curvature tests, they can be combined to more narrowly define the features, as only those cells that match both characteristics will be classified. This essentially means that up to nine additional tests can be done for each site by calculating the results from the previous outputs:

3-15° slope and >0 curvature;

3-15° slope and >3 curvature;

3-15° slope and >5 curvature;

5-15° slope and >0 curvature;

5-15° slope and >3 curvature;

5-15° slope and >5 curvature;

7-15° slope and >0 curvature;

7-15° slope and >3 curvature;

7-15° slope and >5 curvature.

Automated Extraction Algorithm

Representative tables were developed for each layer and the visual data converted into text files containing the geographic location for each cell and its assigned value based on certain attributes. They were then exported for further processing in this format and subsequently fed into the system for pattern analysis and extraction. NDSU computer science analysts Dr. Anne Denton and graduate student Shuhang Li processed the graphical data, or histogram, to determine which range or set of characteristics should be used for programming the algorithm. Although the data reads as a list to the human eye, the processing capabilities of the computer program depict an image and bases the subsequent analysis of the information off that perceived visual representation along with the association of a specific cell with others (Figure 3).

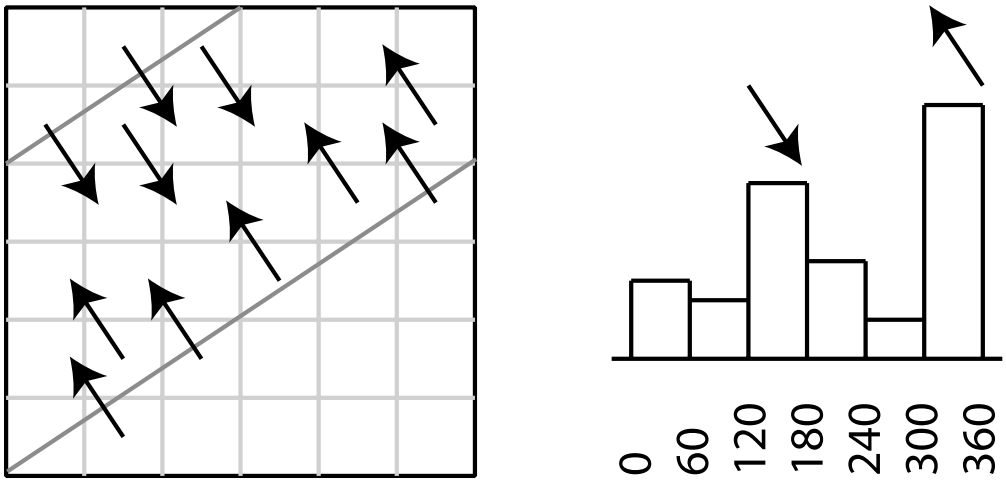

Figure 3. Example of output from aspect and resulting histogram. Arrows representative of surface direction on the slopes of ditch features.

This automated extraction process was completed with WEKA (Waikato Environment for Knowledge Analysis), a suite of machine learning and data mining algorithms used for analysis and predictive modeling through preprocessing, clustering, classification, and selection

of data (Witten et al. 1999). It is an open source program freely available on web-based applications that is coded and scripted in java. The statistical classification of features will be completed through a decision tree-based method, which means that a certain set of attribute criteria must be met to be identified as a specific feature type (Hastie et al. 2001). For this process, the characteristics and values used were slope severity, aspect, and curvature. Since the measurement for the angle of slope may be different from sample to sample, a different range and classification was used for each feature. For aspect, the entire 360 degree spectrum is here represented by eight individual categories in 45-degree increments; 0-45°, 45-90°, 90-135°, 135-180°, 180-225°, 225-270°, 270-315°, and 315-360°. Curvature was characterized into five sequences that ranged in value of severity from less than (-20), (-20) to (-5), (-5) to 5, 5 to 20, and greater than 20. Selection of those cells deemed acceptable as probable features was made available through a text output and subsequently analyzed for accuracy.

Feature characterizations involve many cells, and within each cell multiple types of information. To accomplish this end, a moving window was used in varying sizes to train the data-mining program. As previously stated, a moving window classifies a cell based on a comparison between its own value and those values adjacent to it. Therefore, since the regional topography has relatively low relief, features were defined by the contrasting values of itself and the surrounding landscape. This process yielded a series of instances with an information grid for each data type, and in which the attributes were evaluated together based on their relevance to the classification process (Denton and Wu 2009; Denton et al. 2010; Alnemer et al. 2011). Because the programming of the algorithm was accomplished using only a limited number of features, this technique could provide additional windows of analysis as each instance and pattern of characteristics recorded was considered a feature based on the physical qualities in that

area (Figure 4). Therefore, we have many modes on which to base the algorithm, as multiple instances were recorded for each individual feature. This procedure may produce a problem, however, as the differences exhibited in each window of singular features may provide contrasting datasets and classifications. For example, the steep sides of ditches may pattern differently from the relatively flat bottomed center, and these qualities may affect the output. To mitigate this, it may be necessary to first cluster the windows and use a combination of the resulting patterns for classification (Dorr and Denton 2010). Furthermore, the areas along the arbitrary cutoffs defined by feature edges may not clearly represent a feature or its absence based on that window, which may provide an additional challenge (Denton et al. 2009; Denton 2009).

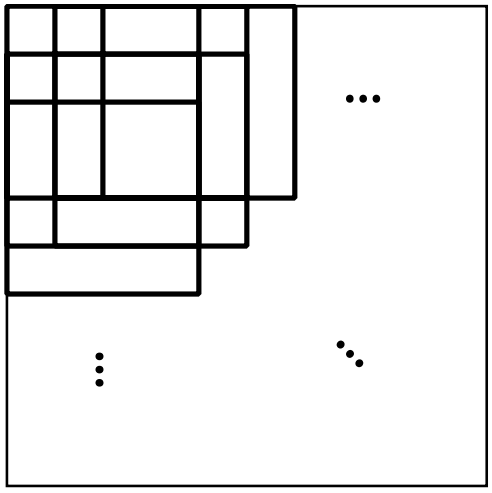

Figure 4. Example of six moving windows overlaying each other.

Training and testing of this method was accomplished using the six previously mentioned archaeological sites to identify similar patterns between the ditched features found at each. To test the efficiency of a computer learning system based on a set of known samples, a cross-validation method should be used to determine the accuracy (Hastie et al. 2001). In this instance,

this means that the system should be trained with five of the previously known sites, and tested on the other (Figure 5). In other words, individual tests were performed on each site with programming that was trained with the other five. If differences were revealed for the separate trials, the degree of accuracy was noted and assessed for each case to help determine inconsistencies between the data used for training. If irregularities were found to occur, this would assist in narrowing down the issues and mitigating the problem. However, if the algorithm performed properly in certain cases, averages were collected and results analyzed to conclude which characteristics best define features in this geographic region for the extraction program.

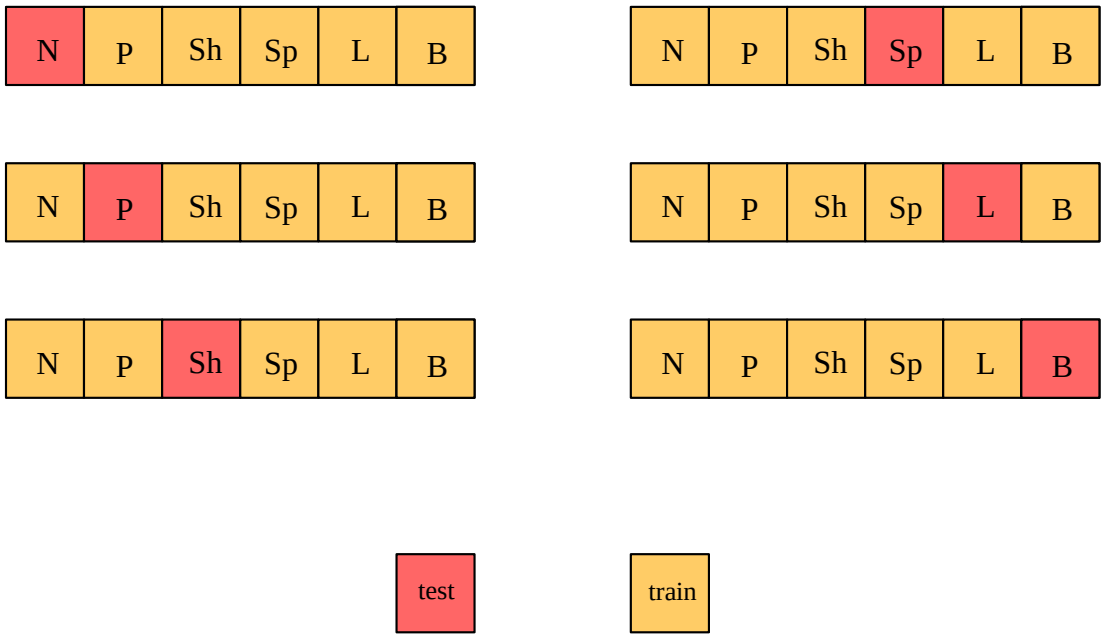

Figure 5. Illustration of cross-validation scheme used for training and testing of site data. (N, Nelson; P, Peterson; Sh, Shea; Sp, Sprunk; L, Lucas; and B, Biesterfeldt).

Visual Inspection and Output Analysis

As output was received from the various tests, the results were placed in a GIS to determine the amount of positively classified points that match the actual boundaries of the delineated feature in the lidar data. To do this, the output table was placed directly into a map document, and displayed as points based on their x and y coordinates. From there they could be immediately inspected to determine if the program functions as intended. If random points were scattered across the test landscape, it was clearly evident that the algorithm did not work as intended. If random points are scattered in clusters, it could be possible that the test worked correctly but picked up small drainages or other topographical features resembling a ditch or trench. In either case, if the ditch was not detected, issues likely occurred and solutions to remedy the problem were examined. However, if the output points roughly match the ditch boundaries, it was determined that a successful attempt to program the algorithm was found. Even in the presence of a substantial amount of false-positive results, whether clustered or not, an effective detection of the feature may signify that the system functioned as intended.

Quantitative analysis of the ratios for true-positive/false-positive results were used to assess the accuracy of the various methods and attributes used for testing. To determine how well the feature detection worked, a percentage was calculated through the number of true-positive cells from the output that match those that were classified as such through preprogramming. These were then compared against other factors, such as the quantity of false-positives, to conclude if any of these methods would produce viable results that can be efficiently used and successfully implemented for further research.

CHAPTER 4. LOCAL ENVIRONMENT AND CULTURES

Bend Region

The Maple and Sheyenne rivers represent the remnants of once prominent watershed systems that fed glacial Lake Agassiz during the ice retreat succeeding the last glacial maximum. The bend region is in the Drift Prairie of the Central Lowlands Physiographic Region (Bluemle 2000). The region contains features resulting from many years of glacial activity including gently rolling grasslands, low ridges and swales, as well as prairie pothole lakes and wetlands. Archaeologically, the area is in the Sheyenne River Study Unit as defined in the *North Dakota Comprehensive Plan for Historic Preservation: Archaeological Component* (SHSND 2008). The dominant landforms include the river floodplain valleys and terraces, old beach ridges, and upland plains.

The Sheyenne River valley was formed by glacial meltwater as it flowed southward, cutting a broad channel into the landscape. As the ice retreated during the terminal Pleistocene, the increased water flow traveled farther south and then eastward, cutting a deep trench as it drained into glacial Lake Agassiz. This area immediately to the east of the bend region is a large expanse of sandy and silty deposits called the Sheyenne Delta, located within the Red River Valley Physiographic Region (Bluemle 2000). It contains a complex topography of alluvial sediment deposits and wind-blown sand dunes with some small ponds present in areas of low relief. When water levels dropped and Lake Agassiz dried up after the glaciers receded, the Sheyenne River cut a trench through the delta and old lakebed, eventually entering what is now the Red River near present-day Fargo, North Dakota.

Soils in the area were formed under a variety of geomorphological factors including processes of glacial, fluvial, and eolian action. The vegetation in the area contains largely mixed prairie grasses and shrubs interspersed with low-lying marshes. Dominant trees in the wooded areas along the Sheyenne River valley include ash, elm, oak, and basswood trees. These locations provide adequate habitats and resources for fauna including white-tailed deer, foxes, coyotes, raccoons, rabbits, squirrels, wild turkey, grouse, pheasants, doves, migratory waterfowl, northern pike, perch, and freshwater mussels. Historically, herd animals such as bison, elk, and antelope would have used the area during their annual migrations (SHSND 2008).

Cultural Traditions

When Euro-Americans first encountered Mandan, Arikara, and Hidatsa groups along the Missouri River in the early 1800s, they were witnessing a traditional Plains Village culture that had existed in the area for the nearly a millennium. The impressive earthlodge villages that Lewis and Clark encountered on their famous expedition would become part of our knowledge of the American West and romanticized in popular literature. Little did people know at the time that the roots of the Plains Village peoples lay with Late Woodland groups who moved into the area in the first millennium AD (SHSND 2008).

Although nomadic groups had used the area since it was first colonized, it wasn't until those eastern groups moved in that a more sedentary lifestyle was adopted. With them they brought new technology including the bow and arrow as well as horticulture and pottery (SHSND 2008). This new lifestyle necessitated an obvious change in settlement patterns as groups remain sedentary to tend their gardens and increasingly utilized more permanent infrastructure. This does not mean less importance was placed on hunting and the gathering of

other resources, but only that as a less mobile lifestyle was adopted, there were many associated cultural implications. The locations of the sedentary sites needed to be situated proximal to major drainages as they provided fertile soil and ensured water availability throughout the growing season. Major river valleys also provided wooded areas suitable hunting grounds. By AD 1000, Plains Village proper was operating as an independent cultural tradition as numerous villages were being constructed along major waterways. These villages were typically made of permanent, earthlodge structures that were constructed of various sized timbers, with mud and sod packed into the top and sides to provide adequate shelter from the elements. A ditch would oftentimes be excavated around the perimeter of the community, which was sometimes accompanied by a wooden palisade. Additional features would include storage and cache pits, as well as large refuse middens.

Plains Village Indians can be separated into three groups: the Southern Plains Tradition in Oklahoma and parts of Kansas, the Central Plains Tradition in Kansas and Nebraska, and the Middle Missouri Tradition in South Dakota and North Dakota (Wood 1974). These groups existed fairly autonomously from each other for a couple hundred years, but by AD 1200, Central Plains groups, which are ancestral to the Arikara, began migrating north into the Middle Missouri territory (Bamforth 1994; Wood 1974). This merging of cultures would later be termed the Coalescent Tradition as it represented a cultural adaptation of multiple groups. During this time a separate cultural tradition was emerging on the plains to the east of the Missouri River, the Northeastern Plains Village (NEPV) complex (Toom 2004).

The NEPV complex (AD 1200-1800) is characterized by occupations primarily located on the James, Sheyenne and Maple Rivers in eastern North Dakota and, based off ceramic assemblages, likely originated from groups that occupied the upper reaches of the Minnesota

River Valley (Toom 2004). The sites of this complex are relatively smaller than their Middle Missouri counterparts but still contain similar features, such as ditched enclosures. Other sites relating to this cultural group are not fortified and likely represent seasonal camps used for hunting and other gathering activities. Based on similarities in ceramic style, Toom (2004) further argues that an NEPV group traveled farther west in the mid fifteenth century and settled on the Missouri River, culminating in the emergence of the Hidatsa Nation. However, other NEPV groups continued to occupy eastern North Dakota for several hundred more years.

The majority of the occupations for this study belong to a cultural tradition known as the Shea Phase, a sub-tradition of the greater NEPV complex (Michlovic 2008). Evidence found in southeastern North Dakota, primarily from the Shea and Sprunk sites along the Maple River, suggest an occupation with dates ranging between AD 1400 and 1600 (Michlovic and Schneider 1993; Michlovic and Holley 2009). Economic activities of the groups that occupied these enclosed village sites focused primarily on hunting bison and other small-to-medium sized game, the foraging of wild plant and marine resources, as well as limited domestic maize production (Michlovic et al. 2008). Although no house depressions can be seen at the surface, geophysical testing has revealed anomalies that likely represent domestic structures. The sites are relatively small and would have been seasonally occupied by no more than a hundred individuals, or several families (Holley et al. 2011).

Fortification Ditches

The frequency of these ditched occupations in North Dakota, especially those of the Middle Missouri Tradition, have been the subject of much analysis in plains archaeology. Their origins and uses have been the object of study and debates by numerous scholars.

Anthropologists have traditionally viewed extreme violence and high-casualty tribal warfare as a product of European contact and the influence it had on indigenous cultures. However, some researchers have attributed the rise in violent warfare between tribal groups in pre-contact settings as an ecological product of changing environmental conditions and external group conflicts (Bamforth 1994). A wealth of evidence for pre-contact warfare exists on the northern plains after the arrival of Central Plains groups from the south beginning around AD 1300. During this time, Middle Missouri occupations exhibited changes that include an increase in community size as well as the construction of defensive works around the site perimeter. These fortified boundaries typically consisted of ditches (Figure 6), several meters deep and wide, that were typically backed by a wooden palisade. These villages were often situated along the steep banks of river floodplains, providing an additional tactical advantage against potential aggressors. Environmental changes occurring during this time created less than ideal conditions for their agricultural economies, stressing the relationship between the encroaching groups and resulting in violent undertakings between them. European contact may have augmented inter-tribal violence during those times, as continued westward advancement constantly displaced indigenous populations, and conflicts arose when groups came into contact with one another. While warfare was increasingly common for post-contact societies, such violence was hardly the product of European influence alone. The prevalence of these ditched sites in the region make for ideal case studies to test the effectiveness of the techniques.

Figure 6. Photograph of ditched feature at Double Ditch site (32BL8).

Another important facet of cultural properties that these types of features represent is a transition to a more sedentary lifestyle. The amount of time and planning it takes to organize such an effort to remove large quantities of earth from the ground is not conducive to a hasty operation. The labor it would take to accomplish that feat would take a significant amount of hours to successfully complete. These efforts would not be made for a temporary occupation and would only be undertaken if they were planning to reside in the area for a significant amount of time, or return to it periodically for seasonal occupations.

Test Sites

A group of local sites in this area that exhibit similar features and characteristics were chosen for this study. The ditched occupations themselves lie on elevated benches above the river valleys and overlook these well-watered and forested areas, which were most likely chosen for their resource availability. Six sites located within this relatively confined geographic region were selected for analysis. The majority of the sites likely represent occupations of the Shea

Phase. However, additional groups in the area had influence as the Biesterfeldt and Lucas site suggest other cultural affiliations.

The following pages provide only a brief summary of the characteristics, classification, and related information for each site in order to provide cultural and historical context. It should be noted, however, that this study is not related to further understanding any of those variables, but examines instead on the development and preliminary testing of a computational or computationally assisted system for locating such sites from remotely sensed data. That system focuses on one specific structural feature that is common at late prehistoric sites in the central and eastern Northern Great Plains, a large defensive ditch.

Shea Site (32CS101)

The Shea site consists of a well-defined, ditched enclosure on an eastern bluff overlooking the Maple River floodplain. Excavations were carried out over a period of five field seasons in the late 1980s. That work was carried out within the village, across the exterior ditch and an interior ditch, near the bluff edges, and just outside the village's outer defensive ditch (Michlovic and Schneider 1993). Evidence collected at the site, together with data from other sites, led Michlovic (2008) to define the Shea Phase as a sub-component of the NEPV tradition.

Materials recovered from site excavations indicate a dual subsistence economy based on hunting/gathering and horticulture. Evidence of bison and other small game hunting was found and additional floral resource use and domestic maize production was noted (Schneider 2002). Though several postholes were identified within the ditch, no patterns could be discerned and no permanent structures were recorded. Additional postholes in linear arrangements immediately interior to the ditch suggest a palisade may have been constructed in conjunction with it.

Perhaps the most notable feature was the discovery of a second, interior ditch that has been almost completely filled in. This piece of information, as well as the intermittent stratigraphic artifact deposits documented during the investigations, suggest it was periodically occupied over a number of years. Charcoal samples from six sources suggest an occupation range between AD 1400 and 1642 (Michlovic and Schneider 1993:124). Although it is possible that separate components may be represented at this site, it is extremely likely that it was revisited by the same group throughout the year depending on seasonal fluctuations and availability of resources. The more prominent ditch at Shea measures three to five meters in width and up to one meter in depth (Michlovic and Holley 2009:22).

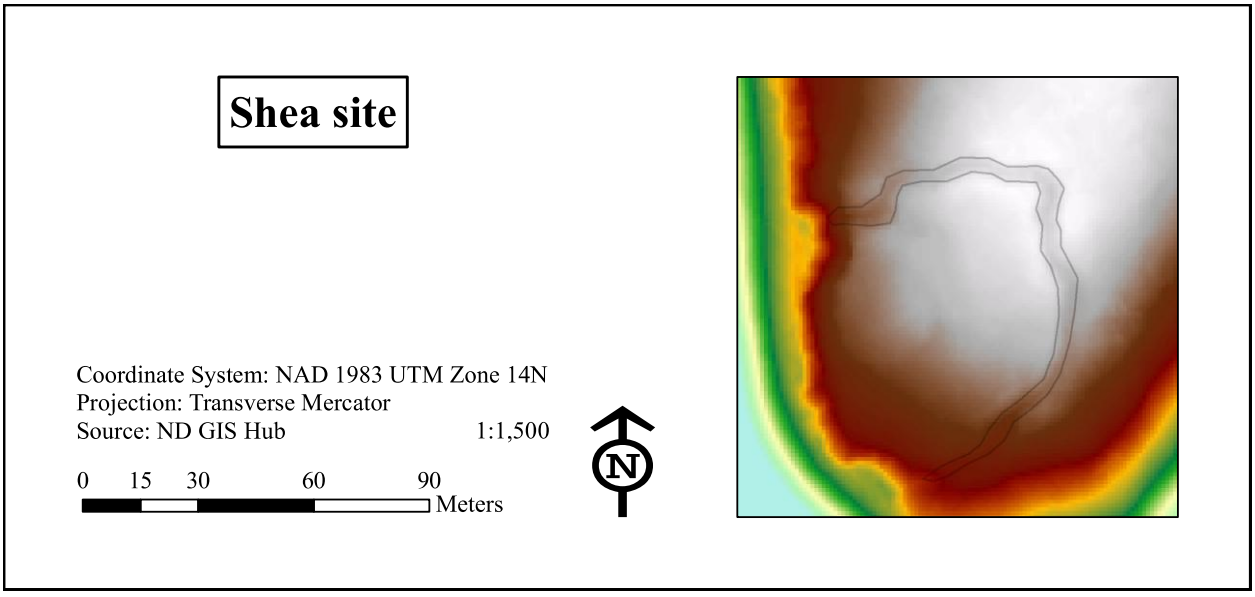

Figure 7. DEM of ditched feature at the Shea site (32CS101). Darker spots in gray area represent the depressions. Edge of river bluff is to the west.

Sprunk Site (32CS4478)

The Sprunk site represents an enclosed, late prehistoric settlement that is situated approximately five kilometers southwest of Shea on a bluff overlooking the Maple River

floodplain (Michlovic and Holley 2009). Evidence from fieldwork during 2004 and 2006 indicate semi-sedentary residency with a mixed subsistence based on bison, small game, waterfowl, and river clams with maize and wild plants supplementing their diet. Two radiocarbon dates suggest an occupation dating between AD 1400 and 1500 (Michlovic and Holley 2009:25). Geophysical surveys revealed several subsurface anomalies that, based on the compacted properties of the soil, possibly represent living surfaces. A single post remnant and a few potential posthole stains were recorded but evidence for permanent structures was not entirely confirmed. Two likely associated and presumed burial mounds are located proximal to the site but not within the boundaries of the fortification. The similarity between the assemblages at Sprunk and Shea suggest that Sprunk also belongs to the Shea Phase of the NEPV tradition (Michlovic 2008). The ditch at the Sprunk site measures two meters in width and only a half-meter in depth (Michlovic and Schneider 1988:6).

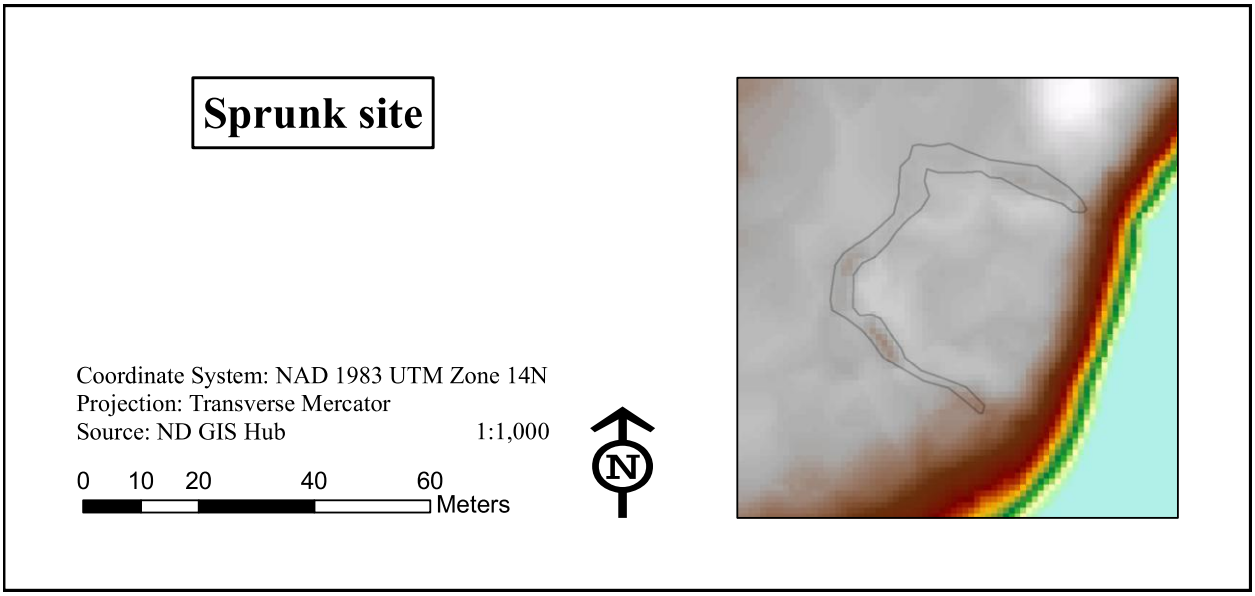

Figure 8. DEM of ditched feature at the Sprunk site (32CS4478). Darker spots in gray area represent the depressions. Edge of river bluff is to the east.

Biesterfeldt Site (32RM1)

First described and mapped during the late 19th and early 20th centuries, excavated by Strong (1940), reported on by Wood (1971), and tested during 2007 and 2008 by archaeological field schools (Holley et al. 2011), this site represents a fortified village on a terrace above an abandoned meander of the Sheyenne River. Containing at least 62 depressions from former earthlodges ranging mostly from four to nine meters, this site was enclosed with a fortification ditch surrounding the perimeter. Other features present include a number of storage pits located throughout the site. As an 18th century, proto-historical occupation, this site contains both traditional Native American artifacts and those produced from Europeans goods: several metal projectile points from the site display evidence of rudimentary manufacturing techniques, suggesting the occupants may have been crafting the artifacts from trade wares. Noted in previous reports, there were indications that catastrophic burning may have destroyed the village, lending credence to the idea of violence and warfare being associated with ditched fortifications. There is evidence of a previous occupation on a buried surface between AD 1200 and 1600 but not enough work has been completed to determine its extent or narrow the timeframe (Holley et al. 2011:42). Damage to the southern portion of the site occurred as it was plowed into agricultural land, making it difficult to discern features at the surface in those areas. However, geophysical surveys completed during 2007 and 2008 revealed subsurface anomalies, and subsequent test excavations performed in 2008 exposed intact living surfaces below the plow zone. Being the only instance of this village type with pronounced depressions in Eastern North Dakota, researchers believe it represents the transition of the Minnesota Cheyenne as they moved across the plains and away from European encroachment (Holley et al. 2011). However, its similarity with the many fortified villages in the Middle Missouri cultural complex must be noted

and may well represent one of those groups occupying the area. In a cross-section from Strong's original excavation, the ditch at the Biesterfeldt site measured between three and four meters wide and about one meter deep (Wood 1971:9).

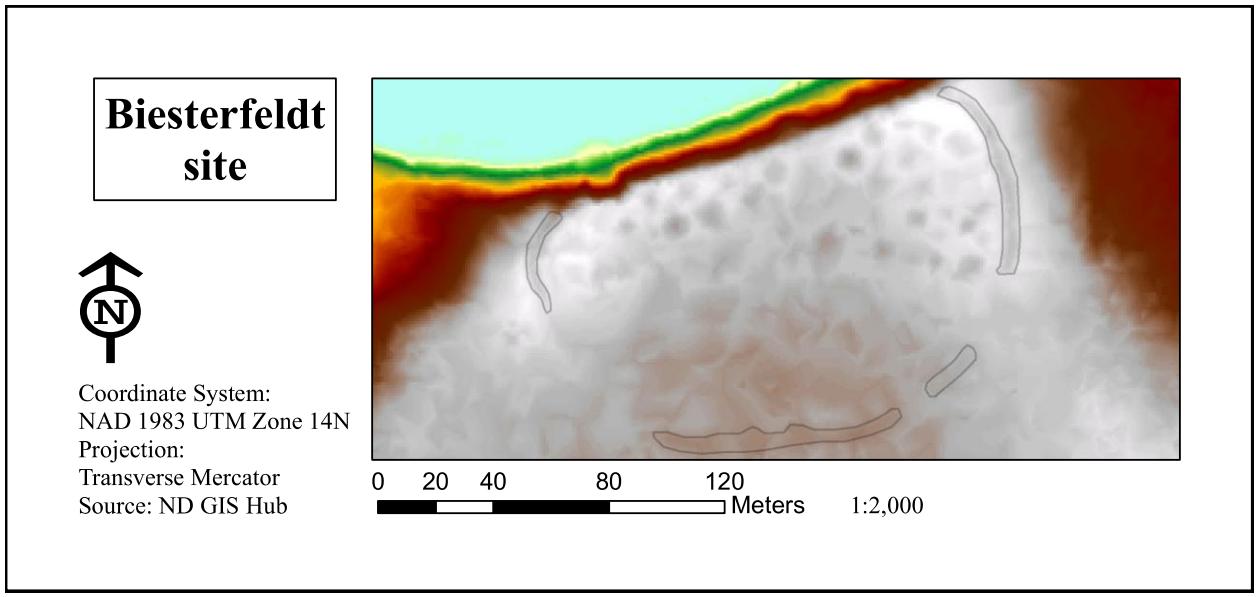

Figure 9. DEM of ditched feature at the Biesterfeldt site (32RM1). Darker spots in gray area represent the depressions. Edge of river bluff is to the north.

Lucas Site (32RM225)

The Lucas site consists of a ditched enclosure with an associated mound cluster in close proximity. It is situated on a southern bluff of the Sheyenne River that overlooks its floodplain. In 1989, a team of archaeologists from Minnesota State University Moorhead carried out test excavations placed both inside and outside of the enclosure, as well as in the ditch itself (Holley and Kalinowski 2008). Although only a limited material assemblage was recovered, the presence of prehistoric ceramics clarifies its association with a Late Woodland culture. The ditch is ovoid in shape and is unique from the other sites discussed in that it is completely enclosed and does not contain refuse debris within the enclosure. An additional feature that

separates it from the others is that spoil removed during the original ditch excavation was placed on the exterior perimeter as a form of embankment. The other examples have spoil placed on the interior edge of the trench and refuse has accumulated within the ditch. These characteristics, as well as its association with a number of nearby mounds, and more notably a set of linear mounds proximal to the enclosure's eastern edge, suggest that it may have been used for ceremonial purposes rather than a residential site. The properties that this site exhibits reduce the probability of its association with the others used for this study and from ceramic analysis it seems to have been occupied at an earlier date, between AD 900-1200 (Holley and Kalinowski 2008:11). The circular ditch at the Lucas site was excavated 85 centimeters below surface and since then, approximately 35 centimeters of sediment has been deposited setting the current depth at about a half-meter (Holley and Kalinowski 2008:2).

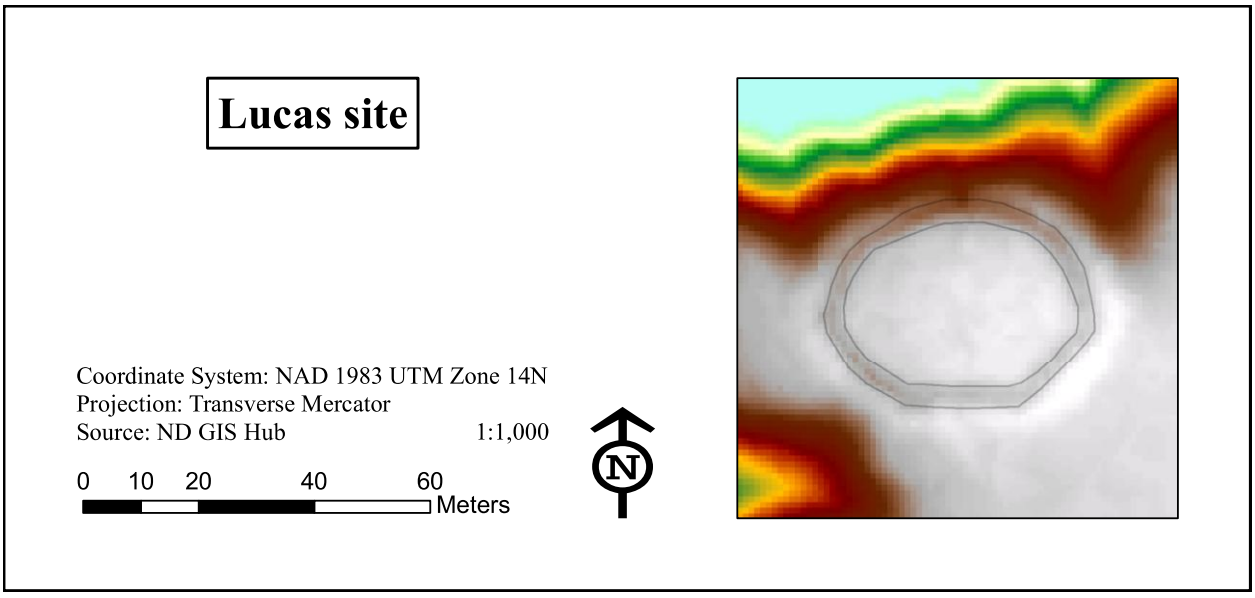

Figure 10. DEM of ditched feature at the Lucas site (32RM225). Darker spots in gray area represent the depressions. Edge of river bluff is to the north.

Peterson Site (32RM401)

The Peterson site is situated west of the Sheyenne River, on a bluff that overlooks the valley floodplain. An ephemeral drainage is located to its north and the site consists of a prehistoric occupation enclosed by a fortification ditch. Although the remains of permanent structures were not found, test excavations carried out there revealed a semi-sedentary lifestyle based on bison hunting and limited maize production, coupled with the supplementary resource acquisition of small game, waterfowl, and river mussels (Michlovic 2008). Several units were placed within the enclosure and one in the ditch. Materials recovered from the site include bone, shell, lithics, and ceramics. An eagle-trapping pit (32RM164) is located directly to the east of the site and is presumed to be associated with the same occupants at that time. Nothing was radiometrically dated from the site but the artifact and feature styles suggest it belongs to the Shea Phase and was occupied sometime around AD 1450 (Michlovic 2008:13).

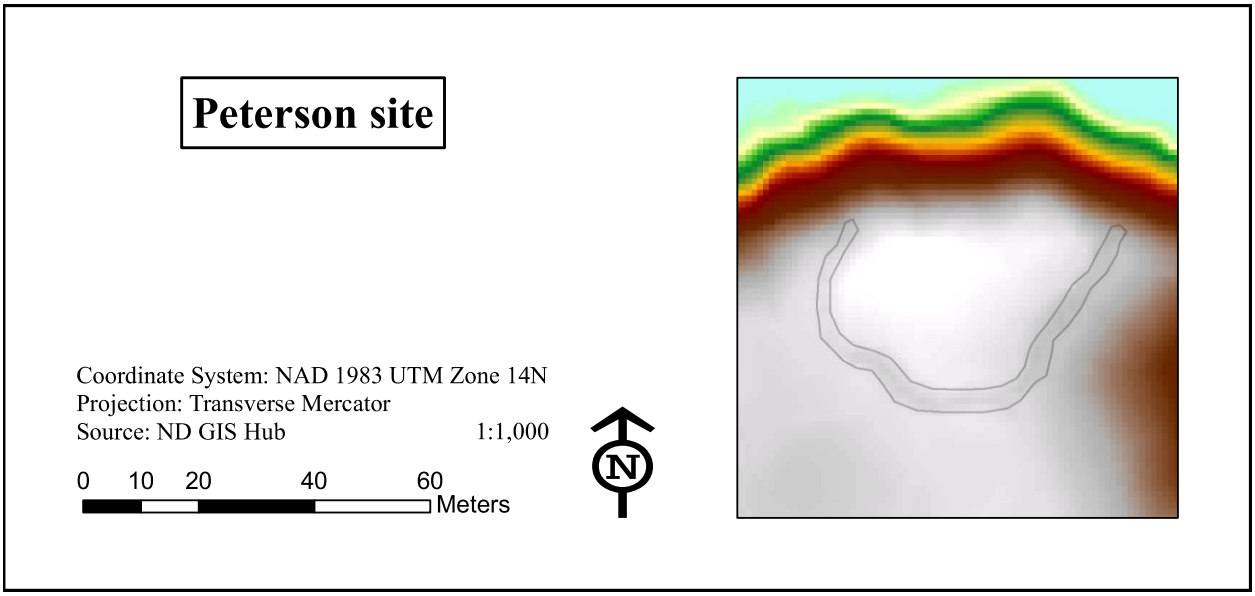

Figure 11. DEM of ditched feature at the Peterson site (32RM401). Darker spots in gray area represent the depressions. Edge of river bluff is to the north.

Nelson Site (32RM402)

The Nelson site is located only a quarter mile away from the Peterson site and like it, contains a fortified ditch enclosure of the same approximate dimensions. Situated between a nearby drainage and overlooking the Sheyenne River Valley, its similarity in style and proximity suggest it is related to the Peterson site, although excavations have not been carried out to confirm this (Michlovic 2008). Unfortunately, the absence of landowner permissions has hindered further work at the site beyond simple classification of the earthworks. Additional features located between the two sites include a pair of mounds (32RM165), presumed to have been used by occupants from both sites for burial purposes. Again, no subsurface testing has been undertaken and the overall information known about the site is fairly limited.

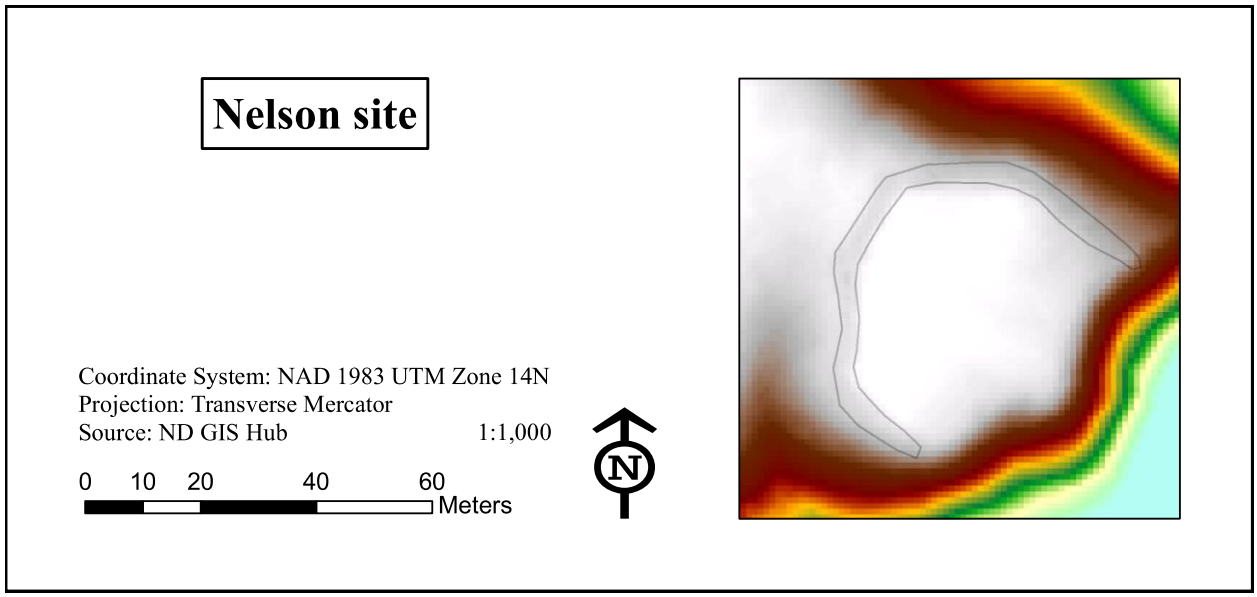

Figure 12. DEM of ditched feature at the Nelson site (32RM402). Darker spots in gray area represent the depressions. Edge of river bluff is to the east.

Summary

In summary, this chapter briefly describes the local cultural traditions and sites used in this study. The majority of these sites including Shea, Sprunk, Peterson, and Nelson, belong to the Shea Phase sub-tradition of the greater NEPV complex (Michlovic 2008). The Lucas site likely represents an earlier occupation, as artifacts recovered as well as differences in the ditch do not match traditions found at the other sites and is likely affiliated with Late Woodland cultures (Holley and Kalinowski 2008). The Biesterfeldt site, containing well-defined earthlodge depressions, as well as a different material assemblage including metal artifacts, represents a post-contact coalescent site that was used some time after those of the aforementioned Shea Phase, although an earlier occupation may be related (Holley et al. 2011). Additionally, it must be noted that the ditched enclosures found at each one of these sites are very similar to the enclosed village occupations found on the Missouri River. Although smaller in size, they represent comparable occupations in that they were used at relatively the same times, and economic activities and artifact styles are somewhat comparable. As such, contact between these groups was likely, especially considering the limited distance between them.

The average size of these ditches in their current state seems to be around three meters wide and up to one or two meters deep (Michlovic 2008). Although there are minor differences between features from the separate sites, the general shape and profiles of these ditches should provide enough similarity for the purposes of this study. Using the methods put forth in the previous chapters, an attempt will be made to classify the unique properties that make up the ditches at these sites, and identify other areas where similar cultural features can be found. If a successful utility can be developed and subsequently applied to a wider range of data, additional sites could potentially be discovered and in turn increase our understanding of the past.

CHAPTER 5. RESULTS AND DISCUSSION

Visualization Results

Separate data frames were created under each site for eight separate visualization techniques: DEM, DEM with hillshade, DEM with multi-directional hillshade, slope severity, directional aspect, curvature profile, constrained color shading, and Local Relief Model (Figures 13-18). To better compare them against each other, they are all represented on a black and white grayscale. Although this will be a subjective comparison, it becomes quite obvious which techniques better define the features. Later on in the discussion section of this chapter, an attempt is made to rank the separate layers by their ability to display the information in better detail and sharper contrasts. At the very least, a short list of the top visualization techniques is provided that seem to best reflect the distinction between the ditched features and the surrounding landscape.

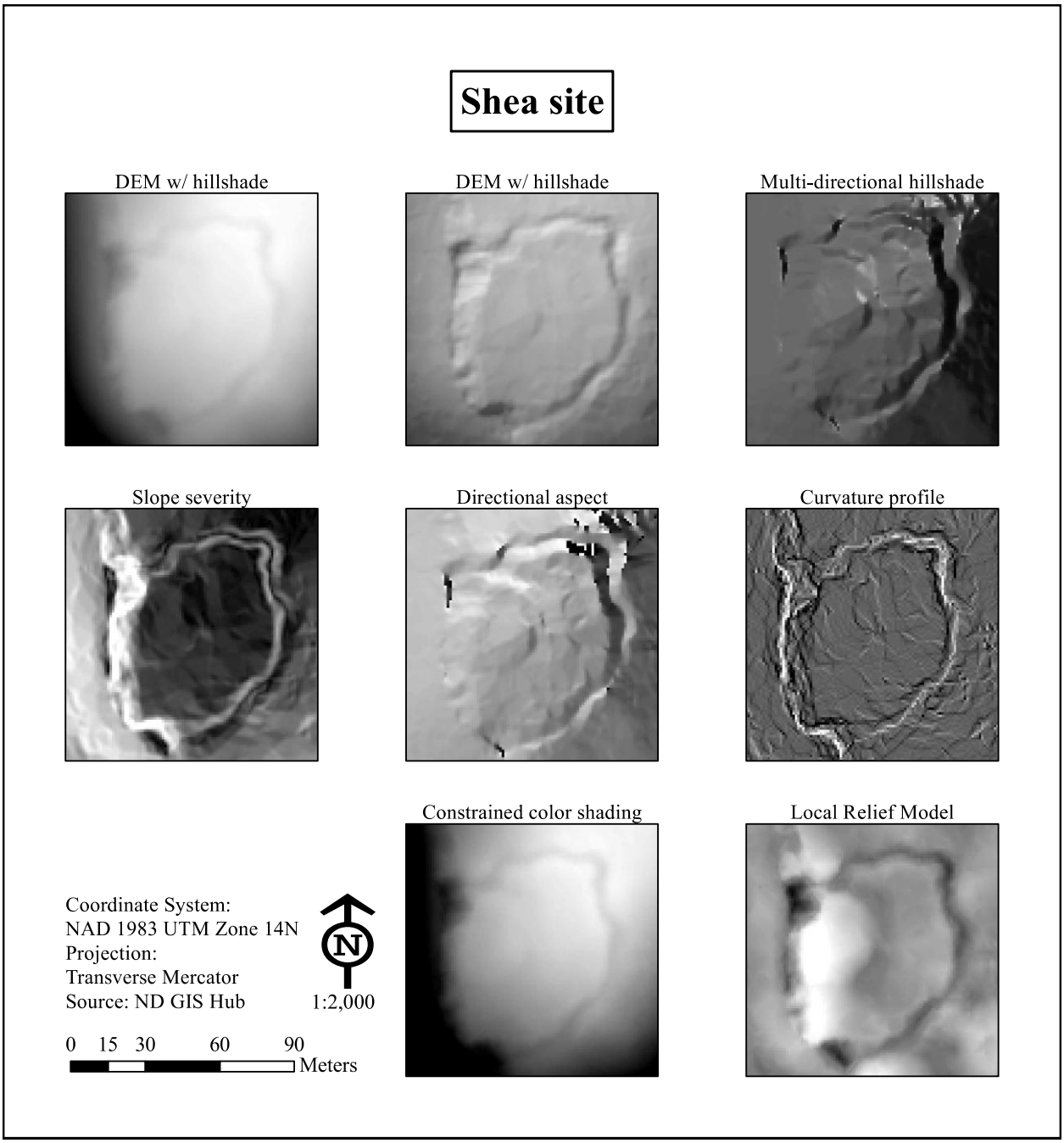

Figure 13. Visualizations of ditched feature at the Shea site.

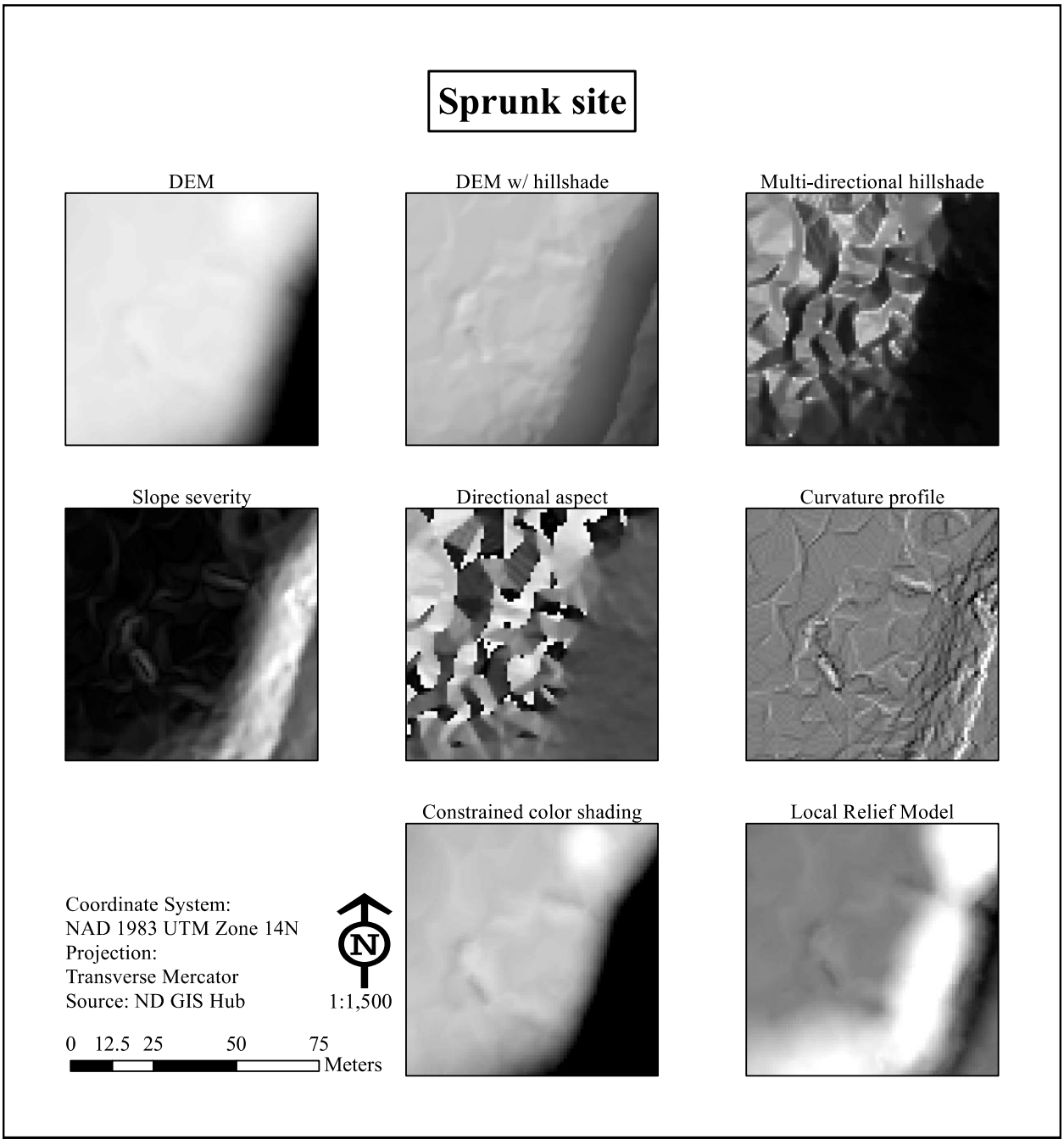

Figure 14. Visualizations of ditched feature at the Sprunk site.

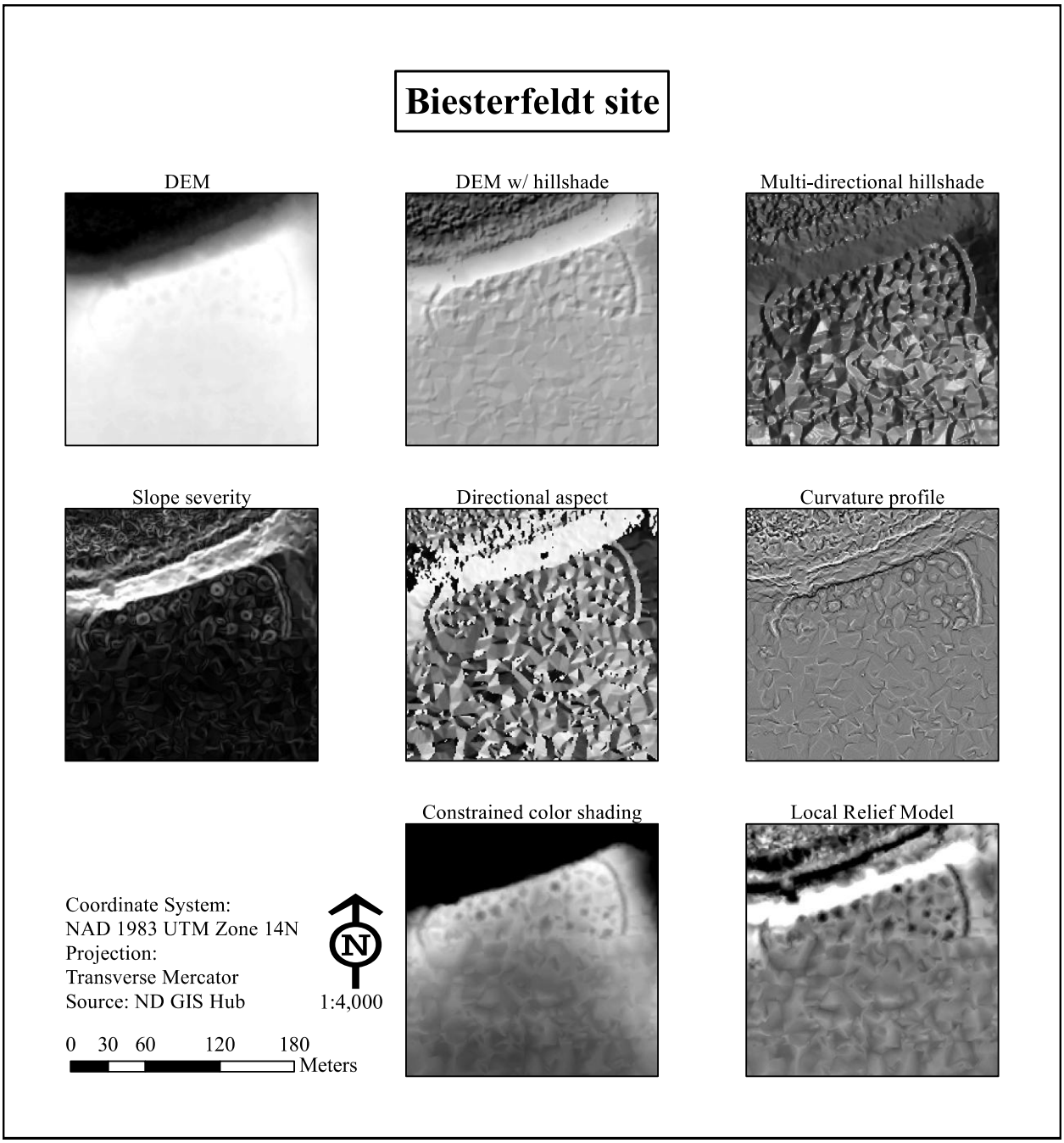

Figure 15. Visualizations of ditched feature at the Biesterfeldt site.

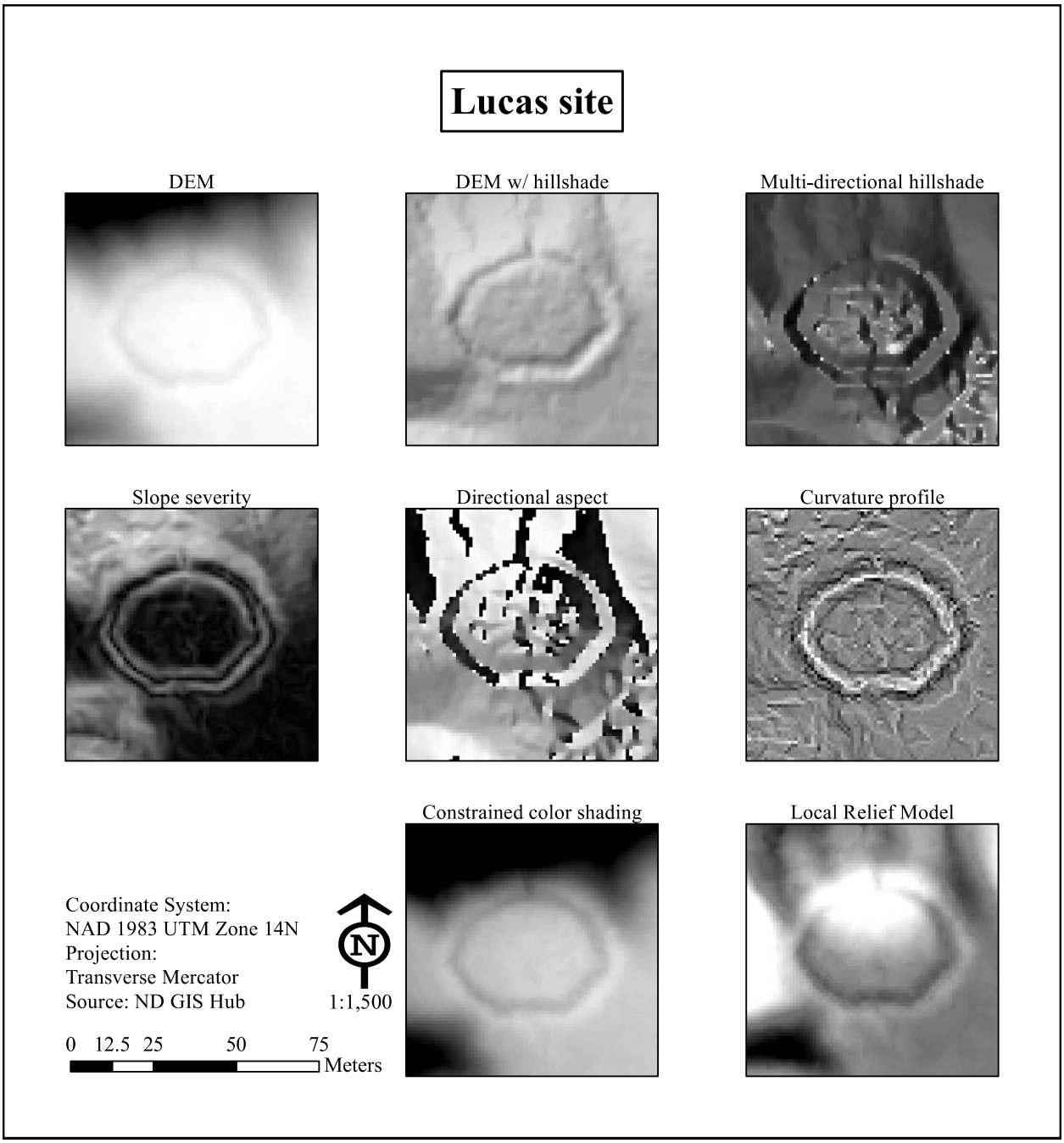

Figure 16. Visualizations of ditched feature at the Lucas site.

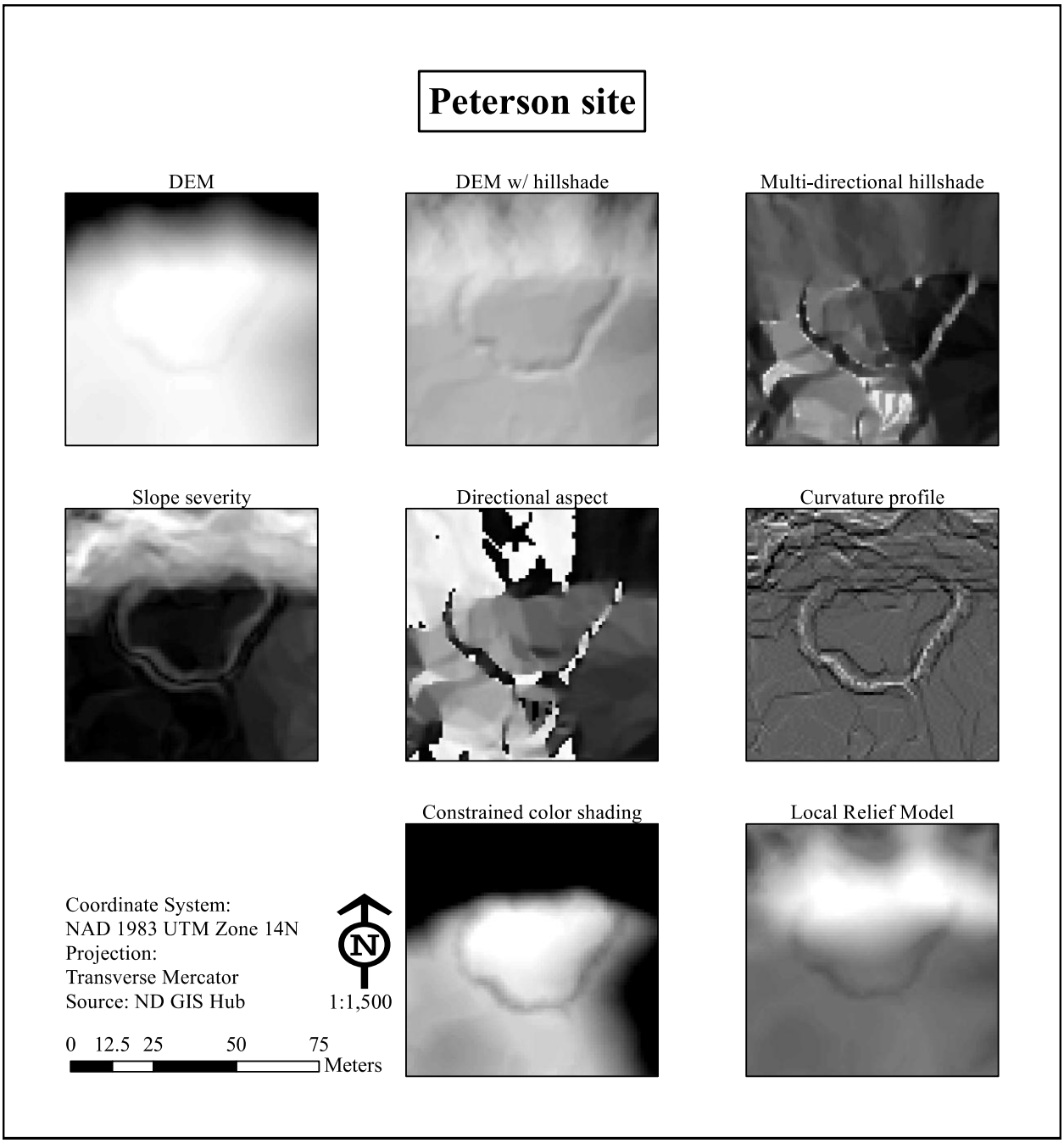

Figure 17. Visualizations of ditched feature at the Peterson site.

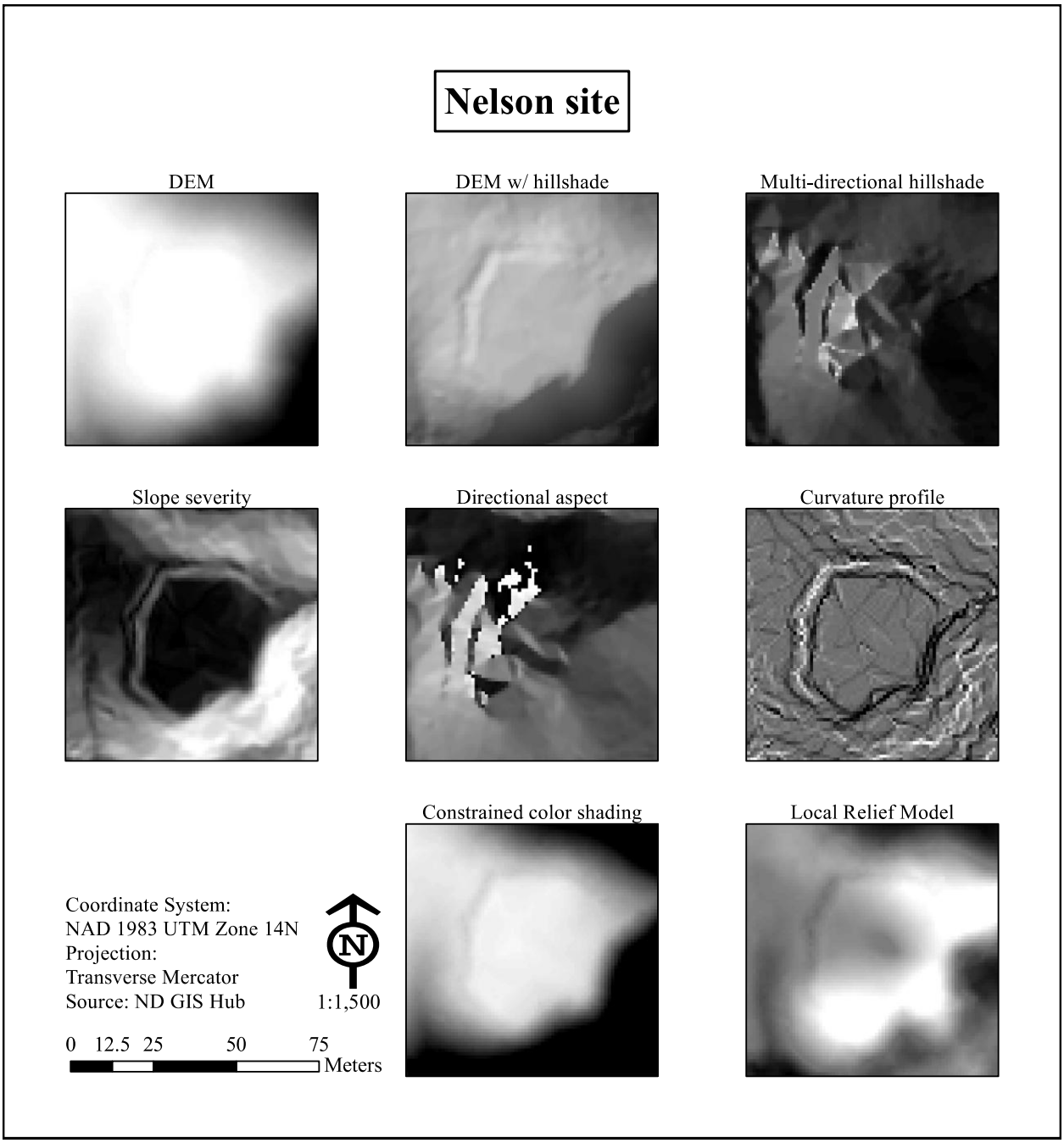

Figure 18. Visualizations of ditched feature at the Nelson site.

Semi-automated Detection Results

The results for the slope and curvature reclassification are displayed here for each site as a simple raster map with two separate colors; purple for the targeted data that attempts to classify the ditch, and gray for everything else in the surrounding landscape that does not fall within the classification range. For example, slope in the 3-15°, 5-15°, or 7°-15° range, curvature that is greater than 0, 3, or 5, or some combination of the two, are displayed as purple cells while everything that falls outside of those parameters is colored gray. A light blue, transparent overlay of the manually defined ditch cells provides a quick guide to visualize how many cells were matched, which can be seen as a darker shade of blue where they overlap.

Figures 19-36 depict the slope, curvature, and combined slope/curavature results for the Shea site (Figures 19-21), Sprunk site (Figures 22-24), Biesterfeldt site (Figures 25-27), Lucas site (Figures 28-30), Peterson site (31-33), and Nelson site (Figure 34-36). Additionally, each data frame within the maps has separate tables displaying the number of true-positive, false-negative, false-positive, and true-negative, as well as the true-positive/false-positive ratios in the form of percentages. In each case, a greater number of true-positive and less false-positive will yield more accurate results.

Shea site

Slope 3-15°	TP/TF	FN/TF	FP/NF	TN/NF
Result	579/643	64/643	30107/48477	18370/48477
Percentage	90	10	62.1	37.9

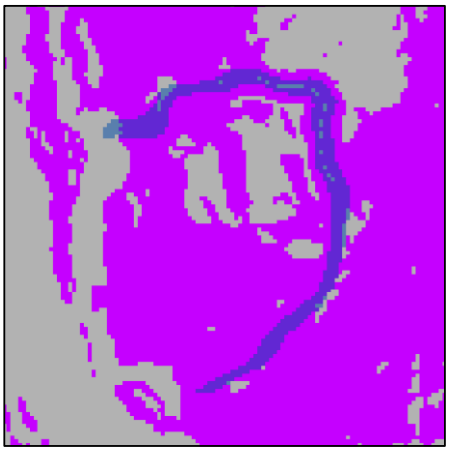

Slope 5-15°	TP/TF	FN/TF	FP/NF	TN/NF
Result	482/643	161/643	24181/48477	24296/48477
Percentage	75	25	49.9	50.1

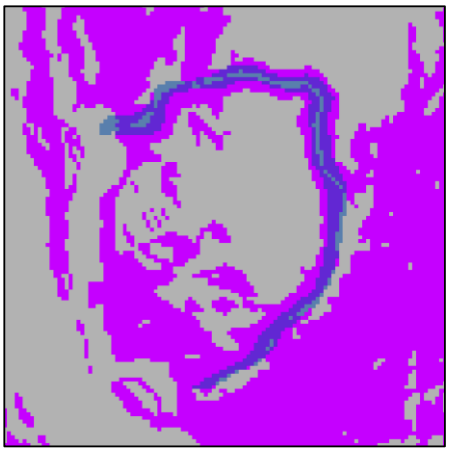

Slope 7-15°	TP/TF	FN/TF	FP/NF	TN/NF
Result	344/643	299/643	13738/48477	34739/48477
Percentage	53.5	46.5	28.3	71.7

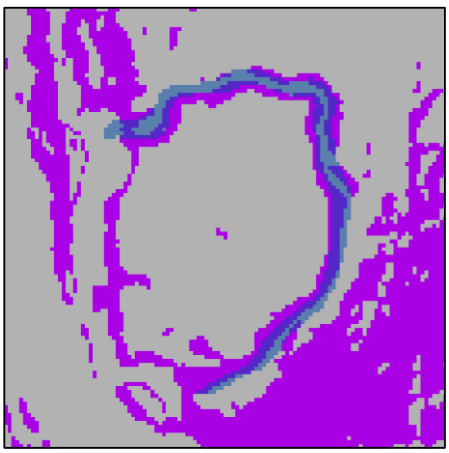

Coordinate System: NAD 1983 UTM Zone 14N
Projection: Transverse Mercator
Source: ND GIS Hub 1:1,500

0 15 30 60 90
Meters

N

Figure 19. Slope reclassification for the Shea site.

Shea site

Curvature >0	TP/TF	FN/TF	FP/NF	TN/NF
Result	460/643	183/643	22718/48477	25759/48477
Percentage	71.5	28.5	46.9	53.1

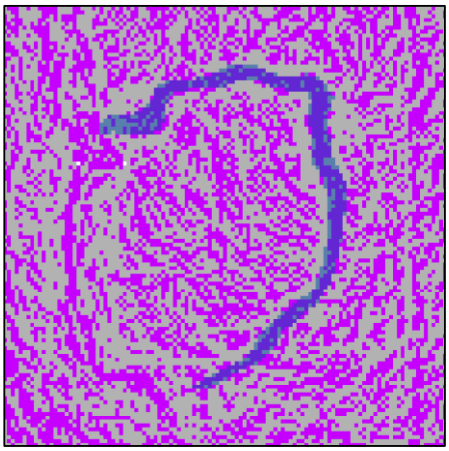

Curvature >3	TP/TF	FN/TF	FP/NF	TN/NF
Result	322/643	321/643	5026/48477	43451/48477
Percentage	50.1	49.9	10.4	89.6

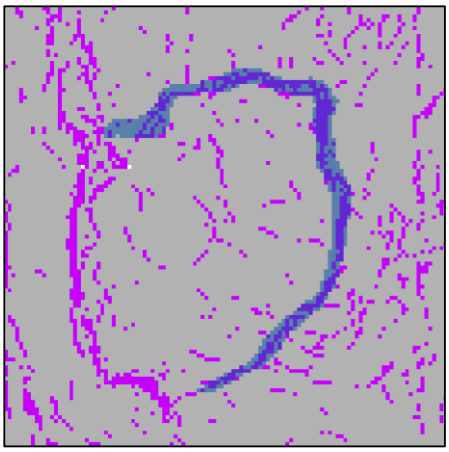

Curvature >5	TP/TF	FN/TF	FP/NF	TN/NF
Result	256/643	387/643	2782/48477	45695/48477
Percentage	39.8	60.2	5.7	94.3

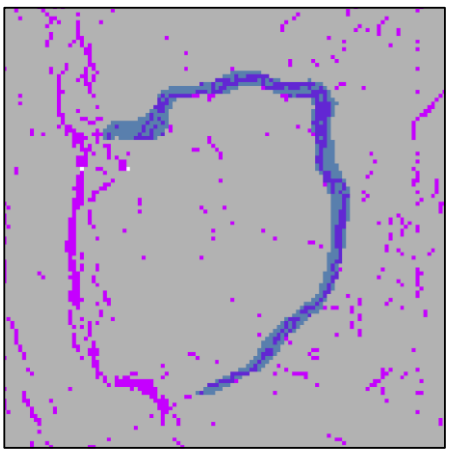

Coordinate System: NAD 1983 UTM Zone 14N
Projection: Transverse Mercator
Source: ND GIS Hub 1:1,500

0 15 30 60 90
Meters

Figure 20. Curvature reclassification for the Shea site.

Shea site

S(3-15°)C(>0)	TP/TF	FN/TF	FP/NF	TN/NF
Result	418/643	225/643	14181/48477	34296/48477
Percentage	65	35	29.3	70.7

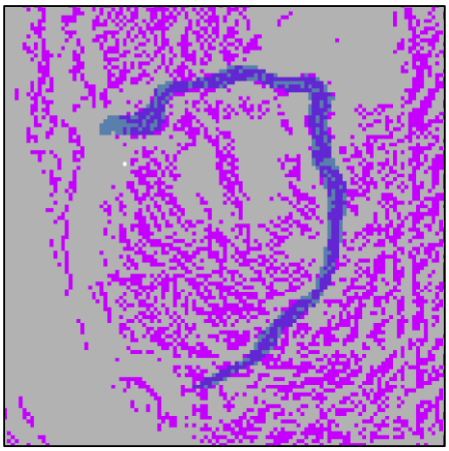

S(3-15°)C(>3)	TP/TF	FN/TF	FP/NF	TN/NF
Result	294/643	349/643	3253/48477	45224/48477
Percentage	45.7	54.3	6.7	93.3

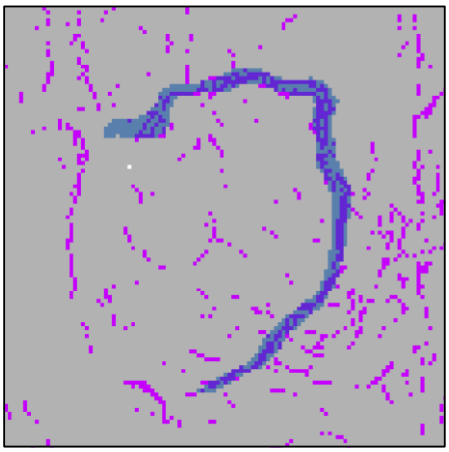

S(3-15°)C(>5)	TP/TF	FN/TF	FP/NF	TN/NF
Result	234/643	409/643	1858/48477	46619/48477
Percentage	36.4	63.6	3.8	96.2

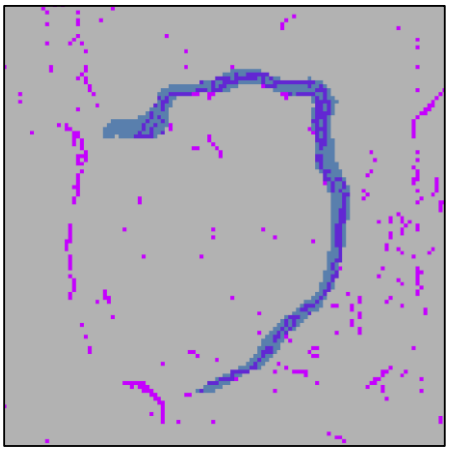

Coordinate System: NAD 1983 UTM Zone 14N
Projection: Transverse Mercator
Source: ND GIS Hub 1:1,500

0 15 30 60 90
Meters

N

Figure 21. Combined slope/curvature reclassification for the Shea site.

Shea site

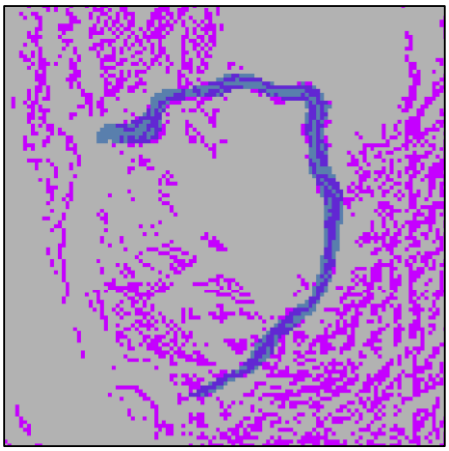

S(5-15°)C(>0)	TP/TF	FN/TF	FP/NF	TN/NF
Result	342/643	301/643	11449/48477	37028/48477
Percentage	53.2	46.8	23.6	76.4

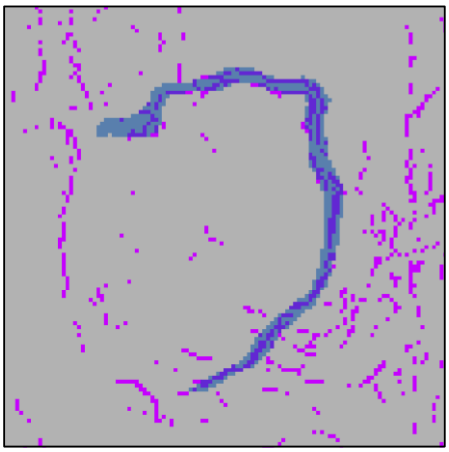

S(5-15°)C(>3)	TP/TF	FN/TF	FP/NF	TN/NF
Result	240/643	403/643	2787/48477	45690/48477
Percentage	37.3	62.7	5.7	94.3

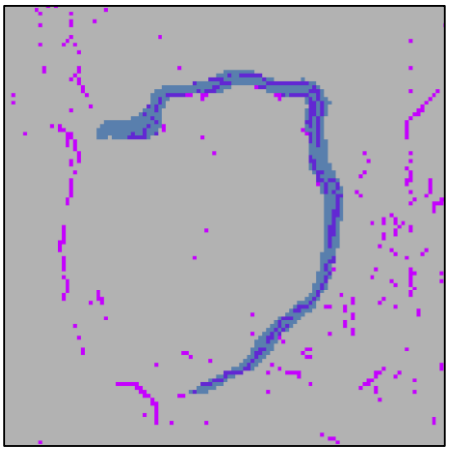

S(5-15°)C(>5)	TP/TF	FN/TF	FP/NF	TN/NF
Result	190/643	453/643	1624/48477	46853/48477
Percentage	29.6	70.4	3.4	96.6

Coordinate System: NAD 1983 UTM Zone 14N
Projection: Transverse Mercator
Source: ND GIS Hub 1:1,500

0 15 30 60 90
Meters

N

Figure 21. Combined slope/curvature reclassification for the Shea site (continued).

Shea site

S(7-15°)C(>0)	TP/TF	FN/TF	FP/NF	TN/NF
Result	228/643	415/643	6447/48477	42030/48477
Percentage	35.5	64.5	13.3	86.7

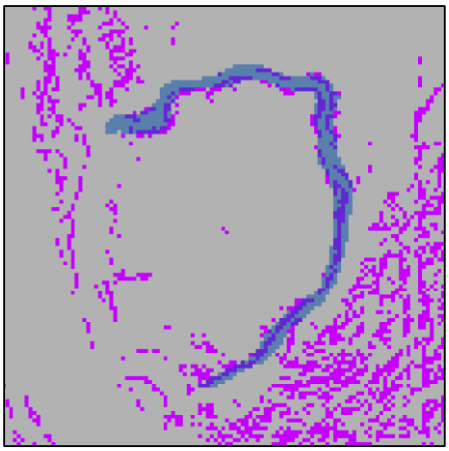

S(7-15°)C(>3)	TP/TF	FN/TF	FP/NF	TN/NF
Result	156/643	487/643	2052/48477	46425/48477
Percentage	24.3	75.7	4.2	95.8

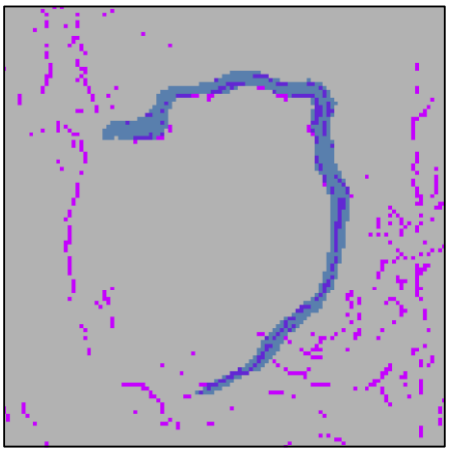

S(7-15°)C(>5)	TP/TF	FN/TF	FP/NF	TN/NF
Result	123/643	520/643	1292/48477	47185/48477
Percentage	19.1	80.9	2.7	97.3

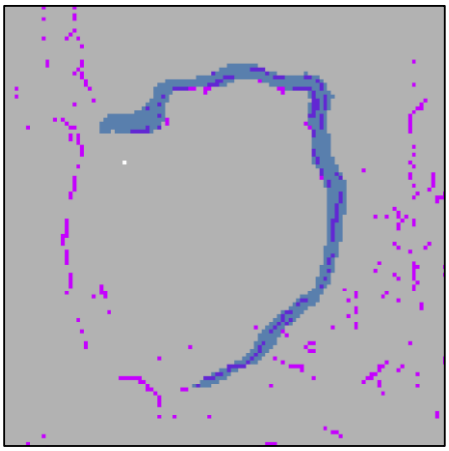

Coordinate System: NAD 1983 UTM Zone 14N
Projection: Transverse Mercator
Source: ND GIS Hub 1:1,500

0 15 30 60 90
Meters

N

Figure 21. Combined slope/curvature reclassification for the Shea site (continued).

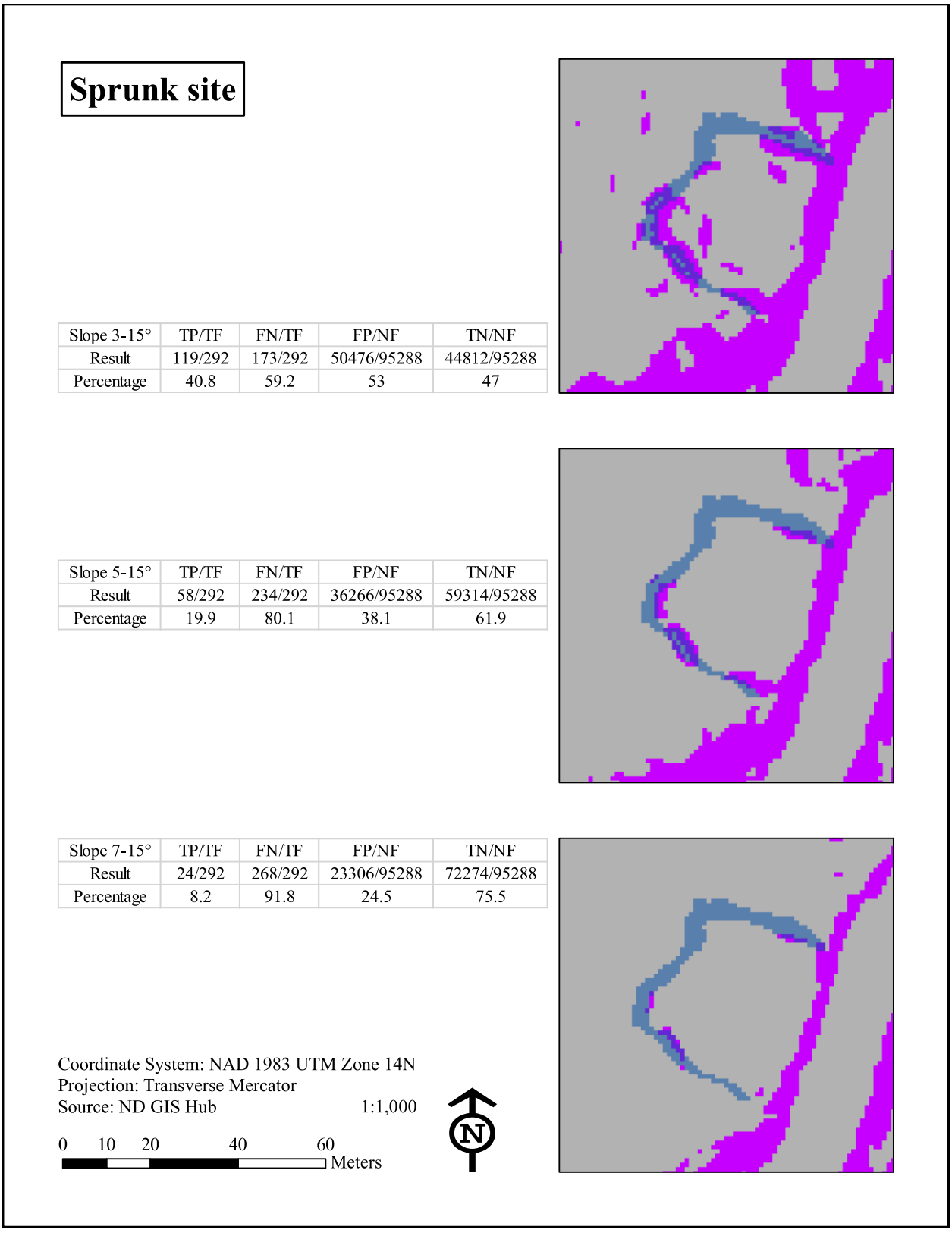

Figure 22. Slope reclassification for the Sprunk site.

Sprunk site

Curvature >0	TP/TF	FN/TF	FP/NF	TN/NF
Result	190/292	102/292	45967/95288	49321/95288
Percentage	65.1	34.9	48.2	51.8

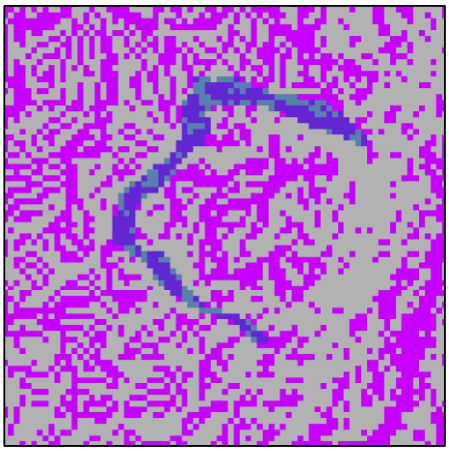

Curvature >3	TP/TF	FN/TF	FP/NF	TN/NF
Result	99/292	193/292	11307/95288	83981/95288
Percentage	33.9	66.1	11.9	88.1

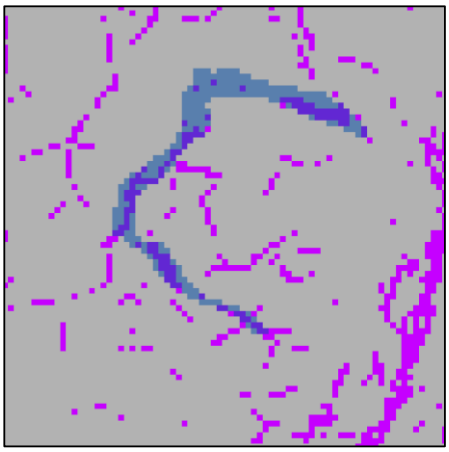

Curvature >5	TP/TF	FN/TF	FP/NF	TN/NF
Result	63/292	229/292	6407/95288	88881/95288
Percentage	21.6	78.4	6.7	93.3

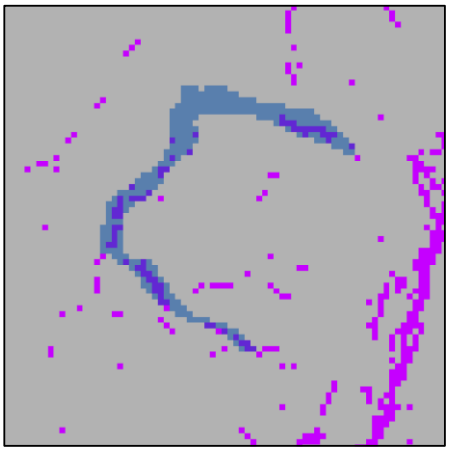

Coordinate System: NAD 1983 UTM Zone 14N
Projection: Transverse Mercator
Source: ND GIS Hub 1:1,000

0 10 20 40 60
Meters

N

Figure 23. Curvature reclassification for the Sprunk site.

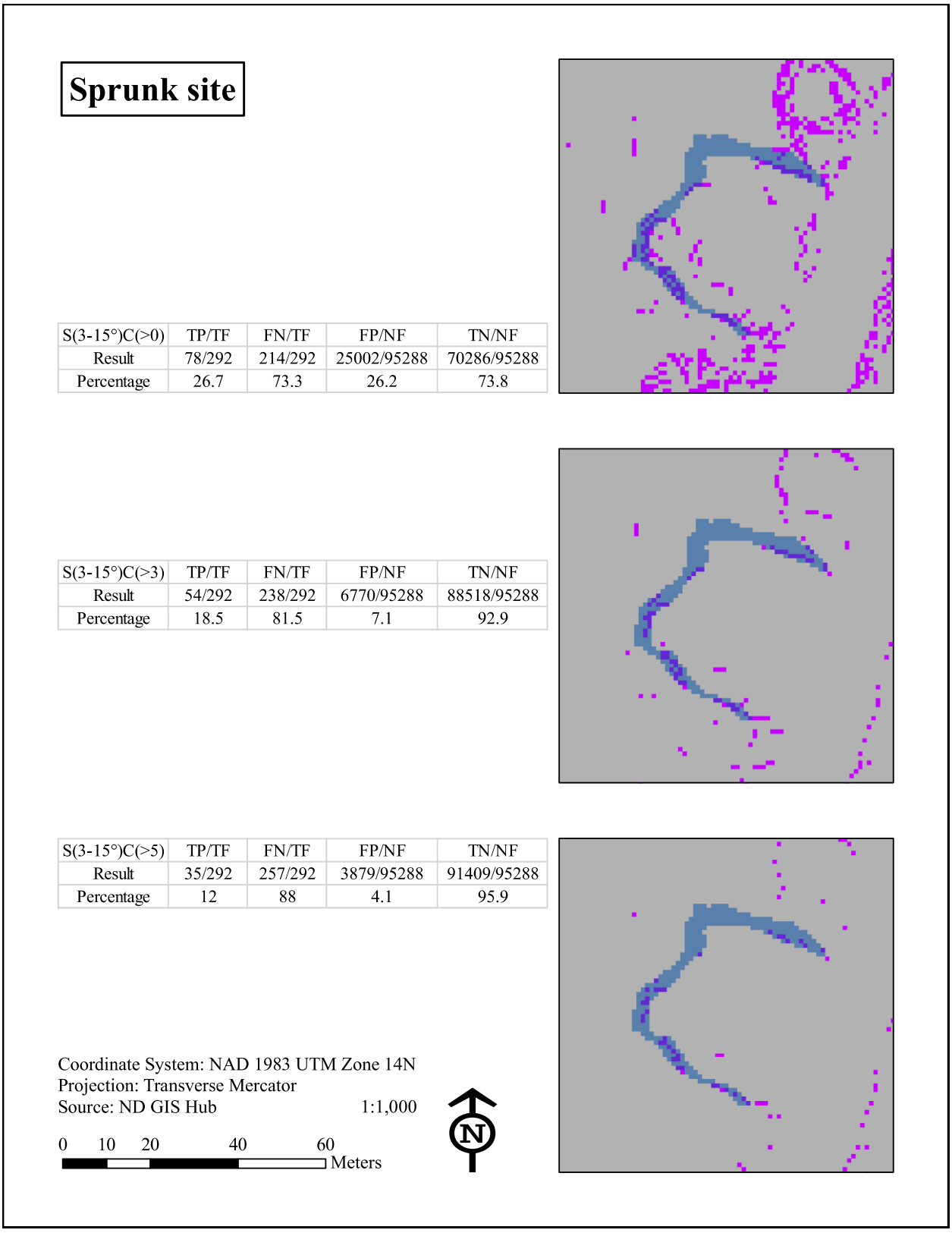

Figure 24. Combined slope/curvature reclassification for the Sprunk site.

Sprunk site

S(5-15°)C(>0)	TP/TF	FN/TF	FP/NF	TN/NF
Result	39/292	253/292	18029/95288	72259/95288
Percentage	13.4	86.6	18.9	81.1

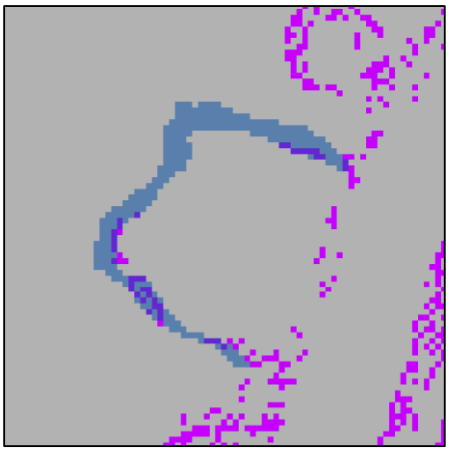

S(5-15°)C(>3)	TP/TF	FN/TF	FP/NF	TN/NF
Result	27/292	265/292	5130/95288	90518/95288
Percentage	9.2	90.8	5.4	94.6

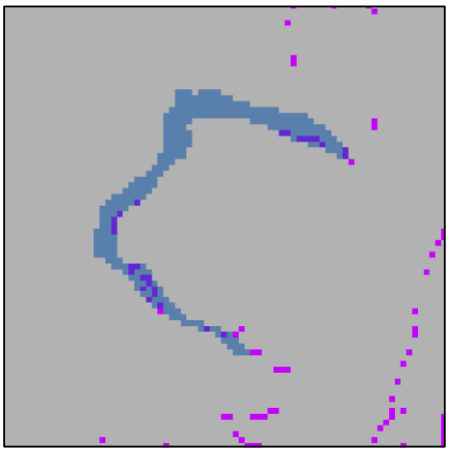

S(5-15°)C(>5)	TP/TF	FN/TF	FP/NF	TN/NF
Result	16/292	276/292	3003/95288	92285/95288
Percentage	5.5	94.5	3.1	96.9

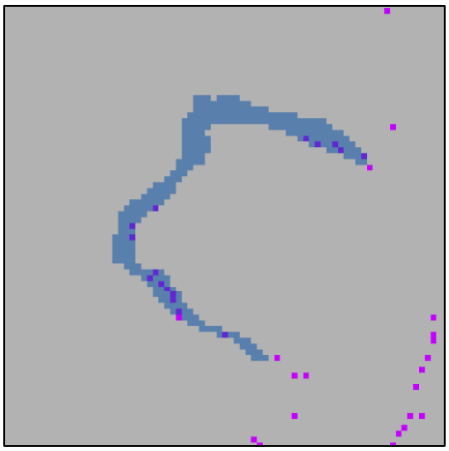

Coordinate System: NAD 1983 UTM Zone 14N
Projection: Transverse Mercator
Source: ND GIS Hub 1:1,000

0 10 20 40 60
Meters

N

Figure 24. Combined slope/curvature reclassification for the Sprunk site (continued).

Sprunk site

S(7-15°)C(>0)	TP/TF	FN/TF	FP/NF	TN/NF
Result	17/292	275/292	11556/95288	83732/95288
Percentage	5.8	94.2	12.1	87.9

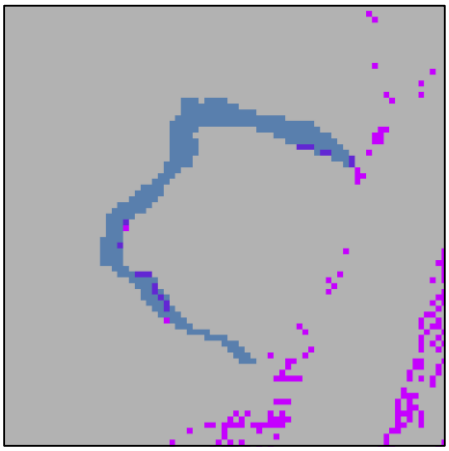

S(7-15°)C(>3)	TP/TF	FN/TF	FP/NF	TN/NF
Result	11/292	281/292	3471/95288	91817/95288
Percentage	3.8	96.2	3.6	96.4

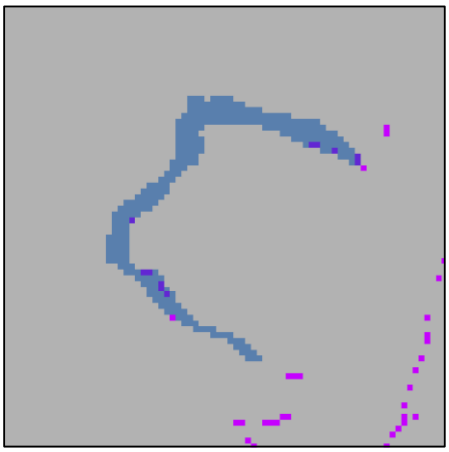

S(7-15°)C(>5)	TP/TF	FN/TF	FP/NF	TN/NF
Result	6/292	286/292	2089/95288	93199/95288
Percentage	2.1	97.9	2.2	97.8

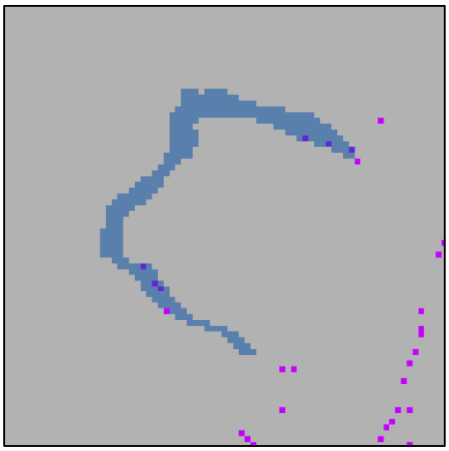

Coordinate System: NAD 1983 UTM Zone 14N
Projection: Transverse Mercator
Source: ND GIS Hub 1:1,000

0 10 20 40 60
Meters

N

Figure 24. Combined slope/curvature reclassification for the Sprunk site (continued).

Beisterfeldt site

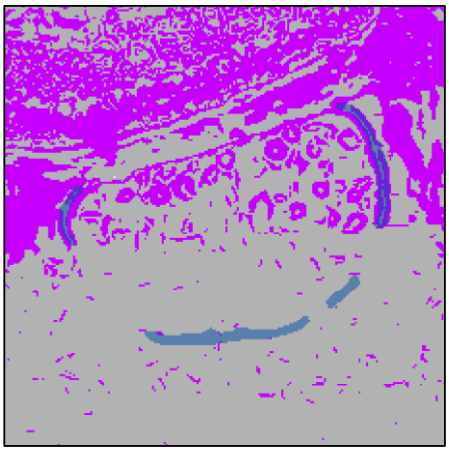

Slope 3-15°	TP/TF	FN/TF	FP/NF	TN/NF
Result	409/1118	709/1118	43022/184690	141668/184690
Percentage	36.6	63.4	23.3	76.7

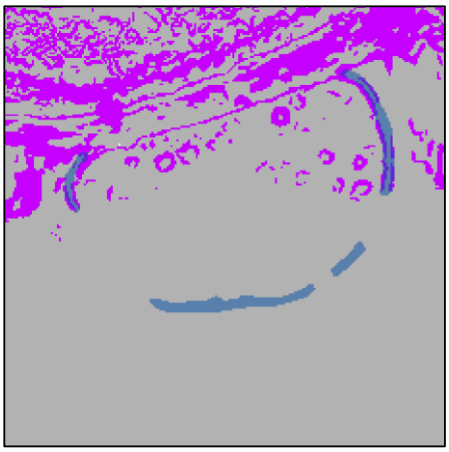

Slope 5-15°	TP/TF	FN/TF	FP/NF	TN/NF
Result	222/1118	896/1118	18849/184690	165841/184690
Percentage	19.9	80.1	10.2	89.8

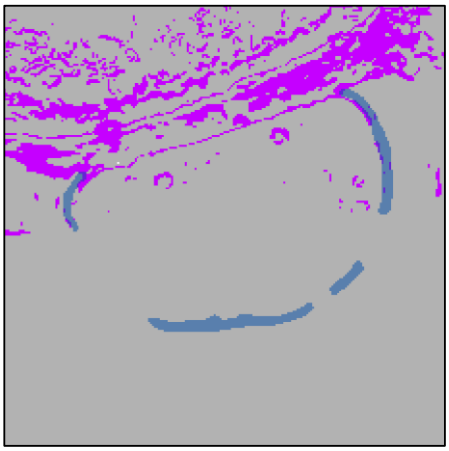

Slope 7-15°	TP/TF	FN/TF	FP/NF	TN/NF
Result	71/1118	1047/1118	8779/184690	175911/184690
Percentage	6.4	93.6	4.8	95.2

Coordinate System: NAD 1983 UTM Zone 14N
Projection: Transverse Mercator
Source: ND GIS Hub 1:3,000

0 30 60 120 180
Meters

N

Figure 25. Slope reclassification for the Biesterfeldt site.

Beisterfeldt site

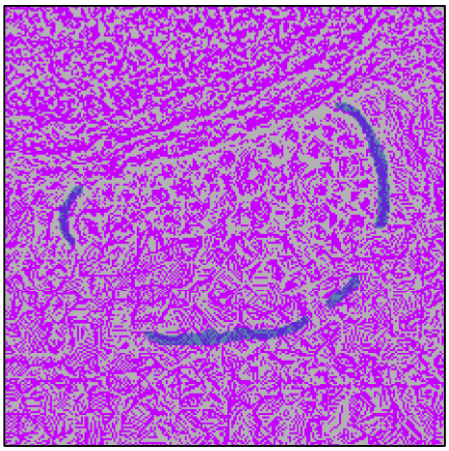

Curvature >0	TP/TF	FN/TF	FP/NF	TN/NF
Result	685/1118	433/1118	88390/184690	96300/184690
Percentage	61.3	38.7	47.9	52.1

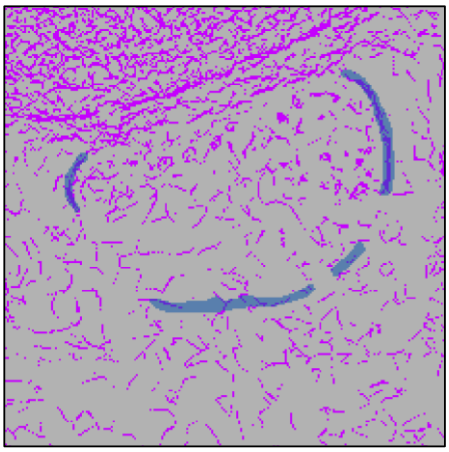

Curvature >3	TP/TF	FN/TF	FP/NF	TN/NF
Result	264/1118	854/1118	23284/184690	161406/184690
Percentage	23.6	76.4	12.6	87.4

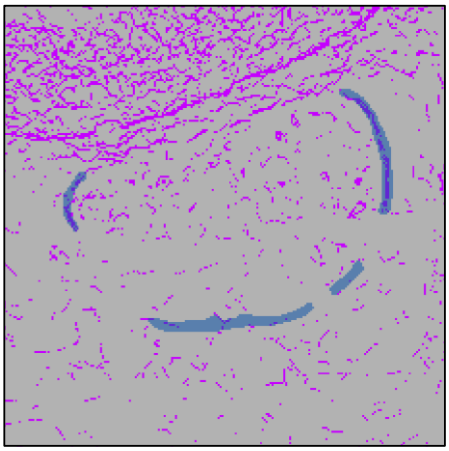

Curvature >5	TP/TF	FN/TF	FP/NF	TN/NF
Result	181/1118	937/1118	13594/184690	171096/184690
Percentage	16.2	83.8	7.4	92.6

Coordinate System: NAD 1983 UTM Zone 14N
Projection: Transverse Mercator
Source: ND GIS Hub 1:3,000

0 30 60 120 180
Meters

N

Figure 26. Curvature reclassification for the Biesterfeldt site.

Beisterfeldt site

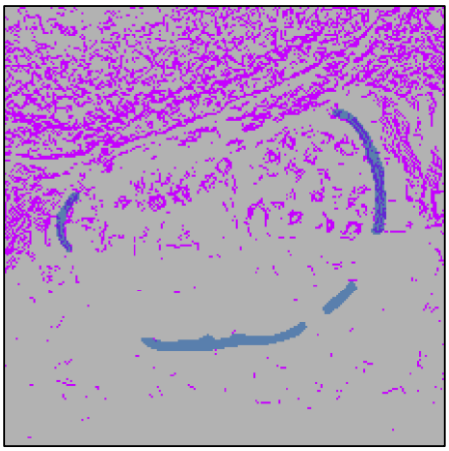

S(3-15°)C(>0)	TP/TF	FN/TF	FP/NF	TN/NF
Result	250/1118	868/1118	21425/184690	163265/184690
Percentage	22.4	77.6	11.6	88.4

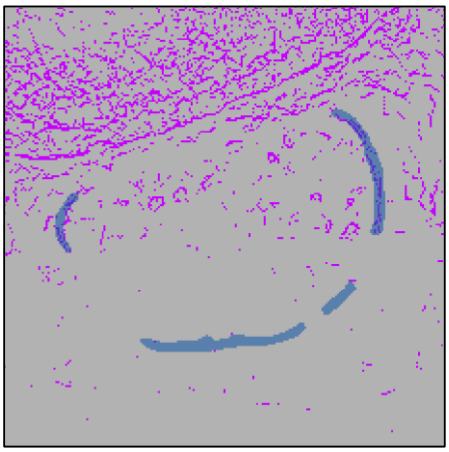

S(3-15°)C(>3)	TP/TF	FN/TF	FP/NF	TN/NF
Result	128/1118	990/1118	10012/184690	174678/184690
Percentage	11.4	88.6	5.4	94.6

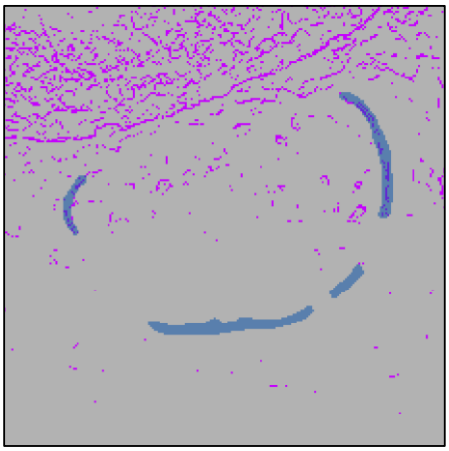

S(3-15°)C(>5)	TP/TF	FN/TF	FP/NF	TN/NF
Result	97/1118	1021/1118	6789/184690	177901/184690
Percentage	8.7	91.3	3.7	96.3

Coordinate System: NAD 1983 UTM Zone 14N
Projection: Transverse Mercator
Source: ND GIS Hub 1:3,000

0 30 60 120 180
Meters

N

Figure 27. Combined slope/curvature reclassification for the Biesterfeldt site.

Beisterfeldt site

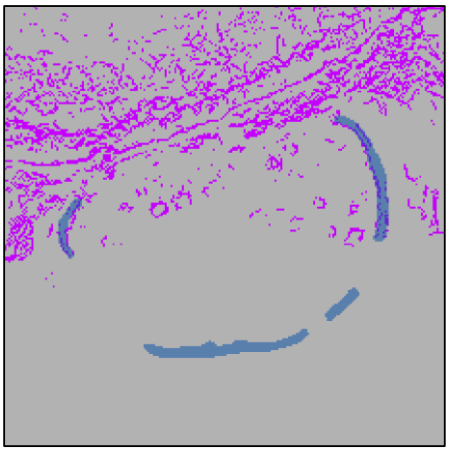

S(5-15°)C(>0)	TP/TF	FN/TF	FP/NF	TN/NF
Result	127/1118	991/1118	9347/184690	175343/184690
Percentage	11.4	88.6	5.1	94.9

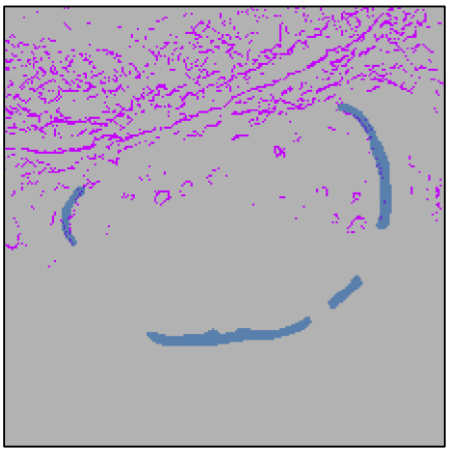

S(5-15°)C(>3)	TP/TF	FN/TF	FP/NF	TN/NF
Result	46/1118	1072/1118	4976/184690	179714/184690
Percentage	4.1	95.9	2.7	97.3

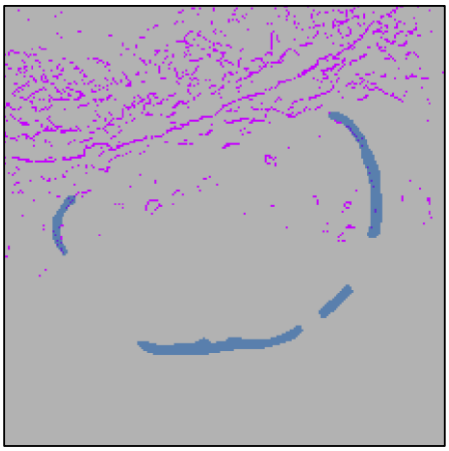

S(5-15°)C(>5)	TP/TF	FN/TF	FP/NF	TN/NF
Result	32/1118	1086/1118	3576/184690	181114/184690
Percentage	2.9	97.1	1.9	98.1

Coordinate System: NAD 1983 UTM Zone 14N
Projection: Transverse Mercator
Source: ND GIS Hub 1:3,000

0 30 60 120 180
Meters

N

Figure 27. Combined slope/curvature reclassification for the Biesterfeldt site (continued).

Beisterfeldt site

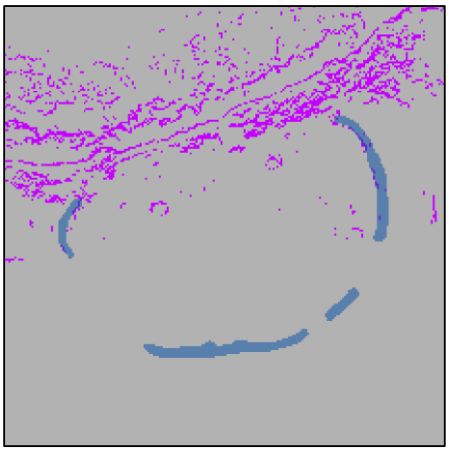

S(7-15°)C(>0)	TP/TF	FN/TF	FP/NF	TN/NF
Result	42/1118	1076/1118	4300/184690	180390/184690
Percentage	3.8	96.2	2.3	97.7

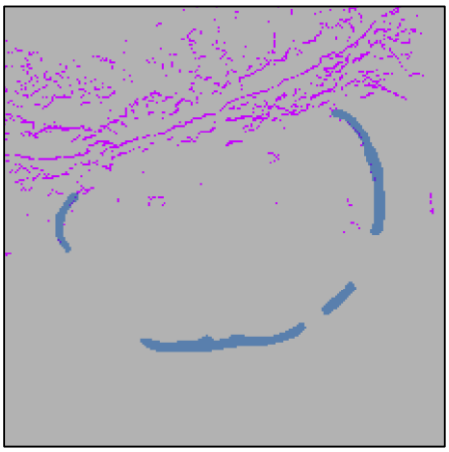

S(7-15°)C(>3)	TP/TF	FN/TF	FP/NF	TN/NF
Result	20/1118	1098/1118	2555/184690	182135/184690
Percentage	1.8	98.2	1.4	98.6

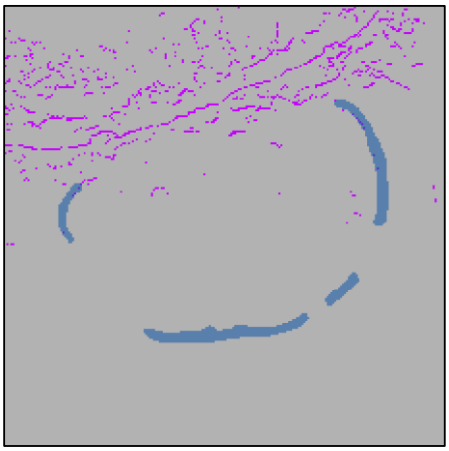

S(7-15°)C(>5)	TP/TF	FN/TF	FP/NF	TN/NF
Result	13/1118	1105/1118	1902/184690	182788/184690
Percentage	1.2	98.8	1	99

Coordinate System: NAD 1983 UTM Zone 14N
Projection: Transverse Mercator
Source: ND GIS Hub 1:3,000

0 30 60 120 180 Meters

N

Figure 27. Combined slope/curvature reclassification for the Biesterfeldt site (continued).

Lucas site

Slope 3-15°	TP/TF	FN/TF	FP/NF	TN/NF
Result	300/397	97/397	4125/10789	6664/10789
Percentage	75.6	24.4	38.2	61.8

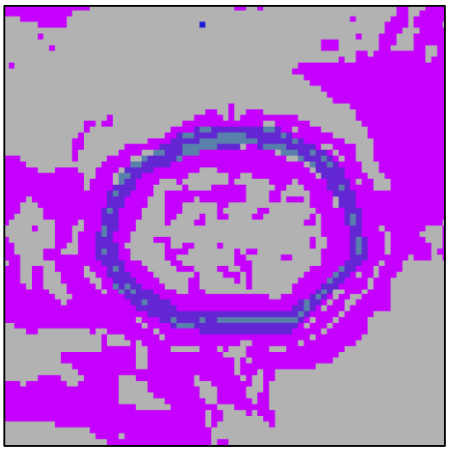

Slope 5-15°	TP/TF	FN/TF	FP/NF	TN/NF
Result	240/397	157/397	3239/10789	7550/10789
Percentage	60.5	39.5	30	70

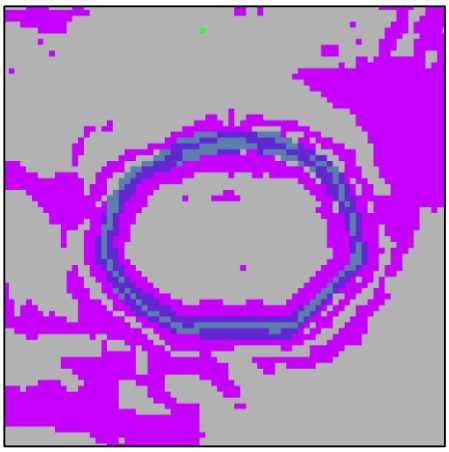

Slope 7-15°	TP/TF	FN/TF	FP/NF	TN/NF
Result	193/397	204/397	2708/10789	8081/10789
Percentage	48.6	51.4	25.1	74.9

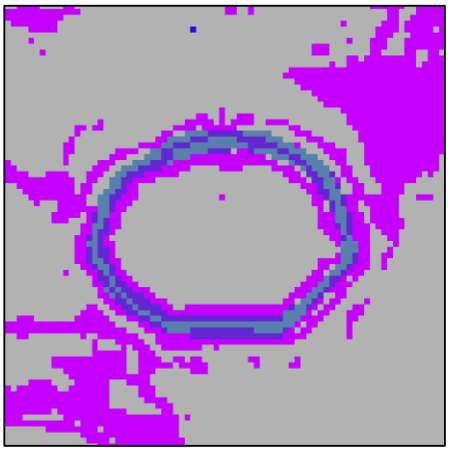

Coordinate System: NAD 1983 UTM Zone 14N
Projection: Transverse Mercator
Source: ND GIS Hub 1:1,000

0 10 20 40 60
Meters

N

Figure 28. Slope reclassification for the Lucas site.

Lucas site

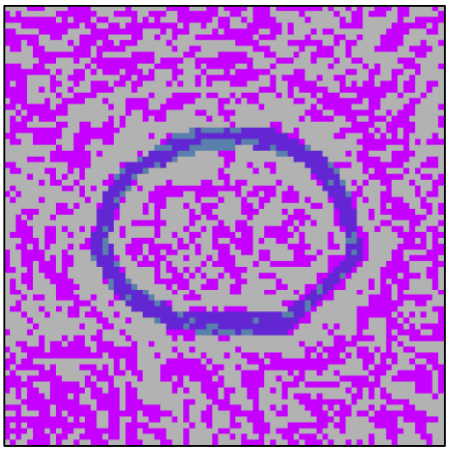

Curvature >0	TP/TF	FN/TF	FP/NF	TN/NF
Result	304/397	93/397	4650/10789	6139/10789
Percentage	76.6	23.4	43.1	56.9

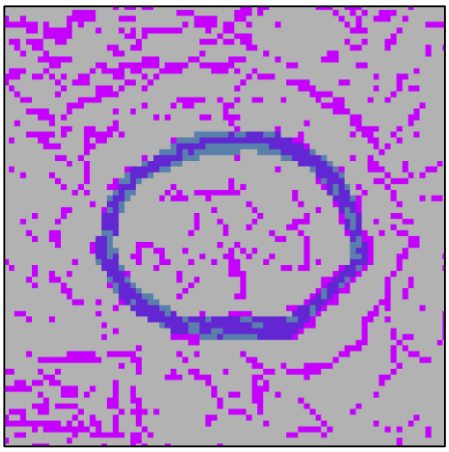

Curvature >3	TP/TF	FN/TF	FP/NF	TN/NF
Result	256/397	141/397	1682/10789	9107/10789
Percentage	64.5	35.5	15.6	84.4

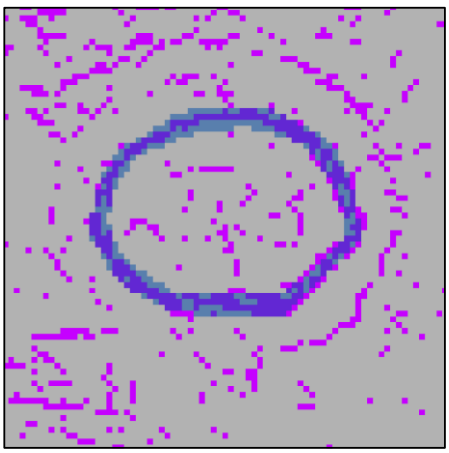

Curvature >5	TP/TF	FN/TF	FP/NF	TN/NF
Result	230/397	167/397	998/10789	9791/10789
Percentage	57.9	62.1	9.3	90.7

Coordinate System: NAD 1983 UTM Zone 14N
Projection: Transverse Mercator
Source: ND GIS Hub 1:1,000

0 10 20 40 60
Meters

N

Figure 29. Curvature reclassification for the Lucas site.

Lucas site

S(3-15°)C(>0)	TP/TF	FN/TF	FP/NF	TN/NF
Result	237/397	160/397	1636/10789	9153/10789
Percentage	59.7	40.3	15.2	84.8

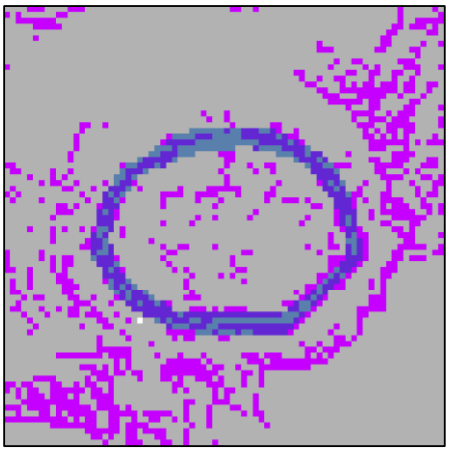

S(3-15°)C(>3)	TP/TF	FN/TF	FP/NF	TN/NF
Result	202/397	195/397	648/10789	10141/10789
Percentage	50.9	49.1	6	94

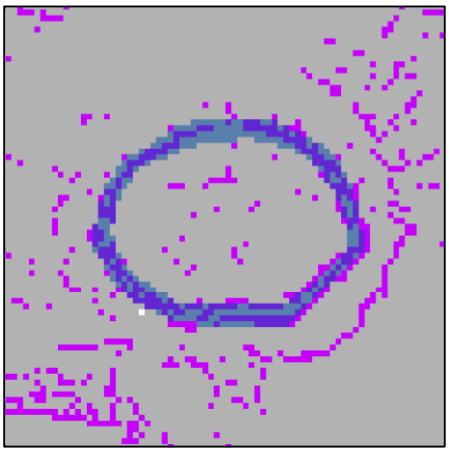

S(3-15°)C(>5)	TP/TF	FN/TF	FP/NF	TN/NF
Result	182/397	215/397	408/10789	10381/10789
Percentage	45.8	54.2	3.8	96.2

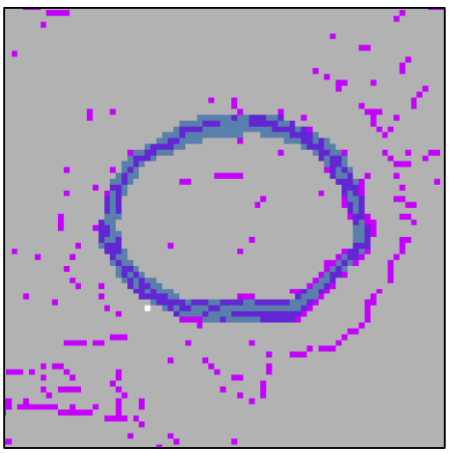

Coordinate System: NAD 1983 UTM Zone 14N
Projection: Transverse Mercator
Source: ND GIS Hub 1:1,000

0 10 20 40 60
Meters

N

Figure 30. Combined slope/curvature reclassification for the Lucas site.

Lucas site

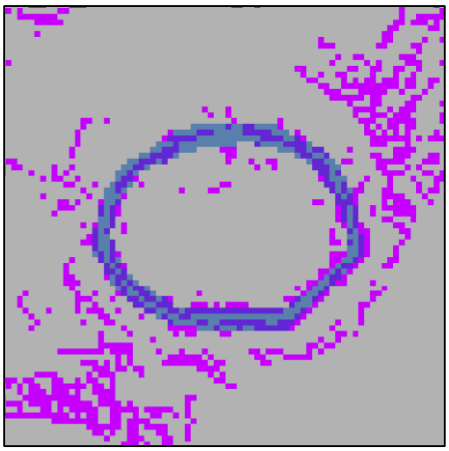

S(5-15°)C(>0)	TP/TF	FN/TF	FP/NF	TN/NF
Result	188/397	209/397	1308/10789	9481/10789
Percentage	47.4	52.6	12.1	87.9

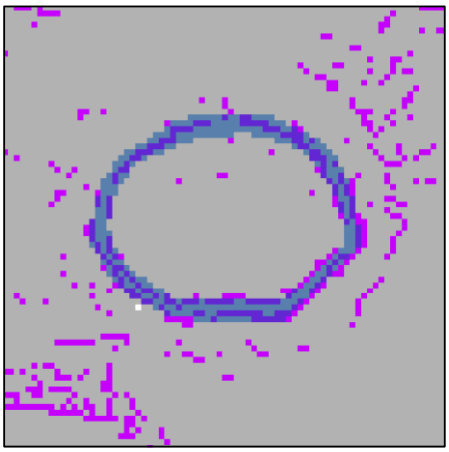

S(5-15°)C(>3)	TP/TF	FN/TF	FP/NF	TN/NF
Result	159/397	238/397	541/10789	10248/10789
Percentage	40.1	59.9	5	95

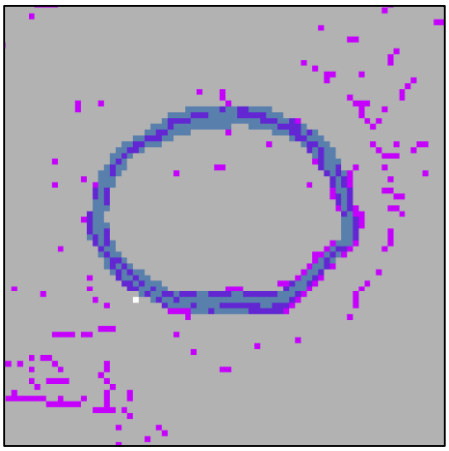

S(5-15°)C(>5)	TP/TF	FN/TF	FP/NF	TN/NF
Result	146/397	251/397	350/10789	10439/10789
Percentage	36.8	63.2	3.2	96.8

Coordinate System: NAD 1983 UTM Zone 14N
Projection: Transverse Mercator
Source: ND GIS Hub 1:1,000

0 10 20 40 60
Meters

N

Figure 30. Combined slope/curvature reclassification for the Lucas site (continued).

Lucas site

S(7-15°)C(>0)	TP/TF	FN/TF	FP/NF	TN/NF
Result	147/397	250/397	1123/10789	9666/10789
Percentage	37	63	10.4	89.6

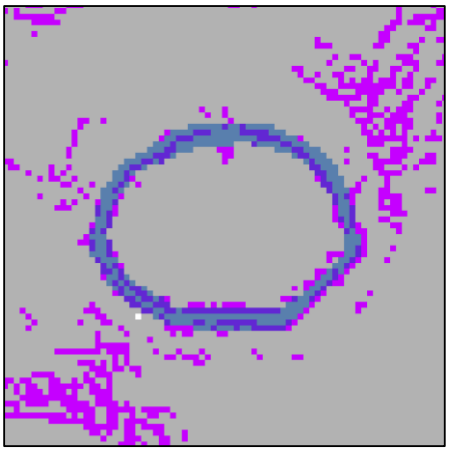

S(7-15°)C(>3)	TP/TF	FN/TF	FP/NF	TN/NF
Result	125/397	272/397	487/10789	10302/10789
Percentage	31.5	68.5	4.5	95.5

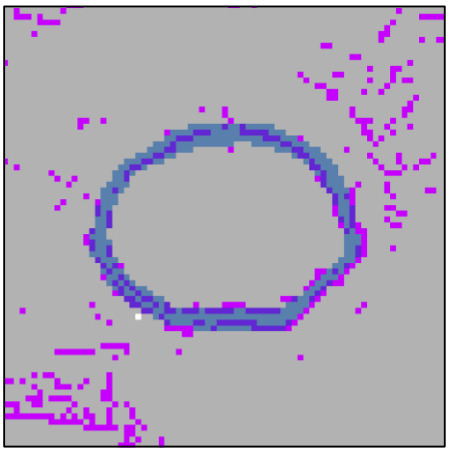

S(7-15°)C(>5)	TP/TF	FN/TF	FP/NF	TN/NF
Result	113/397	284/397	318/10789	10471/10789
Percentage	28.5	71.5	2.9	97.1

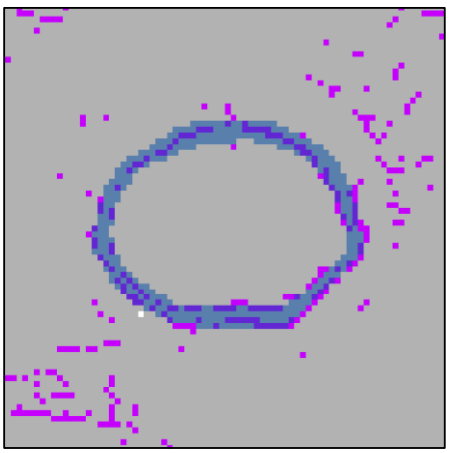

Coordinate System: NAD 1983 UTM Zone 14N
Projection: Transverse Mercator
Source: ND GIS Hub 1:1,000

0 10 20 40 60
Meters

N

Figure 30. Combined slope/curvature reclassification for the Lucas site (continued).

Peterson site

Slope 3-15°	TP/TF	FN/TF	FP/NF	TN/NF
Result	232/296	64/296	5119/14800	9681/14800
Percentage	78.4	21.6	34.6	65.4

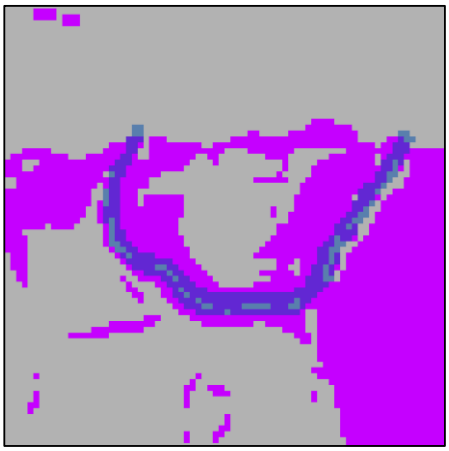

Slope 5-15°	TP/TF	FN/TF	FP/NF	TN/NF
Result	180/296	116/296	4266/14800	10534/14800
Percentage	60.8	39.2	28.8	71.2

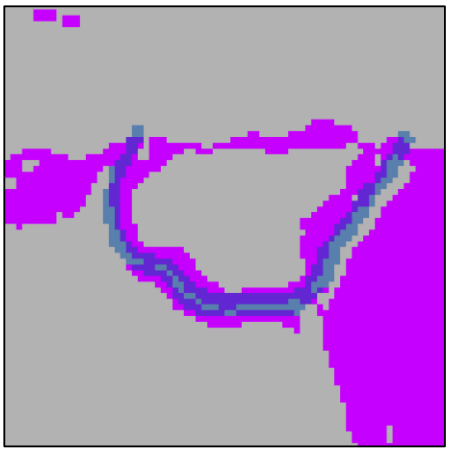

Slope 7-15°	TP/TF	FN/TF	FP/NF	TN/NF
Result	143/296	153/296	3453/14800	11347/14800
Percentage	48.3	51.7	23.3	76.7

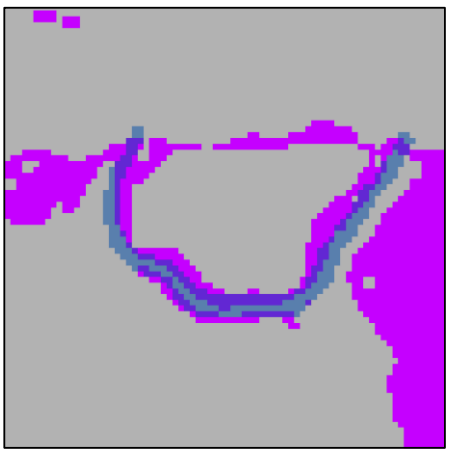

Coordinate System: NAD 1983 UTM Zone 14N
Projection: Transverse Mercator
Source: ND GIS Hub 1:1,000

0 10 20 40 60
Meters

Figure 31. Slope reclassification for the Peterson site.

Peterson site

Curvature >0	TP/TF	FN/TF	FP/NF	TN/NF
Result	218/296	78/296	6423/14800	8377/14800
Percentage	73.6	26.4	43.4	56.6

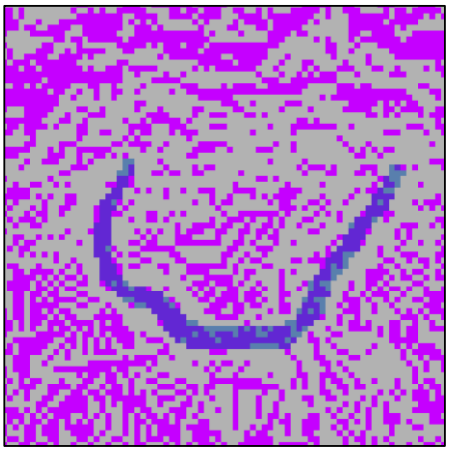

Curvature >3	TP/TF	FN/TF	FP/NF	TN/NF
Result	159/296	137/296	1881/14800	12919/14800
Percentage	53.7	46.3	12.7	87.3

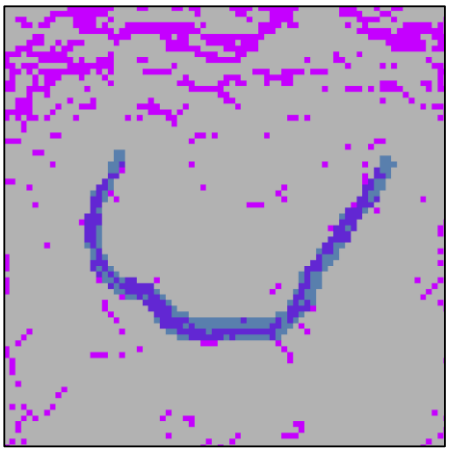

Curvature >5	TP/TF	FN/TF	FP/NF	TN/NF
Result	127/296	169/296	1285/14800	13515/14800
Percentage	42.9	57.1	8.7	91.3

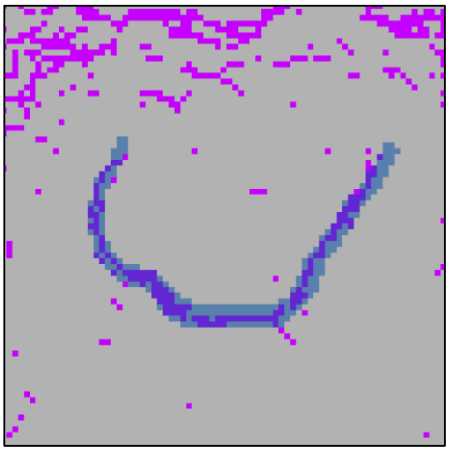

Coordinate System: NAD 1983 UTM Zone 14N
Projection: Transverse Mercator
Source: ND GIS Hub 1:1,000

0 10 20 40 60
Meters

N

Figure 32. Curvature reclassification for the Peterson site.

Peterson site

S(3-15°)C(>0)	TP/TF	FN/TF	FP/NF	TN/NF
Result	170/296	126/296	2105/14800	12695/14800
Percentage	57.4	42.6	14.2	85.8

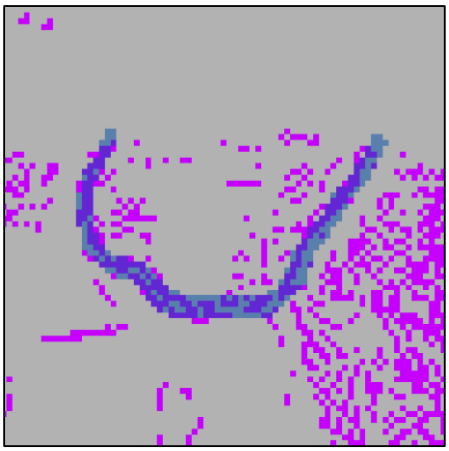

S(3-15°)C(>3)	TP/TF	FN/TF	FP/NF	TN/NF
Result	123/296	173/296	398/14800	14402/14800
Percentage	41.6	58.4	2.7	97.3

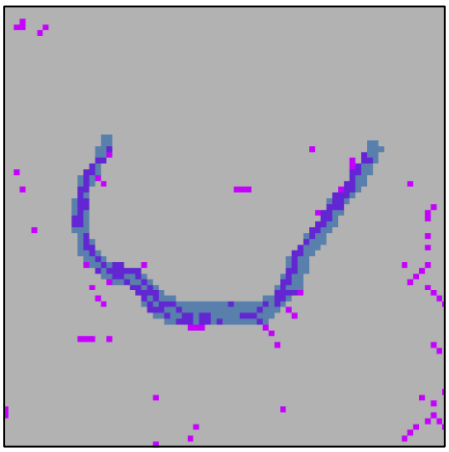

S(3-15°)C(>5)	TP/TF	FN/TF	FP/NF	TN/NF
Result	100/296	196/296	210/14800	14590/14800
Percentage	33.8	66.2	1.4	98.6

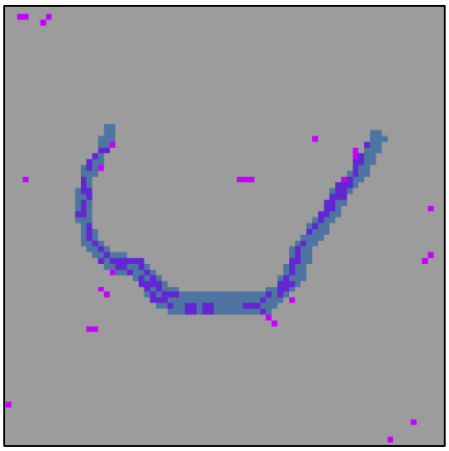

Coordinate System: NAD 1983 UTM Zone 14N
Projection: Transverse Mercator
Source: ND GIS Hub 1:1,000

0 10 20 40 60
Meters

N

Figure 33. Combined slope/curvature reclassification for the Peterson site.

Peterson site

S(5-15°)C(>0)	TP/TF	FN/TF	FP/NF	TN/NF
Result	129/296	167/296	1811/14800	12989/14800
Percentage	43.6	56.4	12.2	87.8

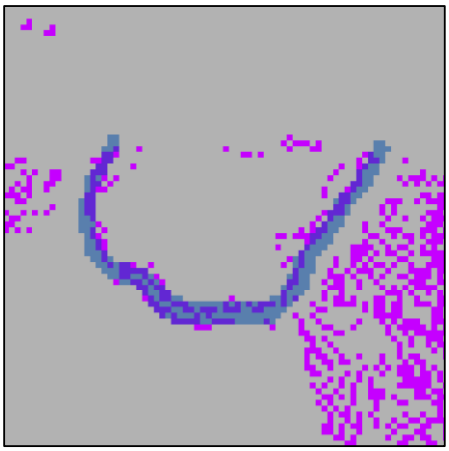

S(5-15°)C(>3)	TP/TF	FN/TF	FP/NF	TN/NF
Result	91/296	205/296	337/14800	14463/14800
Percentage	30.7	69.3	2.3	97.7

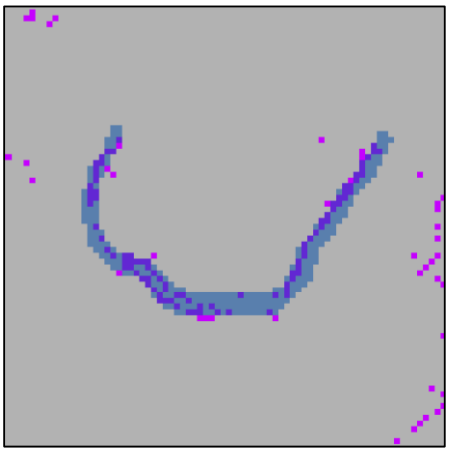

S(5-15°)C(>5)	TP/TF	FN/TF	FP/NF	TN/NF
Result	71/296	225/296	178/14800	14622/14800
Percentage	24	76	1.2	98.8

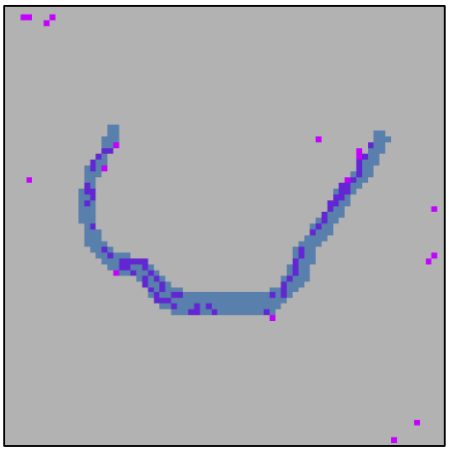

Coordinate System: NAD 1983 UTM Zone 14N
Projection: Transverse Mercator
Source: ND GIS Hub 1:1,000

0 10 20 40 60
Meters

N

Figure 33. Combined slope/curvature reclassification for the Peterson site (continued).

Peterson site

S(7-15°)C(>0)	TP/TF	FN/TF	FP/NF	TN/NF
Result	98/296	198/296	1528/14800	13272/14800
Percentage	33.1	66.9	10.3	89.7

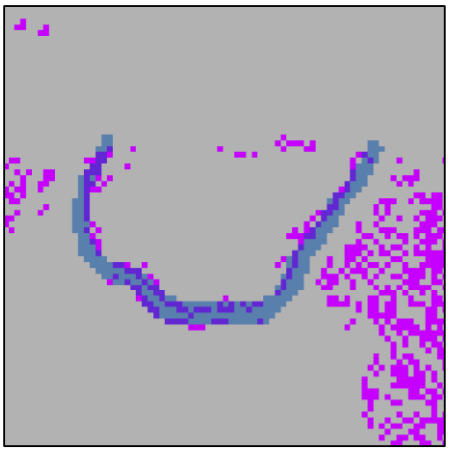

S(7-15°)C(>3)	TP/TF	FN/TF	FP/NF	TN/NF
Result	64/296	232/296	294/14800	14506/14800
Percentage	21.6	78.4	2	98

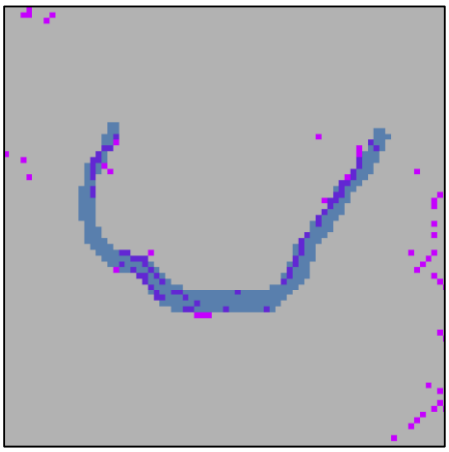

S(7-15°)C(>5)	TP/TF	FN/TF	FP/NF	TN/NF
Result	47/296	249/296	155/14800	14645/14800
Percentage	15.9	84.1	1	99

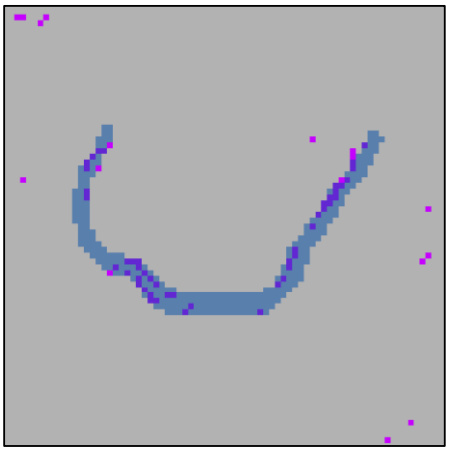

Coordinate System: NAD 1983 UTM Zone 14N
Projection: Transverse Mercator
Source: ND GIS Hub 1:1,000

0 10 20 40 60
Meters

N

Figure 33. Combined slope/curvature reclassification for the Peterson site (continued).

Nelson site

Slope 3-15°	TP/TF	FN/TF	FP/NF	TN/NF
Result	276/381	105/381	31247/62110	30863/62110
Percentage	72.4	27.6	50.3	49.7

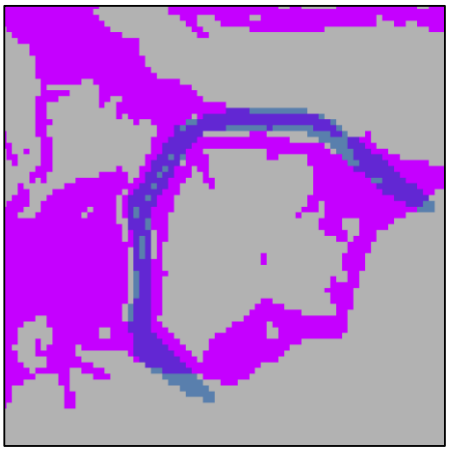

Slope 5-15°	TP/TF	FN/TF	FP/NF	TN/NF
Result	247/381	134/381	22763/62110	39347/62110
Percentage	64.8	35.2	36.6	63.4

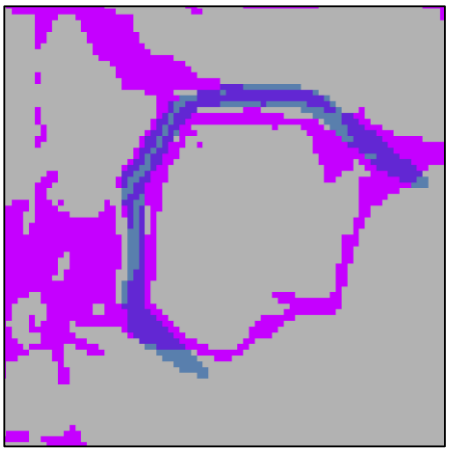

Slope 7-15°	TP/TF	FN/TF	FP/NF	TN/NF
Result	217/381	164/381	14448/62110	47662/62110
Percentage	56	44	23.3	76.7

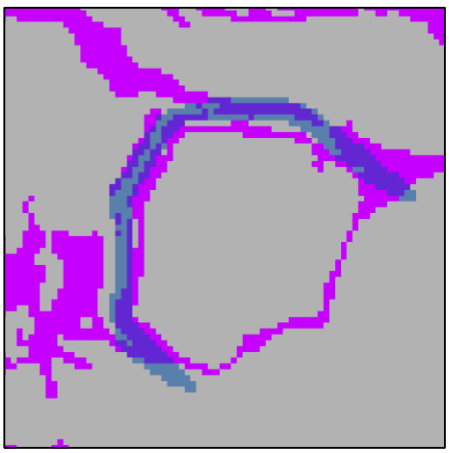

Coordinate System: NAD 1983 UTM Zone 14N
Projection: Transverse Mercator
Source: ND GIS Hub 1:1,000

0 10 20 40 60
Meters

N

Figure 34. Slope reclassification for the Nelson site.

Nelson site

Curvature >0	TP/TF	FN/TF	FP/NF	TN/NF
Result	221/381	160/381	27803/62110	34307/62110
Percentage	58	42	44.8	55.2

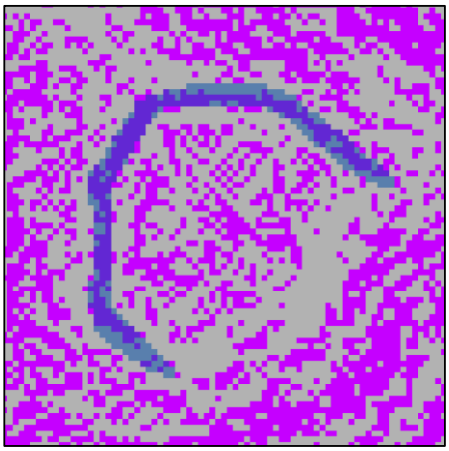

Curvature >3	TP/TF	FN/TF	FP/NF	TN/NF
Result	219/381	162/381	27521/62110	34589/62110
Percentage	57.5	42.5	44.3	55.7

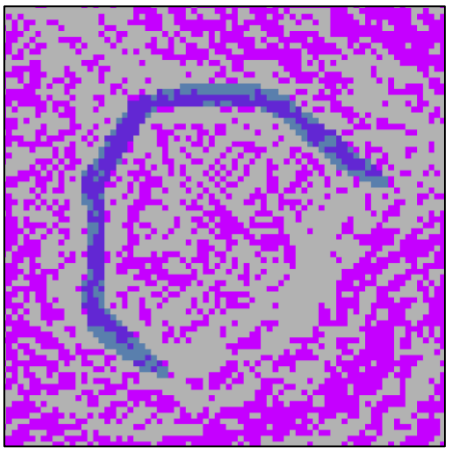

Curvature >5	TP/TF	FN/TF	FP/NF	TN/NF
Result	219/381	162/381	27301/62110	34809/62110
Percentage	57.5	42.5	44	56

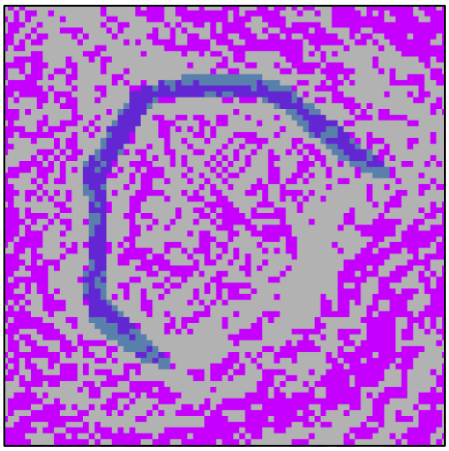

Coordinate System: NAD 1983 UTM Zone 14N
Projection: Transverse Mercator
Source: ND GIS Hub 1:1,000

0 10 20 40 60
Meters

N

Figure 35. Curvature reclassification for the Nelson site.

Nelson site

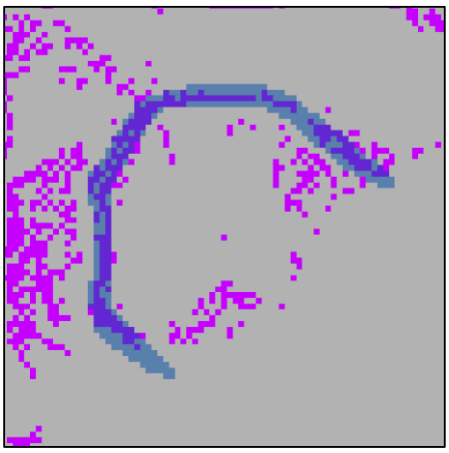

S(3-15°)C(>0)	TP/TF	FN/TF	FP/NF	TN/NF
Result	177/381	204/381	13812/62110	48298/62110
Percentage	46.5	53.5	22.2	77.8

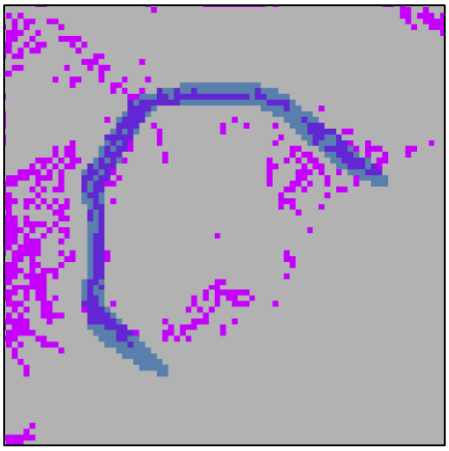

S(3-15°)C(>3)	TP/TF	FN/TF	FP/NF	TN/NF
Result	175/381	206/381	13622/62110	48488/62110
Percentage	45.9	54.1	21.9	78.1

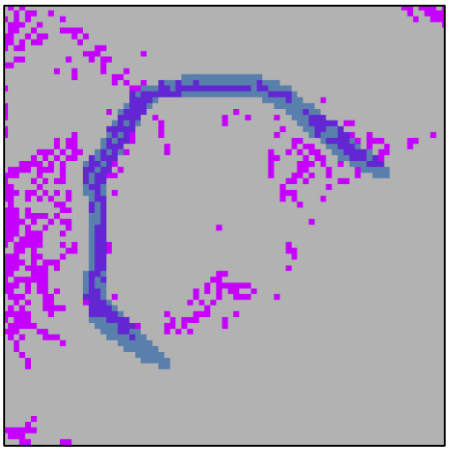

S(3-15°)C(>5)	TP/TF	FN/TF	FP/NF	TN/NF
Result	175/381	206/381	13478/62110	48632/62110
Percentage	45.9	54.1	21.7	78.3

Coordinate System: NAD 1983 UTM Zone 14N
Projection: Transverse Mercator
Source: ND GIS Hub

1:1,000

0 10 20 40 60
Meters

N

Figure 36. Combined slope/curvature reclassification for the Nelson site.

Nelson site

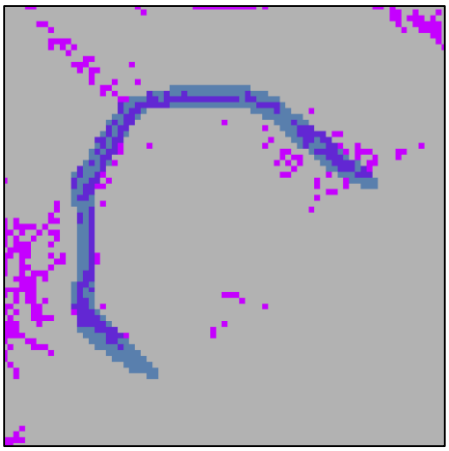

S(5-15°)C(>0)	TP/TF	FN/TF	FP/NF	TN/NF
Result	156/381	225/381	10110/62110	52000/62110
Percentage	40.9	59.1	16.3	83.7

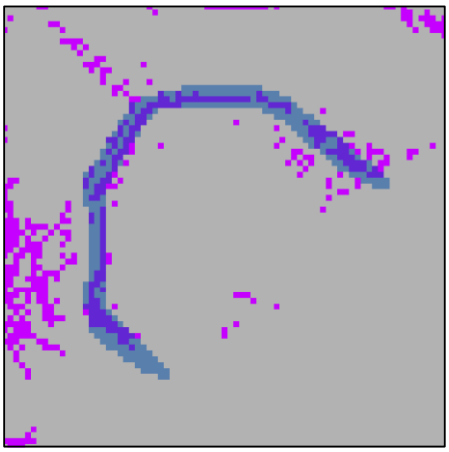

S(5-15°)C(>3)	TP/TF	FN/TF	FP/NF	TN/NF
Result	155/381	226/381	9948/62110	52162/62110
Percentage	40.7	59.3	16	84

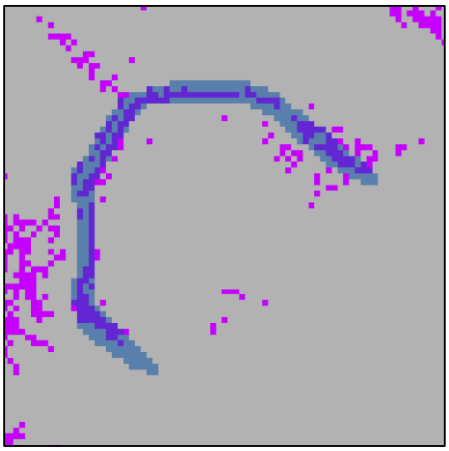

S(5-15°)C(>5)	TP/TF	FN/TF	FP/NF	TN/NF
Result	155/381	226/381	9838/62110	52272/62110
Percentage	40.7	59.3	15.8	84.2

Coordinate System: NAD 1983 UTM Zone 14N
Projection: Transverse Mercator
Source: ND GIS Hub 1:1,000

0 10 20 40 60
Meters

N

Figure 36. Combined slope/curvature reclassification for the Nelson site (continued).

Nelson site

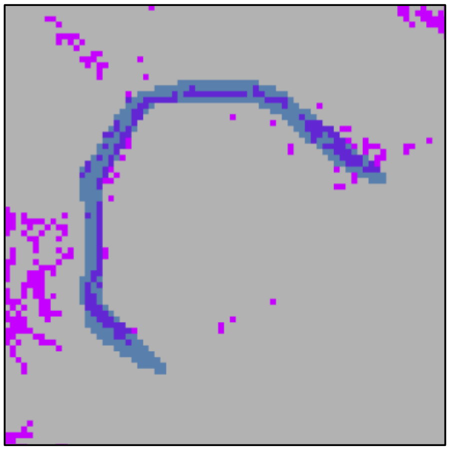

S(7-15°)C(>0)	TP/TF	FN/TF	FP/NF	TN/NF
Result	133/381	248/381	6478/62110	55632/62110
Percentage	34.9	65.1	10.4	89.6

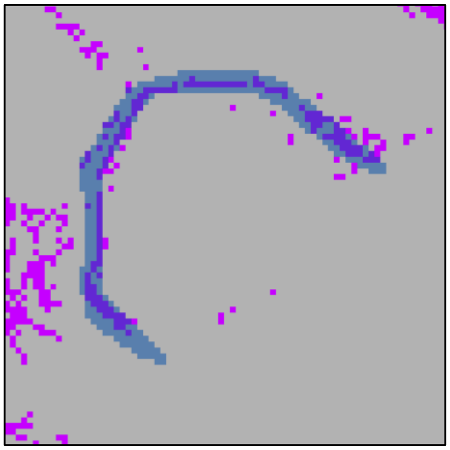

S(7-15°)C(>3)	TP/TF	FN/TF	FP/NF	TN/NF
Result	132/381	249/381	6391/62110	55719/62110
Percentage	34.6	65.4	10.3	89.7

S(7-15°)C(>5)	TP/TF	FN/TF	FP/NF	TN/NF
Result	132/381	249/381	6323/62110	55787/62110
Percentage	34.6	65.4	10.2	89.8

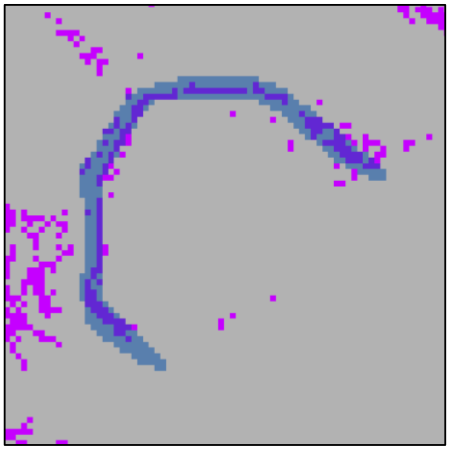

Coordinate System: NAD 1983 UTM Zone 14N
Projection: Transverse Mercator
Source: ND GIS Hub 1:1,000

0 10 20 40 60 Meters

N

Figure 36. Combined slope/curvature reclassification for the Nelson site (continued).

Automated Extraction Results

Output results from the automated extraction algorithm were provided in table format and subsequently displayed as light blue, transparent points within ArcGIS based on their x and y coordinates. This was then overlaid on the raster dataset that included the defined features used for this study (Figures 37-42). The areas where they match is a darker shade of blue to more easily distinguish which cells were correctly classified as the actual features. Because the data frames are concentrated on the actual features to better display the true-positive and false-negative results, false-positive and true-negative points in areas outside of this that were included in the testing are not immediately visible on the maps, although they do exist. Each data frame within the maps has a separate table displaying the number true-positive over, false-negative, false-positive, and true-negative, as well as the true-positive/false-positive ratios in the form of percentages. Again for each case, a greater number of true-positive and less false-positive created more accurate results.

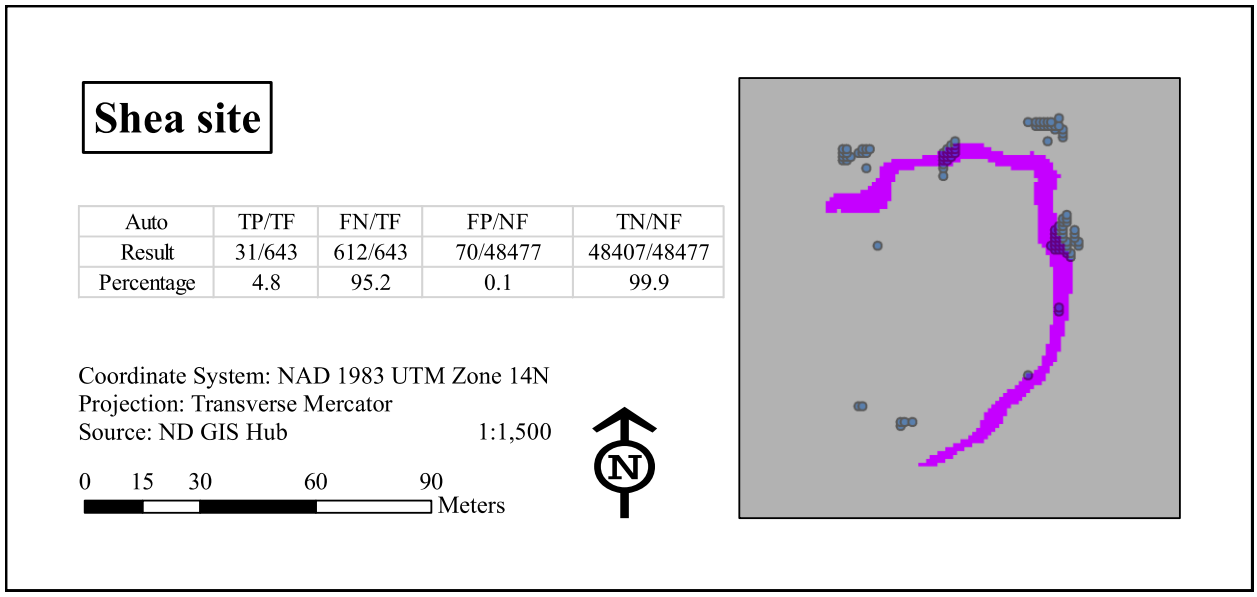

Figure 37. Automated results for the Shea site.

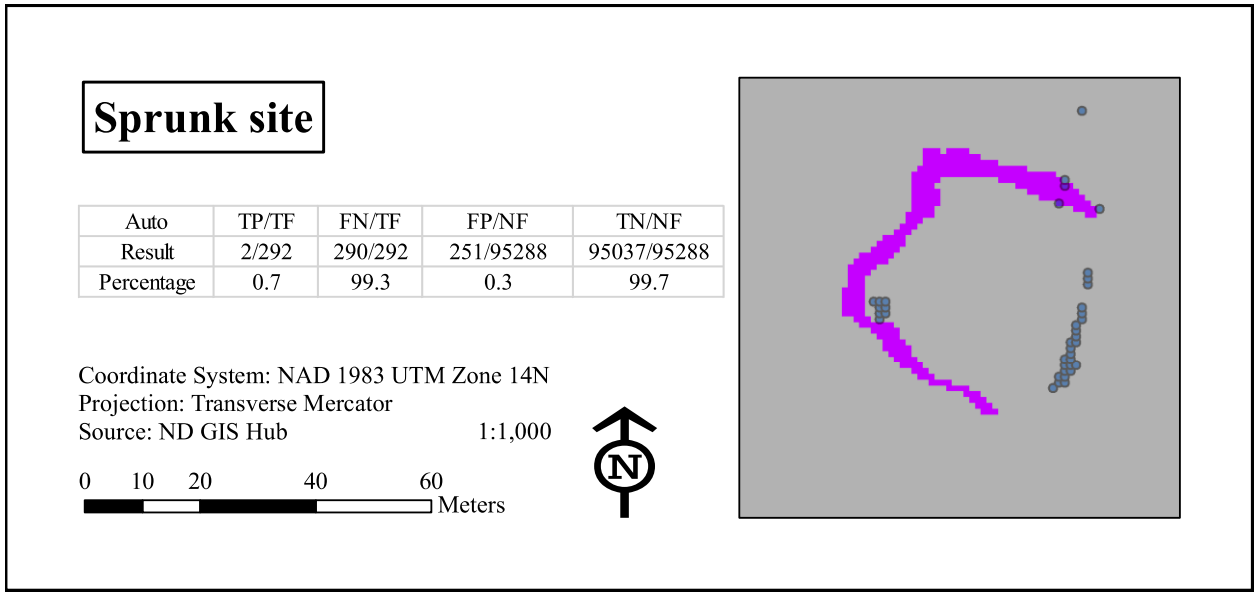

Figure 38. Automated results for the Sprunk site.

Beisterfeldt site

Auto	TP/TF	FN/TF	FP/NF	TN/NF
Result	2/1118	1116/1118	3033/184690	181657/184690
Percentage	0.2	99.8	1.6	98.4

Coordinate System: NAD 1983 UTM Zone 14N
Projection: Transverse Mercator
Source: ND GIS Hub 1:3,000

0 30 60 120 180
Meters

N

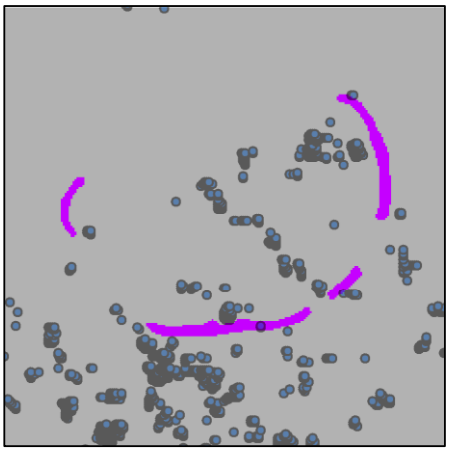

Figure 39. Automated results for the Biesterfeldt site.

Lucas site

Auto	TP/TF	FN/TF	FP/NF	TN/NF
Result	164/397	233/397	507/10789	10282/10789
Percentage	41.3	58.7	4.7	95.3

Coordinate System: NAD 1983 UTM Zone 14N
Projection: Transverse Mercator
Source: ND GIS Hub 1:1,000

0 10 20 40 60
Meters

N

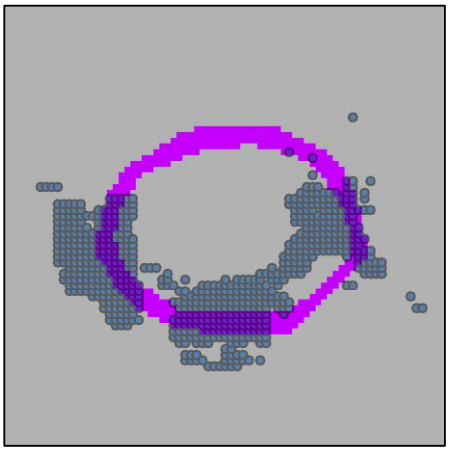

Figure 40. Automated results for the Lucas site.

Peterson site

Auto	TP/TF	FN/TF	FP/NF	TN/NF
Result	38/296	258/296	554/14800	14246/14800
Percentage	12.8	87.2	3.7	96.3

Coordinate System: NAD 1983 UTM Zone 14N
Projection: Transverse Mercator
Source: ND GIS Hub 1:1,000

0 10 20 40 60
Meters

N

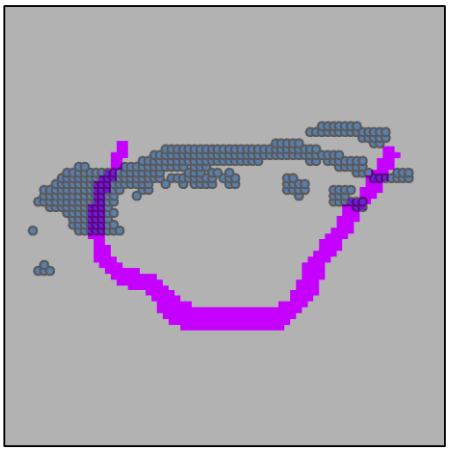

Figure 41. Automated results for the Peterson site.

Nelson site

Auto	TP/TF	FN/TF	FP/NF	TN/NF
Result	0/381	381/381	43/62110	62067/62110
Percentage	0	100	0.1	99.9

Coordinate System: NAD 1983 UTM Zone 14N
Projection: Transverse Mercator
Source: ND GIS Hub 1:1,000

0 10 20 40 60
Meters

N

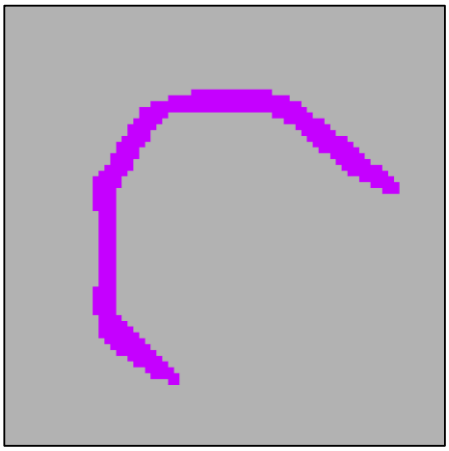

Figure 42. Automated results for the Nelson site.

Discussion

Visualizations

Although the standard DEM is a highly accurate and very useful tool, its effectiveness in contrasting certain features from the surrounding terrain is quite limited. Especially in regard to landscapes with higher degrees of variability, the color scales can only display specific ranges and will result in maps that may not display good contrast for smaller scale landforms. In these examples, the presence of relatively steep slopes along the river valleys constitute the majority of color variation within the sample, leaving only a limited scale to display the features in question. To remedy this, constrained color shading was useful as it more or less cuts out the valley slope by depicting the same color scale over a more limited range of elevation values. This procedure assisted in contrasting ditches from the surrounding landscape, but was still not the most useful tool in displaying the targeted information.

The addition of hillshading to the DEM greatly increased the visibility of the features. Although the single angle of illumination made the features more noticeable, it was still quite limited. Depending on the position of the feature relative to the angle of light, some portions of the ditches may be actually covered by the perceived shadow, making them more difficult to see. This issue was fixed by using a multi-directional hillshade, which illuminated the features from six different angles. This eliminated any instances where portions of the feature may be shaded and resulted in more accurate depictions of the features in their true shape.

Arguably the most useful tool in this package, slope severity displayed the features in great contrast to their surroundings. Since these sites were located on relatively flat bluffs overlooking river valleys, the variation of the landscape only fluctuated by several degrees. Because the sides of ditches had comparably steeper angles of slope, it was very easy to see

where the edges of the features meet the flatter adjacent terrain. Some portions of the ditches may be more difficult to notice, especially where they abut the bluff edge and the downward slope of the valley. A useful visualization technique that fixed this problem was the LRM. This tool works to eliminate larger scale features from the slope model, in this case the steep valleys, and increase the visibility of smaller scale features, so that the ditches became more defined in their depictions. However, this also means that other features that were not very visible in the original relief models became more apparent, which could lead to the false presumption of additional features being present on the landscape if the sizes and shapes are consistent.

The last two visualization tools used for this study, aspect and curvature, may be both as valuable to displaying these features, although they are unrelated to each other in form and function. The directional aspect is useful because it depicts the angle that the surface is facing. Since the plains are mostly flat with undulating hills, their aspect represents a random assortment of directions. But for ditches, we can see a consistent and continuous range where the channel sides face similar directions. In the best cases, where the angles are directly opposite of each other, such as the sides of ditches facing toward each other, we can identify the features quite accurately. The curvature profile accurately reflects the size and shape of the actual ditches and highly contrasts the feature cells from their surroundings. This technique proved to be quite useful in defining them and is one of the reasons it was selected for use in both the semi-automated and automated feature detections.

Although each of these techniques was useful in providing visual representations of these features, a few of them stand out in regard to their ability to distinguish the ditches from their surroundings and accurately reflect on their size and shape. Although it is a subjective endeavor, ranking these techniques in comparison to one another other is necessary. The following list

places them in order from most to least useful: 1, slope severity; 2, curvature profile; 3, Local Relief Model; 4, DEM with multi-directional hillshade; 5, directional aspect; 6, DEM with hillshade; 7, constrained color shading; 8, DEM. Again, it must be stressed that this is only a limited comparison of one feature type on a similar color scale. It is possible to get better contrasting between features by using different styles and ranges of colors, however it was necessary to use the black and white during this evaluation to assess each technique similarly. This is by no means a definitive representation of every visualization and outcome possible, and should be considered as such for any future studies.

Semi-automated Detection

The reclassification schemes in this study had varying degrees of success based on the scales and ranges for the data used during testing. On average there seemed to be an acceptable number of true-positive detections. However, when these statistics are compared to the high amount that are false-positive, it does not seem quite as successful.

For the slope reclassification in the 3-15° range, 65.6% of the features were detected and of the surrounding areas, 43.6% were misclassified. The ratio of true-positive to false-positive detections was 1:85.7. In the 5-15° range, 50.2% of the ditches were classified correctly, including 32.3% of the surrounding area that was not. True-positive to false-positive in this instance had a ratio of 1:76.7. Lastly, for the reclassification in the 7-15° range, 36.8% of the features were positively identified, with 21.6% of the surrounding areas being misclassified, having a true-positive to false-positive ratio of 1:67.

During the reclassification of curvature as >0, 67.7% of the ditches were accurately recognized compared to 45.7% of surrounding areas being misidentified. In this instance, there

was a 1:94.3 ratio for true-positive to false-positive detections. For the scale at >3, 47.2% were positively classified as features and a rate of 17.9% of surrounding areas improperly marked, with a true-positive to false-positive ratio of 1:53.6. During the final reclassification of features as >5, 39.3% of ditches were positively identified while only 13.6% of the surrounding area was misclassified, leaving a ratio of true-positive to false-positive of 1:48.7.

The combination of slope and curvature via a raster calculator yielded even more accurate results. Although the number of true-positive detections decreased slightly, the number of false-positives decreased significantly, resulting in a much more acceptable ratio of the two. The best results seem to have come from the recalculated data with slope in the 3-15° range and curvature at >3. This test had 38.5% of the ditch correctly identified while only misclassifying 8.3% of the surrounding landscape. This resulted in a true-positive to false-negative ratio of 1:35.6. The remaining results from the slope/curvature reclassification can be found below in Table 1. Overall, this technique seemed to work rather well in reducing false positives but less effectively in true positives, but further testing is still necessary to better refine the methodology.

Automated Extraction

At the surface, the automated extraction algorithm for this study proved to be a complete failure. On average, only 10% of the features were classified as true-positive. Although the ratio of true-positive to false-positive was less than the semi-automated detections at 1:18.8, the fact that hardly any of the actual feature cells were identified in the output overshadows this statistic. It must be noted that this technique was experimental in nature and does not have a proven track record in any standardized format. With further testing and analysis, this technique could eventually develop and prove to be a successful utility in the future.

Table 1. Average results for automated methods.

Slope	TP	FP	Ratio
3-15°	65.6%	43.6%	1:85.7
5-15°	50.2%	32.3%	1:76.7
7-15°	36.8%	21.6%	1:67
Curvature	TP	FP	Ratio
>0	67.7%	45.7%	1:94.3
>3	47.2%	17.9%	1:53.6
>5	39.3%	13.6%	1:48.7
Slope/Curvature	TP	FP	Ratio
3-15°+>0	46.3%	19.8%	1:58.8
3-15°+>3	38.5%	8.3%	1:35.6
3-15°+>5	30.4%	6.4%	1:32.3
5-15°+>0	35%	14.7%	1:53.1
5-15°+>3	27%	6.9%	1:33
5-15°+>5	23.3%	4.8%	1:30.4
7-15°+>0	25%	9.8%	1:47.3
7-15°+>3	19.6%	4.3%	1:30
7-15°+>5	16.9%	3.3%	1:27.8
Auto	TP	FP	Ratio
	10%	10.4%	1:18.8

Troubleshooting

Issues will always arise when developing new technologies, and this project was no different. As it was initially a multidisciplinary endeavor to program an automated extraction program, it was necessary to collaborate with individuals from different backgrounds. This proved challenging as geoscience and archaeology have both similar and different terms for the same things, and that information had to be translated to computer science personnel for programming. The issues didn't always get solved but solutions were always attempted.

Several problems arose during the initial programming. When the first sites were trained and tested on themselves to see if it would work, the ditches were not centered on their actual locations and were exaggerated at two to three times their actual size. It was eventually discovered that a larger window size would distort the output, which was subsequently anchored

to a corner of the feature and not its center, resulting in the discrepancies. At one point, the x and y coordinates were reversed and the results were inverted. Although these minor programming issues were ultimately solved, the system was still not able to function as anticipated.

The areas immediately adjacent and outside of the ditches that were included in the manually delineated feature layer could have potentially affected the outcome. It was thought that this would have benefitted the study by providing the algorithm with more data and context with which to work. The ditches are all located on flat terraces and it would seem important for those physical characteristics to be included as they would assist in the identification of the more specific ditched features this study attempts to explore. Perhaps additional testing would clarify this but it is unlikely it would provide any benefits to the program in its current state.

This system did indeed detect the features to a certain extent, but its ratio to false-positive outputs was extremely high, which severely affected the results. If this system were to be successfully programmed, this ratio must be significantly reduced. Even if the features were positively identified in the current system, the additional amount of identified cells not related to the feature could make it difficult to properly assess both on-screen and in the field. An acceptable level of accuracy must be recognized to create useful models that can be adapted for use in field-based surveys. Limiting the thresholds of training samples to stricter parameters will decrease the amount of false-positives, but may additionally limit the amount of true features detected as well. Additionally, the massive amount of data required for analysis presented a challenge to the limited processing capabilities of consumer-based computers. Access to a highly sophisticated and efficient computer system would likely be required for this technology to be fully programmed and utilized.

CHAPTER 6. CONCLUSIONS

Although the extraction system could not be completely developed, it proved to be partially successful. The ditches were positively identified in some areas, and could easily be distinguished from the surrounding landscape. However, it must be noted that there were a significant amount of false-positive results in all of the tests. Regardless, this experiment proved that it is somewhat possible to detect these features in certain contexts, and with further advancement may develop into something extremely productive. These results must not be measured solely on the statistics alone, but by the reasoning that it could eventually supplement or directly support additional testing by future researchers.

To conclude on the results of this analysis, we must examine the original objectives of this study. To reiterate and answer the research questions:

- What visualization technique best represents the physical extent of these features for manual interpretations of the data?

  The many different visualization tools all proved to be useful, but certain techniques were able to better distinguish the ditches from their surroundings. Overall, the Local Relief Model as well as the slope and curvature layers defined the features most clearly, and the latter two were additionally used in subsequent testing.

- Which characteristic of these features, or combination of characteristics, will provide the highest degree of accuracy in detecting known sites through automated and semi-automated methods of feature extraction?

Although the slope and curvature trials yielded some positive results when tested independently, it wasn't until they were used in combination that a more acceptable outcome was attained. Of all the testing, the semi-automated version isolating cells with a slope of 3-15° and curvature >3 generated the best results, with 38.5% true-positive and only 8.3% false-positive detections for a ratio of 1:35.6.

- Since the system will primarily detect anomalies based on morphological shape, is it possible to distinguish between the targeted feature type, and those of similar shape but of other cultural or natural origins, based on interpretations of these non-intrusive datasets alone?

  Depending on the location and context of the identified areas, some places could indeed be disregarded. If a ditch was identified paralleling a road it would be obvious that it would be related to that feature. However, even in conjunction with aerial photographs this may not be very evident based on such limited data. If anything is under suspicion of having prehistoric cultural origins it must be positively verified in the field through ground-truthing.

Even though the results did not fulfill all expectations, they provided enough data for adequate analysis to address the aforementioned research objectives. With additional work there is no doubt that systems such as these could be economically feasible to use on a wide scale. Academics, private consultants, and individual researchers could all benefit from this technology if fully developed. At the current stage it in not quite ready for prime time and it would likely take a dedicated team a significant amount of resources and time to accomplish. Although the

foundation of this methodology is sound, it will require many additional modifications and subsequent testing to improve.

Additional Areas

If this system can eventually demonstrate sufficient productivity, it could be tested in additional areas with known sites that have ditched features to determine its applicability on a wider scale. It is crucial for any scientific experiment to perform tests on unknown variables to obtain as wide a variety of results as possible. In this way, we can eliminate those instances that don't work and develop solutions to problems that may have not occurred during the initial development of the program. All of these results will aid in the understanding of its experimental development, as it is impossible to figure out how something works without additionally figuring out what doesn't work. The most obvious place to turn for subsequent testing would be the many other fortified village sites in North Dakota.

Numerous examples of large fortified villages are located and extend along areas of the Missouri River. Many of them have been preserved for interpretive purposes and multiple excavations have been performed to learn about prehistoric lifeways in that drainage. Although dozens of samples could be considered for analysis, the lidar data are limited to the regions comprising the Missouri River floodplain, and are not currently available for much of the areas beyond. Only three sites are included in the available lidar data that are proximal to the Missouri River: Double Ditch, On a Slant, and Chief Looking's Village. Each of these significantly sized occupations could have supported hundreds or even thousands of people at different times. Additionally, each of these sites has fortification ditches integrated into their site design that provide the testing grounds necessary to complete development.

Returning to the geographic region closest to the training set, other sites in the area provide supplementary samples for even further confirmation testing. Along the Sheyenne River just north of the Fort Ransom mound group is a ditched occupation referred to as the Zeck Site (Michlovic and Holley 2009). The site was recorded, but its geographic location has since been lost and recent attempts to find it have proven futile. Man-made disturbances in the area have altered the topography and the exact boundaries of the ditch cannot be determined. However, if the correct programming can be developed this would be one instance in which the system could be used; the rediscovery of lost sites. Several sites on the James River, Hintz and Hendrickson III sites, as well as a secondary cluster of villages near Lake Traverse and Bigstone Lake along the Minnesota/North Dakota border provide additional areas for testing (Michlovic and Schneider 1993). These sites offer the necessary settings in which to verify the accuracy and precision of the extraction program prior to its application to the detection of unknown sites on larger datasets.

The end goal of this research is not just successfully to create a system that can automatically detect known anthropogenic features based on morphological characteristics, but to apply that system to expanded areas in the hopes of detecting similar, unrecorded features on the landscape. To accomplish this, the system could eventually be tested on greater portions of the Sheyenne and Maple Rivers in search of similar sites to the samples used for training. In addition, since more archaeological work has been done here than in other areas, it would be beneficial to expand this application to areas where previous site inventories are limited. For this reason, it could be proposed to perform additional testing along the nearby James River in Stutsman or La Moure Counties. Aerial lidar data are available for this area in conveniently sized tiles and would provide an advantageous setting to test program suitability in other regions.

If positive classifications did result from this component, ground-truthing can then be conducted to verify the presence of morphological features and eliminate any false-positive results. If cultural properties are identified, specific documentation is required to record the context and integrity of the site.

This research also sets the stage for a broader application of the system that extends past the localized project area. As more data continues to be collected from all regions of the globe, it creates many opportunities for researchers to explore potentially unknown or inaccessible areas. From unexplored jungles in South America to extremist controlled areas in the Levant, similar sites may be found. It must be noted that with increased geographic distance, a greater range in variation between feature types may be observed. Although not universal, the features for this analysis exist in similar forms throughout the world and were chosen as such to demonstrate the system's potential applicability on larger scales for future projects.

Moving Forward

Implications for the successful development of this technology will not only benefit the fields of anthropology and historic preservation, but also environmental studies related to energy production, agriculture, emergency planning, and urban development. More importantly, this system will allow archaeological investigators to review topography and locate features of certain morphological characteristics on the surface that otherwise would be difficult to distinguish in the field due to vegetation cover, terrain, or landowner permissions. Additionally, these methods could reduce the time researchers spend in the field by providing them with a model of potential site locations in areas with differential probabilities for site presence. The mapping of known sites could be recorded in this system to create a database of all known

features, allowing regional, national, and worldwide spatial pattern analysis between samples to determine various statistics, such as the entire range of variation within a feature type. Remote sensing can also provide an avenue for cultural preservationists to monitor archaeological sites and observe their rates of change through time. This would aid in the planning of conservation efforts and any required mitigation to limit further damage of cultural properties.

Having access to the perceived locations of archeological features can reduce the amount of time it takes to perform field-based surveys. Detailed models including the geographic position of anomalies produce accurate maps to easily navigate the landscape and locate the features under question. This allows additional efforts to focus on the validation of those entities that can be attained by either invasive or non-invasive methods. Therefore, the efficiency of this technology will be measured not only in its success at extracting morphological features from the surface, but by its accuracy in detecting true, archaeological features from the false detections.

Using remotely sensed data to explore inaccessible areas, or those with limited surface visibility, can provide valuable details about the landscape and highlights its appeal to researchers from many different disciplines. The successful development of this technology could provide the archaeologist with an important tool to assist in the discovery, documentation, and preservation of cultural materials. This could potentially decrease the amount of time it would take to accomplish fieldwork and provide a more complete record of the site types defined for a given area. Although nothing can replace detailed excavation, the advantages that new technologies can provide are tremendously useful and should be utilized when possible.

It would take a significant amount of time and testing to develop this methodology where it could be universally used and trusted by researchers. Even if this technology does advance to this point, it will never detect every instance of human occupation. This technology, although

extremely useful in archaeology, will never completely replace traditional fieldwork and it must be ultimately stressed that a boots on the ground approach is the only way to truly verify past occupation.

REFERENCES

Ainsworth, S., A. Oswald, and D. Went.
2013 Remotely acquired, not remotely sensed: using lidar as a field survey tool. In Interpreting archaeological topography. R.S. Opitz and D.C. Cowley, eds. 17:206-222.

Alnemer, L.M., O. Al-Azzam, C. Chitranranjan, A.M. Denton, F.M. Bassi, M.J. Iqbal, and S.F. Kianian.
2011 Multiple sources classification of gene position on chromosomes using statistical significance of individual classification results. In International Conference on Machine Learning and Applications, Honolulu, HI, 18-21 Dec. 2011.

Bamforth, D.B.
1994 Indigenous people, indigenous violence: precontact warfare on the North American great plains. Man 29(1):95-115.

Bennett, R., K. Welham, R.A. Hill, and A. Ford.
2012 A Comparison of Visualization Techniques for Models Created from Airborne Laser Scanned Data. Archaeological Prospection 19:41-48.

Bluemle, J.P.
2000 The Face of North Dakota. Eductaion Series 26. North Dakota Geological Survey. Bismarck, North Dakota.

Boast, R. and P. Biehl
2011 Archaeological knowledge production and dissemination in the digital age. Archaeology 2.0: New approaches to communication and collaboration. E.C. Kansa, S.W. Kansa, and E. Watrall eds. 119-155.

Bewley, R.H.
2003 Aerial survey for archaeology. Photogrammetric Record 18(104):273-292.

Challis, K., Z Kokalj, M. Kincey, D. Moscrop, and A.J. Howard.
2008 Airborne lidar and historic environmental records. Antiquity 82:1055-1064.

Challis, K., P. Forlin, and M. Kincey.
2011 A Generic Toolkit for the Visualization of Archaeological Features on Airborne LiDAR Elevation Data. Archaeological Prospection 18:279-289.

Corns, A. and R. Shaw.
2013 Using lidar data – drawing on 10 year's experience at English heritage. In Interpreting archaeological topography. R.S. Opitz and D.C. Cowley, eds. 11:136-145.

Cowley, D.
2009 Remote Sensing for Archaeological Heritage Management. Archaeolingua, Series: EAC Occasional Paper, Volume 5, Budapest.
2012 In with the new, out with the old? Auto-extraction for remote sensing archaeology. C. Bostater Jr., S. Mertikas, X. Neyt, C. Nichol, and D. Cowley, eds. Proceedings of SPIE 8532: 853206.1-183206.9.

Crow, P., S. Benham, B.J. Devereux, and G.S. Amable.
2007 Woodland vegetation and its implications for archaeological survey using LiDAR. Forestry 80(3):241-252.

Crutchley, S.
2013 Lidar and World Heritage Sites in Ireland: why was such a rich data source gathered, how is it being utilised, and what lessons have been learnd? In Interpreting archaeological topography. R.S. Opitz and D.C. Cowley, eds. 12:146-160.

Denton A.M.
2009 Subspace sums for extracting non-random data from massive noise. Knowledge and Information Systems Journal. 20(1):35-62.

Denton, A.M., J. Wu.
2009 Data mining of vector-item patterns using neighborhood histograms. Knowledge and Information Systems Journal. 21:173-199.

Denton, A.M., C.A. Besermann, and D.H. Dorr.
2009 Pattern-based time-series subsequence clustering using radial distribution functions. Knowledge and Information Systems Journal. 18(1):1-27.

Denton A.M., J. Wu, and D.H. Dorr.
2010 Point distribution algorithm for mining vector-item patterns. In Proc. 16th ACM SIGDD Conf. on Knowledge Discovery and Data Mining: Useful Patterns Workshop, Washington DC, 25-28 July 2010.

Devereux, B.J., G.S. Amable, and P. Crow.
2008 Visualisation of LiDAR terrain models for archaeological feature detection. Antiquity 82:470-479.

Devereux, B.J., G.S. Amable, P. Crow, and A.D. Cliff.
2005 The potential of airborne lidar for detection of archaeological features under woodland canopies. Antiquity 79:648-660.

Doneus, M. and C. Briese.
2006 Full-waveform airborne laser scanning as a tool for archaeological reconnaissance. BAR International Series 1568:99-105.

Doneus, M., C. Briese, M. Fera, and M. Janner.
2008 Archaeological prospection of forested areas using full-waveform airborne laser scanning. Journal of Archaeological Science 35:882-893.

Doneus, M. and T. Kuhteiber.
2013 Airborne laser scanning and archaeological interpretation – bringing back the people. In Interpreting archaeological topography. R.S. Opitz and D.C. Cowley, eds. 3:32-50.

Dorr D.H. and A.M. Denton
2010 Generalised sequence signatures through symbolic clustering. International Journal of Data Mining and Bioinformatics 4(6):656-674.

Ebert, D.
2004 Applications of Archaeological GIS. Canadian Journal of Archaeology 28:319-341.

Fry, G.L.A., B. Skar, G. Jerpasen, V. Bakkestuen, and L. Erikstad.
2004 Locating archaeological sites in the landscape: a hierarchical approach based on landscape indicators. Landscape and Urban Planning 67:97-107.

Halliday, S.
2013 I Walked, I Saw, I Surveyed, but what did I see?... and what did I survey. In Interpreting archaeological topography. R.S. Opitz and D.C. Cowley, eds. 5:63-75.

Hastie, T., R. Tibshirani, and J. Friedman
2001 The elements of Statistical learning; data mining, inference, and prediction. Vol. 1. Springer, New York.

Hermosilla, T., L.A. Ruiz, J.A. Recio, and J. Estornell.
2011 Evaluation of Automatic Building Detection Approaches Combining High Resolution Images and LiDAR Data. Remote Sensing 3:1188-1210.

Hesse, R.
2010 Lidar-derived local relief models – a new tool for archaeological prospection. Archaeological Prospection 17:67-72.
2013 The changing picture of archaeological landscapes: lidar prospection over very large areas as part of a cultural heritage strategy. In Interpreting archaeological topography. R.S. Opitz and D.C. Cowley, eds. 14:171-183.

Holley, G.R. and E.M. Kalinowski.
2008 The Lucas Site: Enclosures, Military Camps and the Terminal Late Woodland of the Northeastern Plains. In Journal of the North Dakota Archaeological Association: Papers in Northeastern Prehistory. M.G. Michlovic and D.L. Toom, eds. 8:127-138.

Holley, G.R., M.G. Michlovic, and R.A. Dalan
2011 Report on 2008 Archaeology at the Biesterfeldt Site (32RM1), Ransom County, North Dakota. Minnesota State University Moorhead. Moorhead, MN.

Kokalj, Z., K. Zaksek, and K. Ostir.
2011 Application of sky-view factor for the visualization of historic landscape features in lidar-derived relief models. Antiquity 85:263-273.
2013 Visualizations of lidar derived relief models. In Interpreting archaeological topography. R.S. Opitz and D.C. Cowley, eds. 8:100-114.

Kvamme, K.
1999 Recent Directions and Developments in Geographical Information Systems. Journal of Archaeological Research 7(2):153-201.
2003 Geophysical Surveys as Landscape Archaeology. American Antiquity 68(3):435-457).

Lasaponara, R., R. Colluzi, and N. Masini.
2010 Flights into the past: full-waveform airborne laser scanning data for archaeological investigation. Journal of Archaeological Science 38(9):2061-2070.

Michlovic, M.G.
2008 Archaeological Test Excavations at the Peterson Site (32RM401), Ransom County, North Dakota. Minnesota State University Moorhead. Moorhead, MN.
2008 The Shea Phase of the Northeastern Plains Village Culture. *In* Journal of the North Dakota Archaeological Association. M.G. Michlovic and D.L. Toom eds. 8:35-51.

Michlovic, M.G. and G.R. Holley.
2009 Archaeology of the Sprunk Site (32CS4478). Minnesota State University Moorhead. Moorhead, MN.

Michlovic, M.G. and F.E. Schneider.
1988 The Archaeology of the Shea Site (32CS101). Minnesota State University Moorhead. Moorhead, MN.
1993 The Shea Site: A Prehistoric Fortified Village on the Northeastern Plains. Plains Anthropologist. 38(143):117-137.

McCoy, M.D. and T.N. Ladefoged.
2009 New developments in the use of spatial technology in archaeology. Journal of Archaeological Research 17:263-295.

Neubauer, W.
2004 GIS in Archaeology-the Interface between Prospection and Excavation. Archaeological Prospection 11:159-166.

Ogburn, D.E.
2006 Assessing the level of visibility of cultural objects in past landscapes. Journal of Archaeological Science 33: 405-413.

Opitz, R.S.
2013 An overview of airborne and terrestrial laser scanning in archaeology. In Interpreting archaeological topography. R.S. Opitz and D.C. Cowley, eds. 2:13-31.

Opitz, R.S. and D.C. Cowley.
2013 Interpreting archaeological topography: lasers, 3D data, observation, visualization and applications. In Interpreting archaeological topography. R.S. Opitz and D.C. Cowley, eds. 1:1-12.

Palmer, R.
2013 Reading aerial images. In Interpreting archaeological topography. R.S. Opitz and D.C. Cowley, eds. 5:76-87.

Risbol, O.
2013 Cultivating the 'wilderness' – how lidar can improve archaeological landscape understanding. In Interpreting archaeological topography. R.S. Opitz and D.C. Cowley, eds. 4:51-62.

Rottensteiner, F. and C. Briese.
2002 A new method for building extraction in urban areas from high-resolution LIDAR data. International Archives of Photogrammetry Remote Sensing and Spatial Information Sciences 34.3/A:295-301.

Schneider, F.
2002 Prehistoric horticulture in the northeastern plains. Plains Anthropologist 47(180):33-50.

Sohn, G. and I. Dowman.
2007 Data fusion of high-resolution satellite imagery and LiDAR data for automatic building extraction. ISPRS Journal of Photogrammetry & Remote Sensing 62:43-63.

Stanco, F., S. Battiato, and G. Gallo.
2011 Digital imaging for cultural heritage preservation: analysis, restoration, and reconstruction of ancient artworks. CRC Press, Florida.

State Historical Society of North Dakota (SHSND).
2008 The North Dakota Comprehensive Plan for Historic Preservation: Archeological Component. Electronic document, http://history.nd.gov/hpfomrs.html, accessed July 2015.

Strong, D.W.
1940 From History to Prehistory in the Northern Great Plains. In Essays in Historical Anthropology of North America, Published in Honor of John R. Swanton in Celebration of His Fortieth Year with the Smithsonian Institution. 353-394. Smithsonian Institution Miscellaneous Collections 100. Washington D.C.

Toom, D.L.
2004 Northeastern Plains Village complex timelines and relations. Plains Anthropologist 49(191):281-297.

Trier, O.D., S.O. Larsen, and R. Solberg.
2009 Automatic detection of circular structures in high-resolution satellite images of agricultural land. Archaeological Prospection 16:1-15.

Trier, O.D. and L.H. Pilo,
2012 Automatic Detection of Pit Structures in Airborne Laser Scanning Data. Archaeological Prospection 19:103-121.

Trier, O.D. and Zortea.
2012 Semi-automatic detection of cultural heritage in lidar data. Proceedings of 4th International Conference on Geographic Object-Based Imagae Analysis (GEOBIA) 7-9.

Tripcevich, N.
2004 Interfaces: Mobile GIS in archaeological survey. The SAA Archaeological Record 4(3):17-22.

Tripcevich, N. and S.A. Wernke.
2010 On-site recording of excavation data using mobile GIS. Journal of Field Archaeology 35(4):380-397.

Wehr, A. and U. Lohr.
1999 Airborne laser scanning-an introduction and overiew. ISPRS Journal of Photogrammetry and Remote Sensing 54:68-82.

Whallon Jr., R.
1972 The computer in archaeology: a critical survey. Computers and the Humanities 7(1):29-45.

Witten, I.H., E. Frank, L. Trigg, M. Hall, G. Holmes, and S.J. Cunningham
1999 Weka: Practical machine learning tools and techniques with java implementations. University of Waikato, Department of Computer Science. Hamilton,New Zealand.

Wood, W.R.
1971 Biesterfeldt: a post-contact coalescent site on the northeastern plains. Smithsonian Institution Press. Washington DC.
1974 Northern Plains Village Cultures: Internal Stability and External Relationships. Journal of Anthropological Research 30(1):1-16.

APPENDIX. INDIVIDUAL SITE RESULTS

Table A.1. Shea site results.

Shea					
	Slope 3-15°	TP/TF	FN/TF	FP/NF	TN/NF
Ratio	Result	579/643	64/643	30107/48477	18370/48477
1:52	Percentage	90	10	62.1	37.9
	Slope 5-15°	TP/TF	FN/TF	FP/NF	TN/NF
Ratio	Result	482/643	161/643	24181/48477	24296/48477
1:50.2	Percentage	75	25	49.9	50.1
	Slope 7-15°	TP/TF	FN/TF	FP/NF	TN/NF
Ratio	Result	344/643	299/643	13738/48477	34739/48477
1:39.9	Percentage	53.5	46.5	28.3	71.7
	Curvature >0	TP/TF	FN/TF	FP/NF	TN/NF
Ratio	Result	460/643	183/643	22718/48477	25759/48477
1:49.4	Percentage	71.5	28.5	46.9	53.1
	Curvature >3	TP/TF	FN/TF	FP/NF	TN/NF
Ratio	Result	322/643	321/643	5026/48477	43451/48477
1:15.6	Percentage	50.1	49.9	10.4	89.6
	Curvature >5	TP/TF	FN/TF	FP/NF	TN/NF
Ratio	Result	256/643	387/643	2782/48477	45695/48477
1:10.9	Percentage	39.8	60.2	5.7	94.3
	S(3-15°)C(>0)	TP/TF	FN/TF	FP/NF	TN/NF
Ratio	Result	418/643	225/643	14181/48477	34296/48477
1:33.9	Percentage	65	35	29.3	70.7
	S(3-15°)C(>3)	TP/TF	FN/TF	FP/NF	TN/NF
Ratio	Result	294/643	349/643	3253/48477	45224/48477
1:11.1	Percentage	45.7	54.3	6.7	93.3

Table A.1. Shea site results (continued).

	S(3-15°)C(>5)	TP/TF	FN/TF	FP/NF	TN/NF
Ratio	Result	234/643	409/643	1858/48477	46619/48477
1:7.9	Percentage	36.4	63.6	3.8	96.2
	S(5-15°)C(>0)	TP/TF	FN/TF	FP/NF	TN/NF
Ratio	Result	342/643	301/643	11449/48477	37028/48477
1:33.5	Percentage	53.2	46.8	23.6	76.4
	S(5-15°)C(>3)	TP/TF	FN/TF	FP/NF	TN/NF
Ratio	Result	240/643	403/643	2787/48477	45690/48477
1:11.6	Percentage	37.3	62.7	5.7	94.3
	S(5-15°)C(>5)	TP/TF	FN/TF	FP/NF	TN/NF
Ratio	Result	190/643	453/643	1624/48477	46853/48477
1:8.6	Percentage	29.6	70.4	3.4	96.6
	S(7-15°)C(>0)	TP/TF	FN/TF	FP/NF	TN/NF
Ratio	Result	228/643	415/643	6447/48477	42030/48477
1:28.3	Percentage	35.5	64.5	13.3	86.7
	S(7-15°)C(>3)	TP/TF	FN/TF	FP/NF	TN/NF
Ratio	Result	156/643	487/643	2052/48477	46425/48477
1:13.6	Percentage	24.3	75.7	4.2	95.8
	S(7-15°)C(>5)	TP/TF	FN/TF	FP/NF	TN/NF
Ratio	Result	123/643	520/643	1292/48477	47185/48477
1:10.5	Percentage	19.1	80.9	2.7	97.3
	Auto	TP/TF	FN/TF	FP/NF	TN/NF
Ratio	Result	31/643	612/643	70/48477	48407/48477
1:2.3	Percentage	4.8	95.2	0.1	99.9

Table A.2. Sprunk site results.

Sprunk					
	Slope 3-15°	TP/TF	FN/TF	FP/NF	TN/NF
Ratio	Result	119/292	173/292	50476/95288	44812/95288
1:424.2	Percentage	40.8	59.2	53	47
	Slope 5-15°	TP/TF	FN/TF	FP/NF	TN/NF
Ratio	Result	58/292	234/292	36266/95288	59314/95288
1:625.3	Percentage	19.9	80.1	38.1	61.9
	Slope 7-15°	TP/TF	FN/TF	FP/NF	TN/NF
Ratio	Result	24/292	268/292	23306/95288	72274/95288
1:971.1	Percentage	8.2	91.8	24.5	75.5
	Curvature >0	TP/TF	FN/TF	FP/NF	TN/NF
Ratio	Result	190/292	102/292	45967/95288	49321/95288
1:241.9	Percentage	65.1	34.9	48.2	51.8
	Curvature >3	TP/TF	FN/TF	FP/NF	TN/NF
Ratio	Result	99/292	193/292	11307/95288	83981/95288
1:114.2	Percentage	33.9	66.1	11.9	88.1
	Curvature >5	TP/TF	FN/TF	FP/NF	TN/NF
Ratio	Result	63/292	229/292	6407/95288	88881/95288
1:101.7	Percentage	21.6	78.4	6.7	93.3
	S(3-15°)C(>0)	TP/TF	FN/TF	FP/NF	TN/NF
Ratio	Result	78/292	214/292	25002/95288	70286/95288
1:320.5	Percentage	26.7	73.3	26.2	73.8
	S(3-15°)C(>3)	TP/TF	FN/TF	FP/NF	TN/NF
Ratio	Result	54/292	238/292	6770/95288	88518/95288
1:125.4	Percentage	18.5	81.5	7.1	92.9
	S(3-15°)C(>5)	TP/TF	FN/TF	FP/NF	TN/NF
Ratio	Result	35/292	257/292	3879/95288	91409/95288
1:110.8	Percentage	12	88	4.1	95.9

Table A.2. Sprunk site results (continued).

	S(5-15°)C(>0)	TP/TF	FN/TF	FP/NF	TN/NF
Ratio	Result	39/292	253/292	18029/95288	72259/95288
1:462.3	Percentage	13.4	86.6	18.9	81.1
	S(5-15°)C(>3)	TP/TF	FN/TF	FP/NF	TN/NF
Ratio	Result	27/292	265/292	5130/95288	90518/95288
1:190	Percentage	9.2	90.8	5.4	94.6
	S(5-15°)C(>5)	TP/TF	FN/TF	FP/NF	TN/NF
Ratio	Result	16/292	276/292	3003/95288	92285/95288
1:187.7	Percentage	5.5	94.5	3.1	96.9
	S(7-15°)C(>0)	TP/TF	FN/TF	FP/NF	TN/NF
Ratio	Result	17/292	275/292	11556/95288	83732/95288
1:679.8	Percentage	5.8	94.2	12.1	87.9
	S(7-15°)C(>3)	TP/TF	FN/TF	FP/NF	TN/NF
Ratio	Result	11/292	281/292	3471/95288	91817/95288
1:315.5	Percentage	3.8	96.2	3.6	96.4
	S(7-15°)C(>5)	TP/TF	FN/TF	FP/NF	TN/NF
Ratio	Result	6/292	286/292	2089/95288	93199/95288
1:348.2	Percentage	2.1	97.9	2.2	97.8
	Auto	TP/TF	FN/TF	FP/NF	TN/NF
Ratio	Result	2/292	290/292	251/95288	95037/95288
1:120.5	Percentage	0.7	99.3	0.3	99.7

Table A.3. Biesterfeldt site results.

Biesterfeldt					
	Slope 3-15°	TP/TF	FN/TF	FP/NF	TN/NF
Ratio	Result	409/1118	709/1118	43022/184690	141668/184690
1:105.2	Percentage	36.6	63.4	23.3	76.7
	Slope 5-15°	TP/TF	FN/TF	FP/NF	TN/NF
Ratio	Result	222/1118	896/1118	18849/184690	165841/184690
1:84.9	Percentage	19.9	80.1	10.2	89.8
	Slope 7-15°	TP/TF	FN/TF	FP/NF	TN/NF
Ratio	Result	71/1118	1047/1118	8779/184690	175911/184690
1:123.6	Percentage	6.4	93.6	4.8	95.2
	Curvature >0	TP/TF	FN/TF	FP/NF	TN/NF
Ratio	Result	685/1118	433/1118	88390/184690	96300/184690
1:129	Percentage	61.3	38.7	47.9	52.1
	Curvature >3	TP/TF	FN/TF	FP/NF	TN/NF
Ratio	Result	264/1118	854/1118	23284/184690	161406/184690
1:88.2	Percentage	23.6	76.4	12.6	87.4
	Curvature >5	TP/TF	FN/TF	FP/NF	TN/NF
Ratio	Result	181/1118	937/1118	13594/184690	171096/184690
1:75.1	Percentage	16.2	83.8	7.4	92.6
	S(3-15°)C(>0)	TP/TF	FN/TF	FP/NF	TN/NF
Ratio	Result	250/1118	868/1118	21425/184690	163265/184690
1:85.7	Percentage	22.4	77.6	11.6	88.4
	S(3-15°)C(>3)	TP/TF	FN/TF	FP/NF	TN/NF
Ratio	Result	128/1118	990/1118	10012/184690	174678/184690
1:78.2	Percentage	11.4	88.6	5.4	94.6
	S(3-15°)C(>5)	TP/TF	FN/TF	FP/NF	TN/NF
Ratio	Result	97/1118	1021/1118	6789/184690	177901/184690
1:70	Percentage	8.7	91.3	3.7	96.3

Table A.3. Biesterfeldt site results (continued).

	S(5-15°)C(>0)	TP/TF	FN/TF	FP/NF	TN/NF
Ratio	Result	127/1118	991/1118	9347/184690	175343/184690
1:73.6	Percentage	11.4	88.6	5.1	94.9
	S(5-15°)C(>3)	TP/TF	FN/TF	FP/NF	TN/NF
Ratio	Result	46/1118	1072/1118	4976/184690	179714/184690
1:108.2	Percentage	4.1	95.9	2.7	97.3
	S(5-15°)C(>5)	TP/TF	FN/TF	FP/NF	TN/NF
Ratio	Result	32/1118	1086/1118	3576/184690	181114/184690
1:111.8	Percentage	2.9	97.1	1.9	98.1
	S(7-15°)C(>0)	TP/TF	FN/TF	FP/NF	TN/NF
Ratio	Result	42/1118	1076/1118	4300/184690	180390/184690
1:102.4	Percentage	3.8	96.2	2.3	97.7
	S(7-15°)C(>3)	TP/TF	FN/TF	FP/NF	TN/NF
Ratio	Result	20/1118	1098/1118	2555/184690	182135/184690
1:127.8	Percentage	1.8	98.2	1.4	98.6
	S(7-15°)C(>5)	TP/TF	FN/TF	FP/NF	TN/NF
Ratio	Result	13/1118	1105/1118	1902/184690	182788/184690
1:146.3	Percentage	1.2	98.8	1	99
	Auto	TP/TF	FN/TF	FP/NF	TN/NF
Ratio	Result	2/1118	1116/1118	3033/184690	181657/184690
1:1516.5	Percentage	0.2	99.8	1.6	98.4

Table A.4. Lucas site results.

Lucas					
	Slope 3-15°	TP/TF	FN/TF	FP/NF	TN/NF
Ratio	Result	300/397	97/397	4125/10789	6664/10789
1:13.8	Percentage	75.6	24.4	38.2	61.8
	Slope 5-15°	TP/TF	FN/TF	FP/NF	TN/NF
Ratio	Result	240/397	157/397	3239/10789	7550/10789
1:13.5	Percentage	60.5	39.5	30	70
	Slope 7-15°	TP/TF	FN/TF	FP/NF	TN/NF
Ratio	Result	193/397	204/397	2708/10789	8081/10789
1:14	Percentage	48.6	51.4	25.1	74.9
	Curvature >0	TP/TF	FN/TF	FP/NF	TN/NF
Ratio	Result	304/397	93/397	4650/10789	6139/10789
1:15.3	Percentage	76.6	23.4	43.1	56.9
	Curvature >3	TP/TF	FN/TF	FP/NF	TN/NF
Ratio	Result	256/397	141/397	1682/10789	9107/10789
1:6.6	Percentage	64.5	35.5	15.6	84.4
	Curvature >5	TP/TF	FN/TF	FP/NF	TN/NF
Ratio	Result	230/397	167/397	998/10789	9791/10789
1:4.3	Percentage	57.9	62.1	9.3	90.7
	S(3-15°)C(>0)	TP/TF	FN/TF	FP/NF	TN/NF
Ratio	Result	237/397	160/397	1636/10789	9153/10789
1:6.9	Percentage	59.7	40.3	15.2	84.8
	S(3-15°)C(>3)	TP/TF	FN/TF	FP/NF	TN/NF
Ratio	Result	202/397	195/397	648/10789	10141/10789
1:3.2	Percentage	50.9	49.1	6	94
	S(3-15°)C(>5)	TP/TF	FN/TF	FP/NF	TN/NF
Ratio	Result	182/397	215/397	408/10789	10381/10789
1:2.2	Percentage	45.8	54.2	3.8	96.2

Table A.4. Lucas site results (continued).

	S(5-15°)C(>0)	TP/TF	FN/TF	FP/NF	TN/NF
Ratio	Result	188/397	209/397	1308/10789	9481/10789
1:7	Percentage	47.4	52.6	12.1	87.9
	S(5-15°)C(>3)	TP/TF	FN/TF	FP/NF	TN/NF
Ratio	Result	159/397	238/397	541/10789	10248/10789
1:3.4	Percentage	40.1	59.9	5	95
	S(5-15°)C(>5)	TP/TF	FN/TF	FP/NF	TN/NF
Ratio	Result	146/397	251/397	350/10789	10439/10789
1:2.4	Percentage	36.8	63.2	3.2	96.8
	S(7-15°)C(>0)	TP/TF	FN/TF	FP/NF	TN/NF
Ratio	Result	147/397	250/397	1123/10789	9666/10789
1:7.6	Percentage	37	63	10.4	89.6
	S(7-15°)C(>3)	TP/TF	FN/TF	FP/NF	TN/NF
Ratio	Result	125/397	272/397	487/10789	10302/10789
1:3.9	Percentage	31.5	68.5	4.5	95.5
	S(7-15°)C(>5)	TP/TF	FN/TF	FP/NF	TN/NF
Ratio	Result	113/397	284/397	318/10789	10471/10789
1:2.8	Percentage	28.5	71.5	2.9	97.1
	Auto	TP/TF	FN/TF	FP/NF	TN/NF
Ratio	Result	164/397	233/397	507/10789	10282/10789
1:3.1	Percentage	41.3	58.7	4.7	95.3

Table A.5. Peterson site results.

Peterson					
	Slope 3-15°	TP/TF	FN/TF	FP/NF	TN/NF
Ratio	Result	232/296	64/296	5119/14800	9681/14800
1:22.1	Percentage	78.4	21.6	34.6	65.4
	Slope 5-15°	TP/TF	FN/TF	FP/NF	TN/NF
Ratio	Result	180/296	116/296	4266/14800	10534/14800
1:23.7	Percentage	60.8	39.2	28.8	71.2
	Slope 7-15°	TP/TF	FN/TF	FP/NF	TN/NF
Ratio	Result	143/296	153/296	3453/14800	11347/14800
1:24.1	Percentage	48.3	51.7	23.3	76.7
	Curvature >0	TP/TF	FN/TF	FP/NF	TN/NF
Ratio	Result	218/296	78/296	6423/14800	8377/14800
1:29.5	Percentage	73.6	26.4	43.4	56.6
	Curvature >3	TP/TF	FN/TF	FP/NF	TN/NF
Ratio	Result	159/296	137/296	1881/14800	12919/14800
1:11.8	Percentage	53.7	46.3	12.7	87.3
	Curvature >5	TP/TF	FN/TF	FP/NF	TN/NF
Ratio	Result	127/296	169/296	1285/14800	13515/14800
1:10.1	Percentage	42.9	57.1	8.7	91.3
	S(3-15°)C(>0)	TP/TF	FN/TF	FP/NF	TN/NF
Ratio	Result	170/296	126/296	2105/14800	12695/14800
1:12.4	Percentage	57.4	42.6	14.2	85.8
	S(3-15°)C(>3)	TP/TF	FN/TF	FP/NF	TN/NF
Ratio	Result	123/296	173/296	398/14800	14402/14800
1:3.2	Percentage	41.6	58.4	2.7	97.3
	S(3-15°)C(>5)	TP/TF	FN/TF	FP/NF	TN/NF
Ratio	Result	100/296	196/296	210/14800	14590/14800
1:2.1	Percentage	33.8	66.2	1.4	98.6

Table A.5. Peterson site results (continued).

	S(5-15°)C(>0)	TP/TF	FN/TF	FP/NF	TN/NF
Ratio	Result	129/296	167/296	1811/14800	12989/14800
1:14	Percentage	43.6	56.4	12.2	87.8
	S(5-15°)C(>3)	TP/TF	FN/TF	FP/NF	TN/NF
Ratio	Result	91/296	205/296	337/14800	14463/14800
1:3.7	Percentage	30.7	69.3	2.3	97.7
	S(5-15°)C(>5)	TP/TF	FN/TF	FP/NF	TN/NF
Ratio	Result	71/296	225/296	178/14800	14622/14800
1:2.5	Percentage	24	76	1.2	98.8
	S(7-15°)C(>0)	TP/TF	FN/TF	FP/NF	TN/NF
Ratio	Result	98/296	198/296	1528/14800	13272/14800
1:15.6	Percentage	33.1	66.9	10.3	89.7
	S(7-15°)C(>3)	TP/TF	FN/TF	FP/NF	TN/NF
Ratio	Result	64/296	232/296	294/14800	14506/14800
1:4.6	Percentage	21.6	78.4	2	98
	S(7-15°)C(>5)	TP/TF	FN/TF	FP/NF	TN/NF
Ratio	Result	47/296	249/296	155/14800	14645/14800
1:3.3	Percentage	15.9	84.1	1	99
	Auto	TP/TF	FN/TF	FP/NF	TN/NF
Ratio	Result	38/296	258/296	554/14800	14246/14800
1:14.6	Percentage	12.8	87.2	3.7	96.3

Table A.6. Nelson site results.

Nelson					
	Slope 3-15°	TP/TF	FN/TF	FP/NF	TN/NF
Ratio	Result	276/381	105/381	31247/62110	30863/62110
1:113.2	Percentage	72.4	27.6	50.3	49.7
	Slope 5-15°	TP/TF	FN/TF	FP/NF	TN/NF
Ratio	Result	247/381	134/381	22763/62110	39347/62110
1:92.2	Percentage	64.8	35.2	36.6	63.4
	Slope 7-15°	TP/TF	FN/TF	FP/NF	TN/NF
Ratio	Result	217/381	164/381	14448/62110	47662/62110
1:66.6	Percentage	56	44	23.3	76.7
	Curvature >0	TP/TF	FN/TF	FP/NF	TN/NF
Ratio	Result	221/381	160/381	27803/62110	34307/62110
1:125.8	Percentage	58	42	44.8	55.2
	Curvature >3	TP/TF	FN/TF	FP/NF	TN/NF
Ratio	Result	219/381	162/381	27521/62110	34589/62110
1:124.4	Percentage	57.5	42.5	44.3	55.7
	Curvature >5	TP/TF	FN/TF	FP/NF	TN/NF
Ratio	Result	219/381	162/381	27301/62110	34809/62110
1:124.4	Percentage	57.5	42.5	44	56
	S(3-15°)C(>0)	TP/TF	FN/TF	FP/NF	TN/NF
Ratio	Result	177/381	204/381	13812/62110	48298/62110
1:78	Percentage	46.5	53.5	22.2	77.8
	S(3-15°)C(>3)	TP/TF	FN/TF	FP/NF	TN/NF
Ratio	Result	175/381	206/381	13622/62110	48488/62110
1:77.8	Percentage	45.9	54.1	21.9	78.1
	S(3-15°)C(>5)	TP/TF	FN/TF	FP/NF	TN/NF
Ratio	Result	175/381	206/381	13478/62110	48632/62110
1:77	Percentage	45.9	54.1	21.7	78.3

Table A.6. Nelson site results (continued).

	S(5-15°)C(>0)	TP/TF	FN/TF	FP/NF	TN/NF
Ratio	Result	156/381	225/381	10110/62110	52000/62110
1:64.8	Percentage	40.9	59.1	16.3	83.7
	S(5-15°)C(>3)	TP/TF	FN/TF	FP/NF	TN/NF
Ratio	Result	155/381	226/381	9948/62110	52162/62110
1:64.2	Percentage	40.7	59.3	16	84
	S(5-15°)C(>5)	TP/TF	FN/TF	FP/NF	TN/NF
Ratio	Result	155/381	226/381	9838/62110	52272/62110
1:63.5	Percentage	40.7	59.3	15.8	84.2
	S(7-15°)C(>0)	TP/TF	FN/TF	FP/NF	TN/NF
Ratio	Result	133/381	248/381	6478/62110	55632/62110
1:48.7	Percentage	34.9	65.1	10.4	89.6
	S(7-15°)C(>3)	TP/TF	FN/TF	FP/NF	TN/NF
Ratio	Result	132/381	249/381	6391/62110	55719/62110
1:48.4	Percentage	34.6	65.4	10.3	89.7
	S(7-15°)C(>5)	TP/TF	FN/TF	FP/NF	TN/NF
Ratio	Result	132/381	249/381	6323/62110	55787/62110
1:47.9	Percentage	34.6	65.4	10.2	89.8
	Auto	TP/TF	FN/TF	FP/NF	TN/NF
Ratio	Result	0/381	381/381	43/62110	62067/62110
-	Percentage	0	100	0.1	99.9